Radical polymerization using organoboron or organozinc as initiator

by

Chao ZHAO

Student ID Number: 1208003

A dissertation submitted to the
Engineering Course, Department of Engineering,
Graduate School of Engineering,
Kochi University of Technology,
Kochi, Japan

For the degree of
Doctor of Philosophy

Assessment Committee:
Supervisor: Prof. Ryuichi SUGIMOTO
Co-Supervisor: Prof. Kazuya KOBIRO
Co-Supervisor: Prof. Nagatoshi NISHIWAKI
Prof. Toshiyuki KAWAHARAMURA
Assistant Prof. Akitaka ITO

September, 2019

Abstract

Organozinc compounds like diethylzinc and dimethylzinc have been widely used for nucleophilic addition reactions and transition-metal-catalyzed cross-couplings. Alkylzinc compounds has properties similar to those of alkylboranes, which have become increasingly important as key reagents in radical chemistry. However, like other dialkylzincs, conventional diethylzinc is highly combustible in air, reacts violently with water, and should be kept in an inert atmosphere, which limits its application. In recent years, there have been few reports on the use of diethylzinc as an initiator.

Alkyl-9-borabicyclo-[3.3.1]-nonane (alkyl-9-BBN) and diethyl(1,10-phenanthroline N^1,N10)zinc (Phen-DEZ) were used as initiators in my research. Since alkylboron and diethylzinc are hydrolytically unstable, an emulsion polymerization system was selected to evaluate the initiation properties of these two initiators.

I investigated various polymerization systems and polymerization methods, selected a variety of monomers and substrates, and varied the reaction conditions to study the properties and application conditions of diethylzinc. My experiments were designed to investigate whether polymerization could be performed in an emulsion system and to examine possible grafting substrates. Here, the new efficient initiators Phen-DEZ and alkyl-9-BBN for radical homopolymerization and graft polymerization in different solvents and reaction systems were developed.

The accomplished work in this dissertation:

- Research on the characteristics and kinetic of 9-BBN initiator in emulsion system.
- Study on characteristics and kinetic of homopolymerization initiated by Phen-DEZ in emulsion system.
- Surface modification of polypropylene and polyethylene through graft polymerization initiated by Phen-DEZ in solvent system.
- Surface modification of cotton and silk through graft polymerization initiated by Phen-DEZ in emulsion system.

Author's Declaration

I hereby declare that the work in this dissertation was conducted under the Regulations of Kochi University of Technology, Kochi, Japan. This is my own original work and this thesis has not been presented and submitted in part or in whole to any university or institution for a degree.

Publications

Sections of this work described in this thesis have been reported in the following publications:

1. Zhao C, Sugimoto R, Naruoka Y. A simple method for synthesizing ultra-high-molecular-weight polystyrene through emulsion polymerization using alkyl-9-BBN as an initiator, Chin. J. Polym. Sci., 2018;36:592-597.
2. Zhao C, Okada H, Sugimoto R. Diethyl(1,10-phenanthroline-N^1,N^{10})zinc initiated grafting of styrene on polypropylene/ polyethylene. Bull. Chem. Soc. Jpn. 2018;91:1576-1578.
3. Zhao C, Okada H, Sugimoto R. Polymerization of styrene in aqueous system using a diethylzinc and 1,10-phenanthroline complex. Polymer. 2018;154:211-217.
4. Zhao C, Okada H, Sugimoto R. Surface modification of polypropylene with poly(methyl methacrylate) initiated by a diethylzinc and 1,10-phenanthroline complex. React. Funct. Polym. 2018;132:127-132.

Acknowledgements

Foremost, I would like to express my deep gratitude to my supervisor, Pro. Sugimoto. I thank him for the great trust in me, give me the opportunity to become his student, and complete my Ph.D. degree in Kochi University of Technology (KUT). During this 3 years, he has given me the meticulous consideration, education, and selfless help. No matter what difficulties I met in research, he always there, provide powerful help. He is knowledgeable, amiable, tolerant, and is the best professor I have ever seen in my life. Whether in research or life, he will be my role model that I will follow for life long.

I would like to express my sincere thanks to Prof. KOBIRO, Prof. NISHIWAKI, Prof. KAWAHARAMURA, Prof. ITO, and Prof. OHTANI, thank you for your valuable comments and help during my research.

I am also grateful to all the staffs of International Relation Division for all warm supports and suggestions since I came to Japan. I would like to express my deep thank to Kubo sensei for teaching me Japanese.

Thanks to my lab-mates in Sugimoto lab, An san, Oshima san, Takagi san, Naruka san, Ichigawa san, Morimoto san, Okada san, Matsui san, Komatsu san, Mana chan, etc… They taught me experiments, Japanese, and Japanese culture. We shared little secrets and good news with each other. Thanks to my friend Liuli, nice to meet you. Thank you, all my favorite friends.

Last but not the least, I would like to express my profound gratitude to my family for supporting me in my decisions and their unrequited love. Thanks to my husband for his tolerance and supportive for the past ten years.

Contents

Introduction

Since Frankland first synthesized alkylzinc compounds in 1849, remarkable advances have been made in the field study of organometallic compounds. However, since 1900, due owing to the advent discovery of the Grignard reagents, organozinc compounds have received much less attention and utilization use [1]. Compared to Grignard reagents, organozincs haves a higher functional group tolerance, and for some purposes, their less lower reactivity can be an advantage. Zinc metal has low toxicity, and zinc ions are normally present in biochemical pathways;, because of the biological importance of organozinc compounds, it has they have attracted more and more increasing attention [2]. In According to the papers that have been reportedliterature, organozincs is are widely used as selective alkylating agents in organic synthesis, such asfor example, alkylation of functionalized electrophiles as selective alkylating agents. Addition of oOrganozincs can also be used in the field of the addition to ketones, aldehydes, and imines, and in ring- opening polymerization, and so onhas also been reported [3,4].

With the development of initiators, much attention has been focused on the use of organozinc reagents. The choice of initiator determines the conditions required for a reaction, and widely used initiators such as peroxides and azo compounds often require relatively high reaction temperatures or harsh initiation conditions. However, increasing the reaction temperature increases the difficulty of the reaction and requires excessive energy; furthermore, high temperatures usually result in degradation of the substrate and reduce the molecular weight of the polymer. New free radical initiators are needed to simplify the reaction conditions. Organoborons first attracted attention for this purpose; in the presence of air, trialkylborane can be used for radical polymerization even at −78 °C [5]. Organozincs have properties similar to those of organoborons. Owing to the higher activity of organic zinc, the reaction conditions are difficult to control. In the past 70 years, research on the polymerization of organic zinc has almost ceased. By contrast, organoborons have received extensive attention. They were first used as an initiator for olefin polymerization in 1955 [6]. To date, organoborons have been widely used for radical polymerization. Their use has resulted in the development of many useful synthetic and novel applications. However, because the reaction mechanism is complex, the initiation mechanism of organoborons has not been clearly defined, and its initiation mechanism is still under debate. Although the mechanism is not yet fully understood, a plausible proposal is as follows (Equation 1).

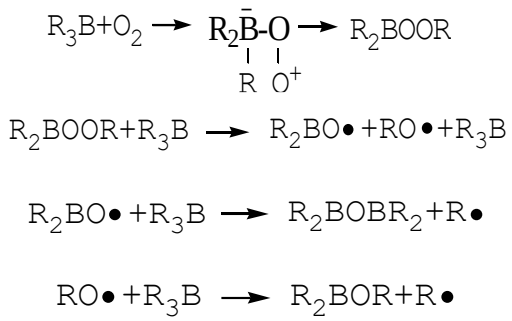

(1)

Organoborons react with oxygen via simultaneous or stepwise reactions to generate alkylperoxyborane. The resulting peroxide then causes hemolytic cleavage at the O–O bond, producing alkoxy radicals.

Alkyl-9-borabicyclo-[3.3.1]-nonanes (alkyl-9-BBNs) were recently applied as a new type of borane initiator. Since a report by Masuda in 1991, 9-borabicyclo-[3.3.1]-nonanes (9-BBNs) have been used as radical polymerization initiators [7]. In the presence of oxygen, alkyl-9-BBNs form complexes that rearrange to become alkylperoxyboron compounds (C–O–O–B), which are easily homolytically cleaved at ambient temperature to generate an alkoxy radical and a stable borane radical [8]. Chung et al. [9] successfully used 1-octyl-9-BBN to initiate the polymerization of methyl methacrylate (MMA), which exhibited the characteristics of living polymerization. Chung's group has also conducted considerable research on graft polymerization and block copolymerization using this stable borane radical as an initiator [10,11]. 9-BBNs are widely applied because they have only one B–H bond; thus, they meet the conditions for initiation of living radical polymerization. In 1996, Chung [12] reported that 9-BBNs are capable of initiating living polymerization. By using a 9-BBN initiator, a product with well-controlled molecular structure can be obtained at ambient temperature. However, alkylboranes are hydrolytically and oxidatively unstable; they decompose in water very rapidly to borate esters and boric acid. Therefore, the application of alkyl-9-BBN in aqueous systems has not been reported. In emulsion polymerization systems, radical polymerization occurs in oil-in-water micelles formed from monomers, water, and surfactants. Because of the unique segregation effect [13,14], high-molecular-weight polymers can be synthesized. Owing to the unique characteristics of emulsion polymerization, I wondered whether alkyl-9-BBN can be applied in emulsion polymerization systems. Therefore, a series of experiments was conducted using sodium dodecyl sulfate (SDS) as an emulsifier to investigate whether alkyl-9-BBN can be applied in an emulsion system and to examine the effects of different reaction conditions on the polymerization. The results show that a stable radical generated from the oxidation adduct of alkyl-9-BBN was able to initiate emulsion polymerization of styrene within a short time and produce polystyrene with a high yield and ultrahigh molecular weight.

Alkylzinc has properties similar to those of alkylborane. The initiation mechanism of diethylzinc (DEZ) has been discussed for decades, and many researchers have proposed possible reaction mechanisms. In contrast to the use of alkylboranes, the use of alkylzinc as an initiator in polymerization, in particular its initiation mechanism, has not been widely studied. Polymerization initiated by alkylzinc was initially considered to be typical cationic polymerization [15,16]. However, an increasing number of researchers have proved experimentally that initiation by DEZ should follow the mechanism of free radical initiation [17,18]. In 1864, Lissenko claimed that auto-oxidation of DEZ produced EtZnOEt [19]. However, most early researchers subsequently believed that auto-oxidation of DEZ yielded zinc dialkoxides. (Equation 2)

$$R_2Zn + O_2 \longrightarrow Zn(OR)_2 \quad (2)$$

One proposal attracted considerable attention, as it suggested that oxygen in the air is involved in the generation of free radicals. For the R2M/O2 system, it is usually assumed that the alkyl radicals R• are formed in the initial step (Equation 3) and initiate the subsequent polymerization.

$$R_2Zn + O_2 \longrightarrow RZnOO\cdot + R\cdot \quad (3)$$

However, this conclusion is inconsistent with recent studies. The latest experimental results show that R2Zn and O2 can react in a highly controlled manner without evidence of generation of free alkyl radicals [20–22]. Julien Maury and his team [23] recently confirmed that both alkyl and alkoxyl radicals were generated during autoxidation via EPR spectroscopy using spin-trapping techniques. However, the debate continues, and there is no clear answer to the question. The development of organoborons and organozincs has contributed greatly to radical polymerization.

Diethylzinc DEZ is well known for its air-sensitivity to air. Neat DEZ is a highly flammable liquid, and ignites spontaneously ignition in air. It is not possible to use wWater cannot be used as a solvent because it reacts violently with water. Therefore, it has hitherto been impossible to carry out perform radical polymerization using DEZ in aqueous mediaum. At the same timeFurther, both storage and use of DEZ require protection from must be stored and used under an inert gases and at an appropriate temperatures.

It is known that organic substrates having electron donor sites can form Lewis acid–-base adducts with alkyl zinc [24]. In recent years, many researchers have tried attempted to use different ligands to form complexes with DEZ [25–-27]. The electrochemical behavior of organozinc complexes with 1.10-phenanthroline, 2.2-bipyridine, 1.2-bipyridine, and di-2-

pyridylketone as ligands were was investigated [28]. By using ligands to form complex with organozinc, and the active organozinc can be stabilized to form complexes. The use of 1,10-phenanthroline as a ligand is of considerable interest because the skeleton structure is fixed and commercially available. The complex formed by DEZ and 1,10-phenanthroline has certain stability is stable to some extent in water and air, and it there is does not burning or smokeing phenomenon, so the diethylzinc-1,10-phenanthroline complex is it can be used for subsequent research.

Because of our ongoing interest in DEZ and the desire to expand its application, we have investigated various polymerization systems and polymerization methods, selected a variety of monomers and substrates, and varied the reaction conditions to study the properties and application conditions of DEZ. My experiments were designed to investigate whether polymerization could be conducted in emulsion systems and to examine possible grafting substrates. Here, a new efficient diethyl(1,10-phenanthroline N^1,N10)zinc (Phen-DEZ) initiator for radical homopolymerization and graft polymerization in different solvent and reaction systems was developed. The results showed that DEZ can initiate homopolymerization and graft polymerization at low reaction temperatures in bulk solvent and emulsion systems capable of initiating graft polymerization on polypropylene (PP), polyethylene (PE), cotton, and silk. I also designed experiments to study the initiation mechanism of DEZ by synthesizing low-molecular-weight PP and using nuclear magnetic resonance (NMR) and matrix-assisted laser desorption/ionization time-of-flight mass spectrometry (MALDI-TOF-MS) to detect free radicals generated in the reaction. The mild reaction conditions, high reactivity, fast reaction speed, wide application range, and good product yield suggest that DEZ shows promise for use as an initiator.

Styrene emulsion polymerization using alkyl-9-BBN synthesized by reacting 9-BBN and styrene in an aqueous SDS solution was studied. Ultrahigh-molecular-weight (>107) polystyrene was synthesized using a radical initiator formed by aerobic oxidation of the alkyl-9-BBN in high yield (>80%). The kinetics of this emulsion polymerization of styrene by alkyl-9-BBN were investigated. We confirmed that in the initial stage of polymerization, the initial reaction rate followed the first-order kinetics. The activation energy of this emulsion polymerization of styrene was approximately 56.2 kJ/mol.

Furthermore, the dissertation demonstrates the stabilization of DEZ by the formation of complexes with 1,10-phenanthroline and successful emulsion polymerization of styrene using Phen-DEZ. Ultrahigh-molecular-weight polymers (Mw > 107) were obtained in high yield (80%) using SDS as an emulsifier in this emulsion system at 23 °C. The kinetics of styrene emulsion polymerization initiated by Phen-DEZ was studied. In the early stage of

polymerization, an almost linear first-order kinetic plot was observed, and the overall activation energy of this polymerization system was 31.0 kJ/mol. MMA and styrene were grafted onto the surface of PP films and fibers by simple radical polymerization of Phen-DEZ using oxygen molecules as the radical initiator. The grafting yield could be changed by varying the reaction time, temperature, and amount of solvent. The resultant grafted PP films were characterized by Fourier transform infrared (FT-IR) spectroscopy, Raman spectroscopy, and X-ray diffraction (XRD) measurements, as well as thermogravimetric analysis (TGA). The surface morphology of the grafted PP films was analyzed using an atomic force microscope. Furthermore, the usually hydrophobic surface of the PP films became hydrophilic, as indicated by a change in the water contact angle (from 106.1° to 64.8°) after grafting with MMA. Scanning electron microscopy (SEM) images showed that graft polymerization did not change the original microstructure of the PP fibers. The results of these analyses proved that MMA could be grafted to PP films using the novel Phen-DEZ/O2 initiator.

Highly efficient and environmentally friendly graft polymerization of MMA onto cotton and silk was performed using an alkylzinc initiator in an emulsion system. Using this method, a high-molecular-weight (Mw > 106) polymer was grafted onto cotton fibers with a high graft yield at ambient temperature. The grafted cotton fibers were characterized by FT-IR spectroscopy, XRD analysis, and TGA. The surface morphologies of the unmodified and grafted cotton were analyzed by SEM. Furthermore, the grafted cotton produced by this novel surface modification method showed improved compatibility with a number of organic solvents. The dyeing performance of the modified silk was significantly increased.

References:

1. Seyferth, D. Zinc alkyls, Edward Frankland, and the beginnings of main-group organometallic chemistry. Organometallics. 2001, 20(14), 2940-2955.

2. Schwach, G.; Coudane, J.; Engel, R.; Vert, M. Ring opening polymerization of DL-lactide in the presence of zinc metal and zinc lactate. Polym. Int. 1998, 46(3), 177-182.

3. Botta, M. C.; Biava, H. D.; Spanevello, R. A.; Mata, E. G.; Suarez, A. G. Development of polymer-supported chiral aminoalcohols derived from biomass and their application to asymmetric alkylation. Tetrahedron Lett. 2016, 57(20), 2186-2189.

4. Anderson, J. C.; Harding, M. The importance of nitrogen substituents in chiral amino thiol ligands for the asymmetric addition of diethylzinc to aromatic aldehydes. Chem. Commun. (Cambridge). 1998, (3), 393-394.

5. Ollivier, C.; Renaud, P. Organoboranes as a Source of Radicals. Chem. Rev. (Washington, D. C.). 2001, 101(11), 3415-3434.

6. Furukawa, J.; Tsuruta, T.; Inoue, S. Triethylboron as an initiator for vinyl polymerization. J. Poly. Sci. 1957, 26, 234-6.

7. Masuda, Y.; Hoshi, M.; Nunokawa, Y.; Arase, A. A remarkably efficient initiation by 9-BBN in the radical addition reactions of alkanethiols to alk-1-enes. Journal of the Chemical Society, Chem. Communi. 1991, (20), 1444-5.

8. Chung, T. C.; Janvikul, W.; Lu, H. L. A Novel "Stable" Radical Initiator Based on the Oxidation Adducts of Alkyl-9-BBN. J. Am. Chem. Soc. 1996, 118(3), 705-6.

9. Chung, T. C.; Lu, H. L.; Janvikul, W. A novel synthesis of PP-b-PMMA copolymers via metallocene catalysis and borane chemistry. Polymer. 1997, 38(6), 1495-1502.

10. Chung, T. C.; Xu, G.; Lu, Yingying; Hu, Youliang. Metallocene-Mediated Olefin Polymerization with B-H Chain Transfer Agents: Synthesis of Chain-End Functionalized Polyolefins and Diblock Copolymers. Macromolecules. 2001, 34(23), 8040-8050.

11. Kitayama, Y.; Okubo, M. A synthetic route to ultra-high molecular weight polystyrene ($>10^6$) with narrow molecular weight distribution by emulsifier-free, emulsion organotellurium-mediated living radical polymerization (emulsion TERP). Polym. Chem. 2016, 7(14), 2573-2580.

12. Jang, Y.; Choi, D. S.; Kim, J. G. First Emulsion Polymerization of Styrene with Sodium Borohydride: Evidence of the Generation of Radical Intermediates by Sodium Borohydride in H2O. Langmuir. 2004, 20(16), 6570-6574.

13. Furukawa, J.; Tsuruta, T.; Inoue, S.; Kawasaki, A.; Kawabata, N. Calcium-zinc tetraethyl complex as an initiator for vinyl polymerization. J. Polym. Sci. 1959, 35, 268-71.

14. Inoue, S.; Tsuruta, T.; Furukawa, J. Catalytic reactivity of organometallic compounds for olefin polymerization. IV. Vinyl polymerization by organocalcium compounds. Angew.

Makromol. Chem. 1959, 32, 97-111.
15. Sakata, R.; Tsuruta, T.; Saigusa, T.; Furukawa, J. Polymerization of propylene oxide and vinyl compounds with diethylzinc in the presence of cocatalysts. Kogyo Kagaku Zasshi. 1960, 63, 1817-22.
16. Makimoto, T.; Tsuruta, T.; Furukawa, J. Vinyl polymerization with organometallic compound carbon disulfide systems. Angew. Makromol. Chem. 1962, 52, 239-41.
17. Folkertsma, E.; Benthem, S. H.; Jastrzebski, J. T. B. H.; Lutz, M.; Moret, M.; Klein G.; Robertus J. M. 1,2-Addition of Diethylzinc to a Bis(Imidazolyl)ketone Ligand. Eur. J. Inorg. Chem. 2018, 2018(10), 1167-1175.
18. Mukherjee, D.; Ellern, A.; Sadow, A. D. Remarkably Robust Monomeric Alkylperoxyzinc Compounds from Tris(oxazolinyl)boratozinc Alkyls and O_2. J. Am. Chem. Soc. 2012, 134(31), 13018-13026.
19. Kubisiak, M.; Zelga, K.; Justyniak, I.; Tratkiewicz, E.; Pietrzak, T.; Keeri, A. R.; Ochal, Z.; Hartenstein, L.; Roesky, P. W.; Lewinski, J. Catalytic Epoxidation of Enones Mediated by Zinc Alkylperoxide/tert-BuOOH Systems. Organometallics. 2013, 32(19), 5263-5265.
20. Hollingsworth, N.; Johnson, A. L.; Kingsley, A.; Kociok-Kohn, G.; Molloy, K. C. Structural study of the reaction of methylzinc amino alcoholates with oxygen. Organometallics. 2010, 29(15), 3318-3326.
21. Maury, J.; Feray, L.; Bazin, S.; Clement, J.; Marque, S. R. A.; Siri, D.; Bertrand, M. P. Spin-Trapping Evidence for the Formation of Alkyl, Alkoxyl, and Alkylperoxyl Radicals in the Reactions of Dialkylzincs with Oxygen. Chem. – Eur. J. 2011, 17(5), 1586-1595, S1586/1-S1586/38.
22. Lewinski, J.; Sliwinski, W.; Dranka, M.; Justyniak, I.; Lipkowski, J. Reactions of [ZnR2(L)] complexes with dioxygen: a new look at an old problem. Angew. Chem. Int. Edit. 2006, 45(29), 4826-4829.
23. Aleksanyan, D. V.; Kozlov, V. A.; Petrov, B. I.; Balashova, T. V.; Pushkarev, A. P.; Dmitrienko, A. O. Lithium, zinc and scandium complexes of phosphorylated salicylaldimines: synthesis, structure, thermochemical and photophysical properties, and application in OLEDs. RSC Adv. 2013, 3(46), 24484-24491.
24. Krahmer, J.; Beckhaus, R.; Saak, W.; Haase, D. Chelating complexes of diethylzinc and ZnCl2 with 2,2-bipyridine and 1,6,7,12,13,18-hexaazatrinaphthylene (HATN) as ligands. Z. Anorg. Allg. Chem. 2008, 634(10), 1696-1702.
25. Vaughan, B. A.; Arsenault, E. M.; Chan, S. M.; Waterman, R. Synthesis and characterization of zinc complexes and reactivity with primary phosphines. J. Organomet. Chem. 2012, 696(26), 4327-4331.

26. El-Shazly, M. F. Electrochemical reduction and electron spin resonance studies of organozinc complexes. Inorg. Chim. Acta. 1978, 26(2), 173-6.

Chapter 1:

Synthesizing Ultra-high-molecular-weight Polystyrene through Emulsion Polymerization Using Alkyl-9-BBN as an Initiator

1.1 Introduction

Organoboranes and their derivatives are becoming increasingly important as key reagents in radical chemistry [1]. One widely used organoborane is tributylborane (TBB), which has been used as a polymerization initiator. Welch [2] has reported the polymerization of vinyl monomers initiated by alkylboranes in the presence of oxygen or electron donors; polymerization proceeded via a free-radical mechanism.

Alkyl-9-borabicyclo-[3.3.1]-nonanes (BBNs) have been used as radical polymerization initiators since the report by Masuda et al. [3] in 1991. Chung et al. [4] successfully used 1-octyl-9-BBN to initiate the polymerization of methyl methacrylate, which exhibited characteristics of living polymerization. In the presence of oxygen, alkyl-9-BBNs will form complexes that rearrange to alkylperoxyboron compounds (C-O-O-B), which are easily homolytically cleaved at ambient temperature to generate an alkoxy radical and a stable borinate radical [4]. Chung's group has also conducted a lot of research on graft polymerization [5,6] and block copolymerization using this stable borinate radical as an initiator [7,8]. However, since these alkyl boron compounds are hydrolytically unstable, there are very few reports on polymerization in aqueous systems.

Recently, a number of publications have appeared that describe the syntheses of ultra-high-molecular-weight polymers through living radical polymerization processes, including atom transfer radical polymerization (ATRP) [9] (24 h, 50 °C, poly[2-dimethylamino]-ethyl methacrylate, Mw (weight average molecular weight) = ~1.1×10^6), reverse addition fragmentation chain transfer (RAFT) [10,11], and organotellurium-mediated living radical emulsion polymerization (emulsion TERP) [12] (24 h, 60 °C, polystyrene, Mn = ~1.2×10^6). Although living polymerization provides a means to synthesize ultra-high-molecular-weight polymers, it has a major drawback, which is that long reaction times are required.

High-speed processes for polymerization that are less energy intensive are thus highly desired for industry. Emulsion polymerization has a unique advantage in the production of

ultra-high-molecular-weight polymers [12,13] due to the segregation effect [14-16], and provides a facile route for the syntheses of high-molecular-weight polymers with high reaction rates.

Emulsion polymerization of vinyl monomers in aqueous media has been carried out using various initiator systems [17-19]; however, the use of a conventional thermal initiator, e.g., persulfate, has been reported for most polymerizations. No information appears to be available for emulsion polymerization induced by alkyl-9-BBNs. This is because trialkylboranes are hydrolytically and oxidatively unstable, decomposing in water very rapidly to trialkylboroxines, borate esters, and boric acid.

The oxidized adduct that forms upon mixing an alkyl-9-BBN with oxygen homolytically decomposes to produce alkoxy radicals and stable borate radicals. Using this stable borate radical to initiate polymerization is advantageous in terms of energy conservation owing to its rapid decomposition at lower temperatures. Hence, the polymerization can be conducted at a lower reaction temperature than those used when conventional thermal initiators are employed, which are usually in the 70–90 °C range.

Recently, we attempted the emulsion polymerization of styrene using an alkyl-9-BBN in an aqueous sodium dodecyl sulfate (SDS) solution. A stable borinate radical generated from the oxidation adduct of the alkyl-9-BBN was found to be able to initiate the emulsion polymerization of styrene within a short time and produce polystyrene with a high yield and ultra-high molecular weight. We also report the kinetics of this emulsion polymerization of styrene initiated by an alkyl-9-BBN in this paper.

1.2 Experimental

1.2.1 Materials

9-BBN (0.5 M in tetrahydrofuran) was purchased from Sigma-Aldrich. Styrene was purchased from Wako Pure Chemical Industry, Ltd., and purified by washing with a 10% aqueous solution of sodium hydroxide and treated with anhydrous sodium sulfate. SDS, tetrahydrofuran, NaOH, and $MgSO_4$ were purchased from Wako Pure Chemical Industry, Ltd. and were used as received. All aqueous solutions were prepared with deionized (DI) water that was generated using a Millipore MilliQ Academic Water Purification System and deoxygenated by sparging with argon for 30 min.

1.2.2 Characterization and measurements

Size-exclusion chromatography (SEC) was carried out using a system equipped with a Jasco PU-2080 Plus pump and a Jasco RI-2031 Plus Intelligent RI detector. The molecular weights and molecular weight distributions (PDI) of the polymers relative to a polystyrene standard were determined using Chrom NAV software. Chloroform served as the polymer solvent and eluent in an equilibrated system at 40 °C. A Malvern Zetasizer Nano series instrument was used to measure the diameters of the polymer particles, and average particle diameter distributions were determined in cumulant mode using Zetasizer v7.11 software.

1.2.3 Polymerization procedure

All experiments were conducted under an argon atmosphere. The emulsion polymerizations were carried out in 50 mL double-neck round bottom flasks connected with an argon gas inlet and with a magnetic stirrer. SDS was first dissolved in degassed water, and then styrene monomer was added to the solution while it was stirred at 400 rpm. The initiator was prepared by mixing 9-BBN and styrene (molar ratio = 1:1) in another 50 mL flask and stirring at 23 °C for 1 h just before use. The two solutions were combined, and the resulting solution was stirred at 400 rpm for 48 h under an argon atmosphere.

A fixed amount of latex was removed from the reaction mixture at regular time intervals and the size of the polymer particles was measured. Then, the polystyrene was precipitated in methanol and collected, and the conversion, molecular weight, and molecular weight distribution of the polymer were determined. Polymerization was repeated three times for each set of reaction conditions.

1.3 Results and discussion

1.3.1 Effect of amount of emulsifier on reaction

The effect of SDS surfactant concentration on polymerization yield in the emulsion polymerization of styrene was investigated.

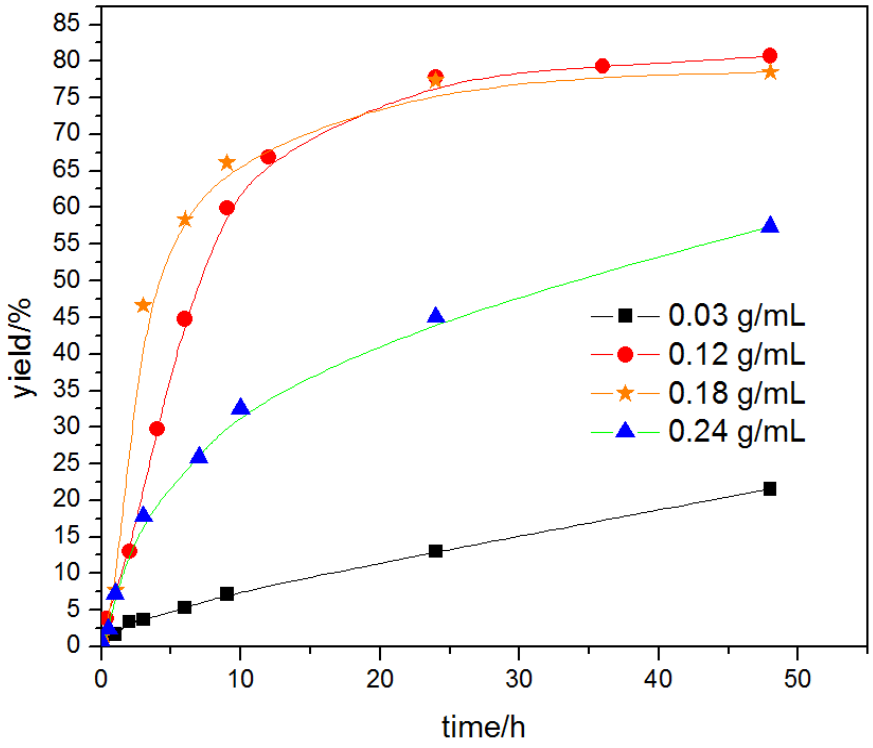

Figure 1. Effect of SDS surfactant concentration on polymerization yield in emulsion polymerizations of styrene (SDS g/ monomer mL)

The emulsion polymerization reactions were carried out at 23 °C with a constant styrene/alkyl-9-BBN ratio of 1000:1. Figure 1 shows the plots of polymerization time versus yield with different amounts of SDS. The yield increased monotonically with the polymerization time in the initial stage of the reaction. When the SDS concentration was 0.12g/mL and 0.18g/mL, yield reached a certain value after approximately 24 h. However, yield of the other two groups kept increasing as the reaction time increased.

The yield after polymerization for 48 h with an SDS concentration of 0.03 g/mL was 22%. In addition, the yield after polymerization for 48 h increased from 22% to 81% when the SDS concentration was increased by four times from 0.03 to 0.12 g/mL. When the amount of emulsifier increases within a specific range, the micelle becomes more stable and the number of micelle increases. As a result, the initiator content in each micelle decreases. While the rate of chain initiation and propagation is not affected, so the reaction time of each macromolecule becomes shorter. Similar results could be obtained when the SDS amount was 0.18 g/mL. However, when the SDS concentration was further increased to 0.24 g/mL, the yield decreased to 57%.

Figure 2 shows the plots of polymerization time versus molecular weight (Mw) with different amounts of SDS under similar conditions. Very-high-molecular-weight polystyrene (Mw > 5×10^6) was obtained with all SDS concentrations. In particular, ultra-high-molecular-weight (Mw = 1.2×10^7) polystyrene was obtained with a high yield of 81% when 0.12 g/mL of SDS was used. It is known that as the surfactant concentration increases and the initiator concentration decreases, the molecular weight increases with conventional surfactants. So the molecular weight obtained by using 0.12 g/mL and 0.18 g/mL SDS were higher than that of using 0.03 g/mL SDS. Under the protection of enough emulsifier, the initiator can keep long reaction time and free monomer can enter the emulsion particle to participate in the reaction. However, when the amount of SDS was doubled to 0.24 g/mL, the molecular weight of polystyrene decreased slightly to 9.3×10^6. By analyzing the particle size data, an increased in particle size cause the micelle to become unstable and inhibited monomer transport into micelles. Therefore, the yield of polymer prepared with 0.24 g/mL SDS was decreases and increased slowly than the polymer synthesized with 0.12 g/mL SDS.

Figure 3 shows the plots of particle size versus polymerization time with different amounts of SDS under similar conditions. With an SDS concentration of 0.03 g/mL, the particle size increased from 110 to 220 nm as the polymerization progressed. On the other hand, when the amount of SDS was very high (0.24 g/mL), the particle size increased continuously from 190 to 320 nm as polymerization proceeded. However, when the amount of SDS was 0.12 g/mL and 0.18 g/mL, the particle size was quite stable throughout the polymerization. The particle size data of SDS concentration of 0.18 g/mL were slightly larger than that of 0.12 g/mL group. There are two possible reasons for the phenomenon of increased particle size at SDS concentrations above 0.12g/mL. The first reason is that the excess emulsifier in water phase leads to fusion of several particles or deformation of micelle particles. Another reason is that the water content of the surrounding hydration layer increases because of many emulsifiers located at the oil-water interface. As the result, transport of monomer into micelles was hindered and the yield using 0.24 g/mL SDS decreased to 57%. That is, when the amount of SDS is too small or too large, particle formation becomes unstable, and it was found that there exists an optimum amount of SDS for the stabilization of the particle diameter. Since the appropriate SDS concentration for polymerization was 0.12 g/mL based on these results, it was used in subsequent experiments.

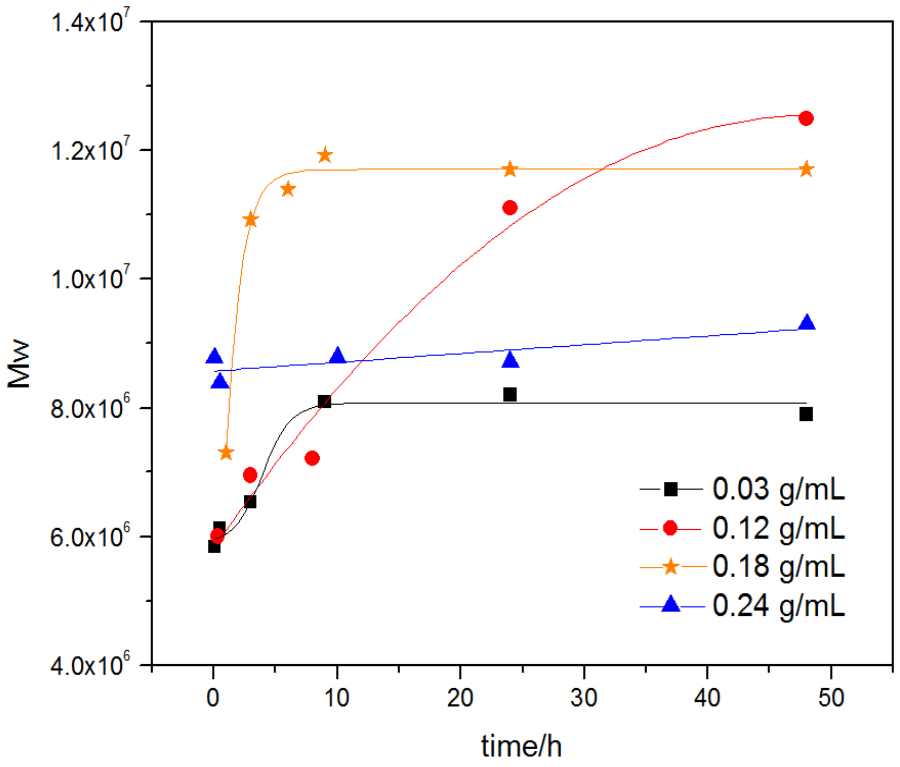

Figure 2. Time dependence of molecular weight in the emulsion polymerization of styrene with 9-BBN using different amounts of SDS (Mw: weight average molecular weight)

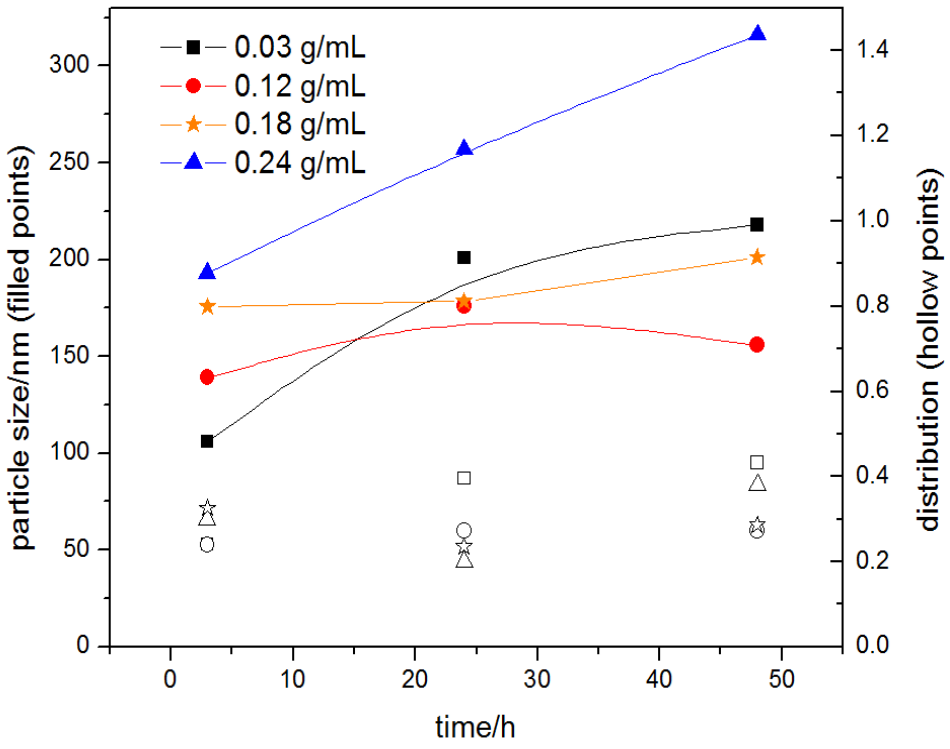

Figure 3. Particle size (nm) and distribution of polystyrene particles prepared via emulsion polymerization

1.3.2 Influence of the ratio between initiator and monomer

Figure 4 shows the effect of the monomer/initiator molar ratio on the polymerization. In the early stages of the polymerization of styrene using an alkyl-9-BBN as the initiator, the reaction rates were slower when higher amounts of initiator were used. However, in polymerization using conventional radical initiators, it is known that the reaction rate becomes higher as the amount of initiator increases because more radicals are generated [20]. In the polymerization of styrene using this alkyl-9-BBN, radicals are generated through the decomposition of the oxidized adduct formed via the reaction between the alkyl-9-BBN and oxygen. Therefore, the presence of an excess amount of the alkyl-9-BBN leads to the formation of more radical species, increasing the probability of the coupling of the generated radicals. As a result, the coupling of excess radicals occurs preferentially, decreasing the amount of effective active species and, consequently, the polymerization rate. At the same time, the lifetime of free radicals were shortened and the molecular weight decreased. When the polymerization time exceeded 20 h, the relationship between the yield and the amount of initiator was the opposite of that in the initial stage of polymerization. Since the alkyl borane compound reacts with water easily, when the polymerization time exceeds 20 h, the apparent reaction rate is considered to become slow because the amount of radicals generated in proportion to the amount of the alkyl-9-BBN decreases.

Figure 5 shows the Mw of polystyrene prepared using different monomer/initiator molar ratios. The molecular weight of polystyrene changed markedly as a result of changing the monomer-to-initiator molar ratio; the molecular weight of polystyrene can be increased significantly by decreasing the monomer-to-initiator molar ratio. Because of the segregation effect, when the initiator concentration decreases, the radical termination rate decreases, which increases the lifetime of the radical species; as a result, the Mw of polystyrene will increase [12, 14, 15]. When the monomer-to-initiator molar ratio was 6000:60 or 6000:20, the Mw of polystyrene was between 1×10^6 and 3×10^6 regardless of the polymerization time. These molecular weights are relatively high, but one order of magnitude lower than those of polystyrene obtained with the other two ratios. When an excess amount of the alkyl-9-BBN is used, the yield of polystyrene increases, but the chain termination reaction between the radical and the growing polymer chain occurs more frequently, so the molecular weight decreases [13]. Another possible reason that excess alkyl-9-BBN may reduce the Mw of the polymer is that it acts as a chain transfer agent. When the monomer-to-initiator molar ratio was 6000:3, the Mw exceeded 1×10^7 within 10 h, and radical termination such as through chain termination reactions hardly occurred,

so ultra-high-molecular-weight polystyrene was obtained. When the monomer-to-initiator molar ratio was 6000:6, the increase in the molecular weight was slower, and ultra-high-molecular-weight polystyrene with a Mw exceeding 1×10^7 was obtained after 24 h. When the monomer-to-initiator molar ratio was 6000:20 or lower, the Mw of polystyrene was constant irrespective of the polymerization time. However, when the molar ratio was 6000:6 or higher, the molecular weight was 6–7 times higher after 48 h, and ultra-high-molecular-weight polystyrene with a Mw exceeding 1.2×10^7 was obtained. In all cases, the polystyrene emulsion particles were stable and did not coagulate.

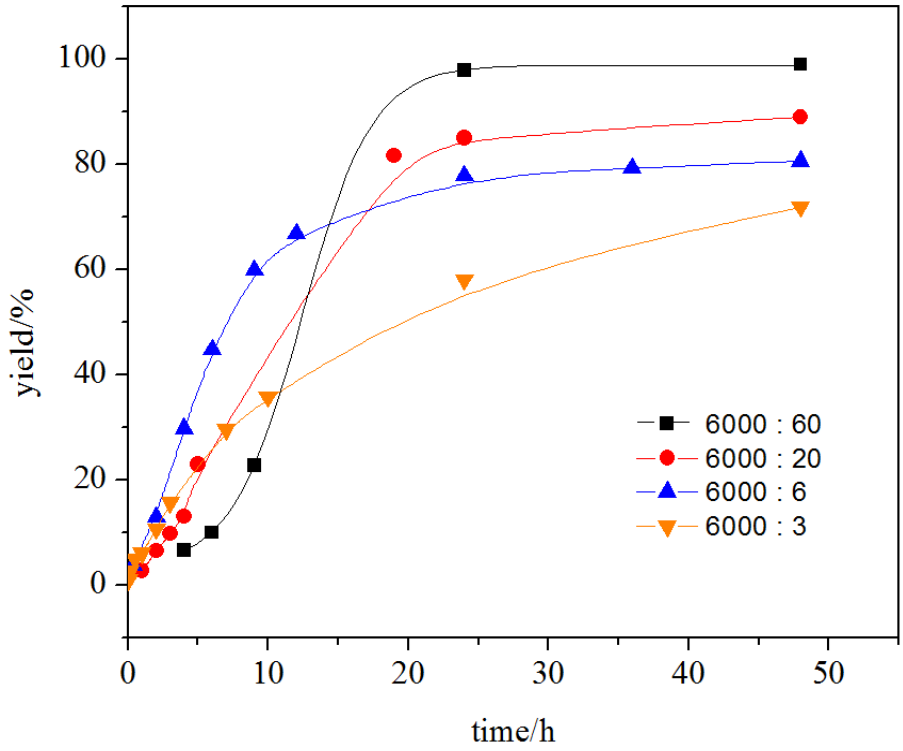

Figure 4. Plots of yield versus time for the emulsion polymerization of styrene with 9-BBN using different monomer-to-initiator ratios of 6000:60 (■), 6000:20 (●), 6000:6 (▲), and 6000:3 (▼)

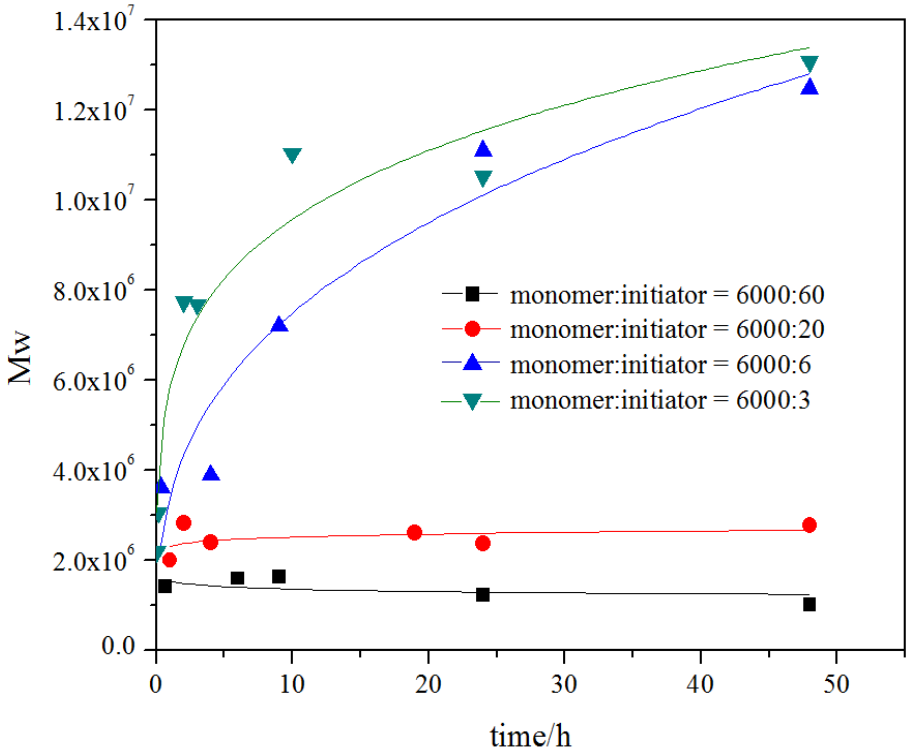

Figure 5. Plots of polymerization time versus Mw for the emulsion polymerization of styrene with 9-BBN using different monomer-to-initiator ratios.

1.3.3 Kinetic studies

In order to gain a better understanding of the characteristics of styrene polymerization initiated by 9-BBN, a kinetic study was performed at four different polymerization temperatures: 23, 40, 60, and 80 °C. The effects of variations in the reaction temperature on the yield and Mw of polystyrene were investigated.

Table 1 summarizes the results of the emulsion polymerization of styrene for 48 h at different reaction temperatures. The Mw was higher than 1×10^7 when the polymerization temperature was 40 °C or lower, but decreased when the reaction temperature was increased to higher than 60 °C, which may be because of the promotion of the generation of free radicals at higher temperatures. As has already been discussed, increasing the concentration of radicals will lead to lower molecular weights.

Table 1. Results of emulsion polymerization of styrene at different temperatures

Temperature (°C)	Yield (%)	Mw ($\times 10^6$)	PDI
23	81	12	2.45
40	92	10	2.69
60	89	6.6	2.54
80	96	3.3	1.93

The profile of the emulsion polymerization of styrene was obtained by monitoring the progress of the reaction. The polymerization rate (Rp) was calculated using the following equation: $Rp = (dC/dt) \times [M_0]$.

As can be seen from Figure 6, it is clear that the Rp increased and reached a maximum in a very short time. Thereafter, the reaction rate decreased sharply, and the polymerization was complete within 30 min, giving a 96% yield at 80 °C. This indicates that there was no induction period before polymerization started. Higher monomer conversions could be achieved at higher temperatures perhaps because of the lower solution viscosity at higher temperatures, which facilitates monomer consumption [9]. Even with a polymerization temperature of 60 °C, the Rp increased rapidly to the maximum in the same way and was followed by rapid retardation, and the polymerization was complete in 6 h. When the reaction temperature was decreased to 40 and 23 °C, the Rp decreased further, and the time required for the reaction to reach completion increased. The results showed that a long polymerization time is required, since the polymerization activity is relatively low under mild reaction conditions.

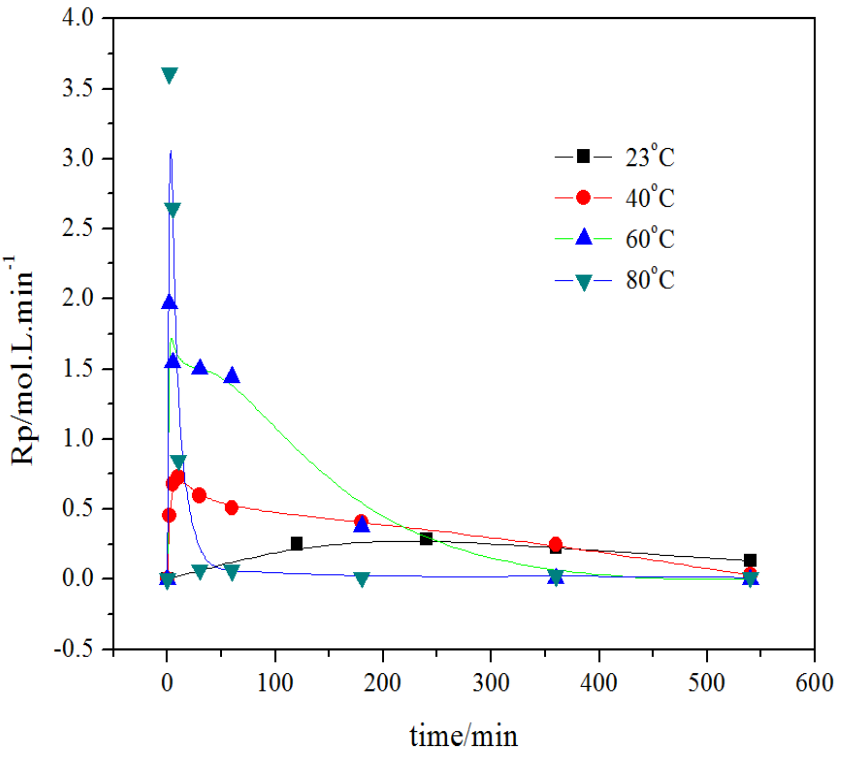

Figure 6. Time dependence of Rp

The study of the dynamics was conducted at the early stages of the polymerization of styrene using the alkyl-9-BBN. The plots of polymerization time versus −ln (1 − X), where X is the fraction conversion, showed linear relationships, as shown in Figure 7. For this polymerization of styrene using an alkyl-9-BBN, we confirmed that the initial reaction rate followed first-order kinetics in the initial stage.

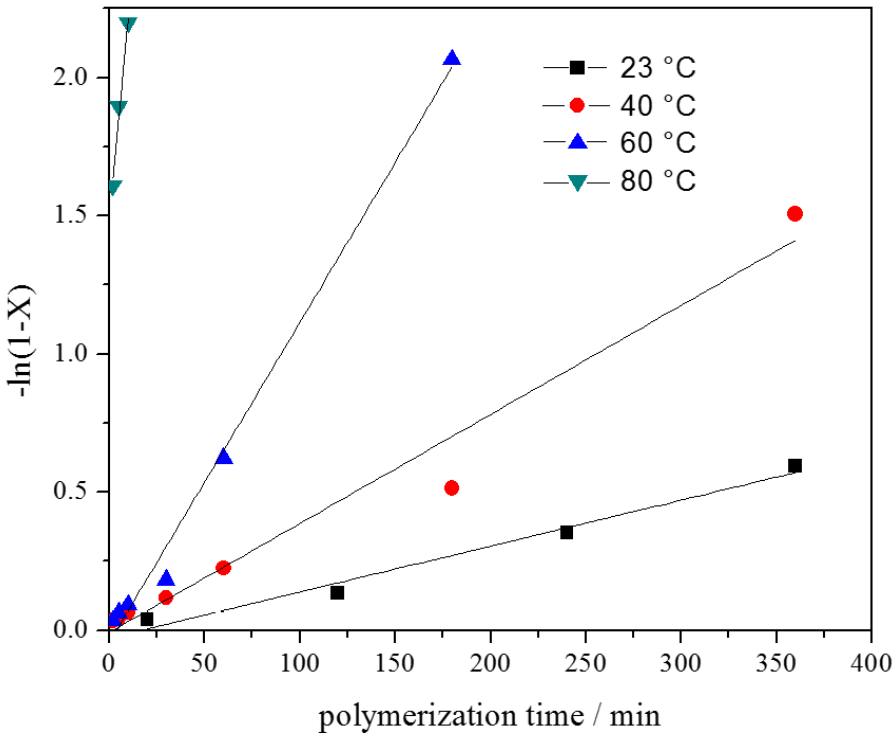

Figure 7. Polymerization time versus −ln (1 − X) for the emulsion polymerization at 23 (■), 40 (●), 60 (▲), and 80 °C (▼)

Then, the polymerization rate constants at different temperatures were determined from the slopes of these lines. The Arrhenius equation is used to calculate the overall activation energy and is as follows:

$$\ln k = -\frac{Ea}{RT} + \ln A$$

The Arrhenius plot of ln k versus 1/T showed a good linear relationship and the activation energy for the emulsion polymerization of styrene was estimated to be approximately 56.2 kJ/mol (Figure 8).

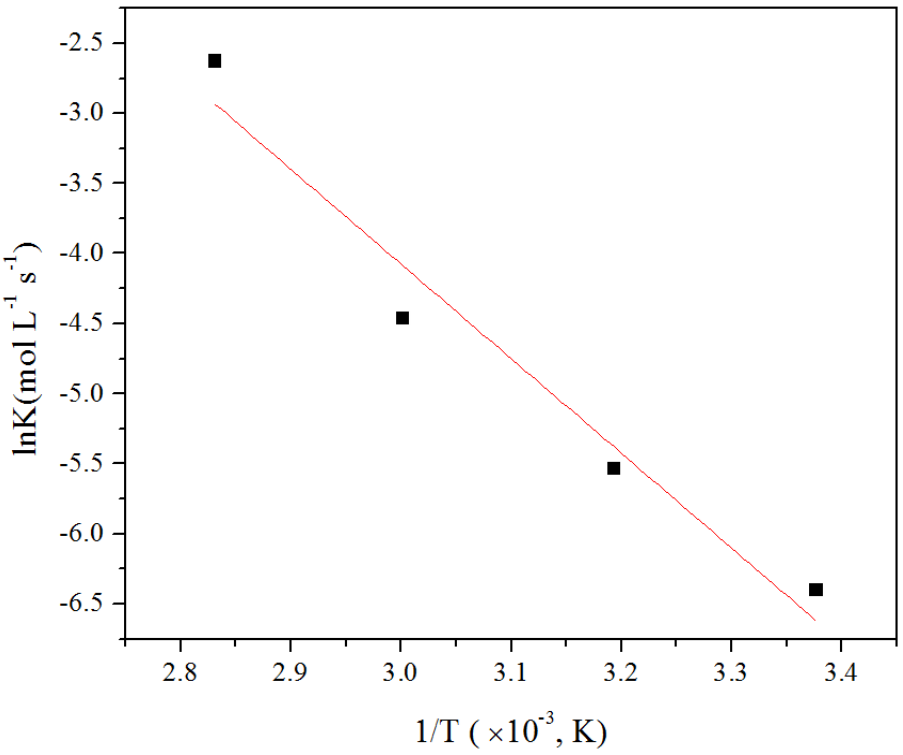

Figure 8. Arrhenius plot for the emulsion polymerization of styrene with an alkyl-9-BBN at 23–80 °C

1.4 Conclusion

We have demonstrated that a hydrolytically unstable alkyl-9-BBN can be used as an emulsion polymerization initiator for the efficient polymerization of styrene at room temperature. Furthermore, we have developed a new and convenient method to synthesize ultra-high-molecular-weight (>10 000 000) polystyrene at room temperature and low pressure and with a short reaction time via emulsion polymerization using an alkyl-9-BBN as an initiator in an aqueous SDS solution. The optimum amount of SDS was 0.12 g/mL, and if the amount of SDS is too large or too small, particle formation becomes unstable. The activation energy for this emulsion polymerization of styrene was estimated to be approximately 56.2 kJ/mol based on a kinetic study. This novel polymerization process is not limited to the preparation of polystyrene but can be extended to the polymerizations of many other vinyl monomers, such as methyl methacrylate. This research is currently underway and the results will be reported in the near future.

1.5 References

1. Philippe, R.; Beauseigneur, A.; Brecht-Forster, A.; Becattini, B.; Darmency, V.; Kandhasamy, S.; Montermini, F.; Ollivier, C.; Panchaud, P.; Pozzi, D.; Scanlan, E. M.; Schaffner, A.; Weber, V. Boron: a key element in radical reactions. Pure and Appl. Chem. 2007, 79(2), 223-233.

2. Welch, F. J. Polymerization of methyl methacrylate by triethylboron-oxygen mixtures. J. Polym. Sci. 1962, 61, 243-251.

3. Yuzuru, M.; Masayuki, H.; Yutaka, N.; Akira, A. A remarkably efficient initiation by 9-BBN in the radical addition reactions of alkanethiols to alk-1-enes. J. Chem. Soc., Chem. Commun. 1991, (20), 1444-1445.

4. Chung, T. C.; Janvikul, W.; Lu, H. L. A Novel "Stable" Radical Initiator Based on the Oxidation Adducts of Alkyl-9-BBN. J.Am.Chem. Soc. 1996, 118(3), 705-706.

5. Chung, T. C.; Rhubright, D.; Jiang, G. J. Synthesis of polypropylene-graft-poly(methyl methacrylate) copolymers by the borane approach. Macromolecules. 1993, 26(14), 3467-3471.

6. Dong, J. Y.; Manias, E.; Chung, T. C. Functionalized Syndiotactic Polystyrene Polymers Prepared by the Combination of Metallocene Catalyst and Borane Comonomer. Macromolecules. 2002, 35(9), 3439-3447.

7. Chung, T. C.; Lu, H. L.; Janvikul, W. A novel synthesis of PP-b-PMMA copolymers via metallocene catalysis and borane chemistry. Polymer. 1997, 38(6), 1495-1502.

8. Chung, T. C.; Xu, G. Metallocene-Mediated Olefin Polymerization with B-H Chain Transfer Agents: Synthesis of Chain-End Functionalized Polyolefins and Diblock Copolymers. Macromolecules. 2001, 34(23), 8040-8050.

9. Mao, B. W.; Gan, L. H.; Gan, Y. Y. Ultra high molar mass poly[2-(dimethylamino)ethyl methacrylate] via atom transfer radical polymerization. Polymer. 2006, 47(9), 3017-3020.

10. Truong, N. P.; Dussert, M. V.; Whittaker, M. R.; Quinn, J. F.; Davis, T. P. Rapid synthesis of ultrahigh molecular weight and low polydispersity polystyrene diblock copolymers by RAFT-mediated emulsion polymerization. Polym. Chem. 2015, 6(20), 3865-3874.

11. Read, E.; Guinaudeau, A.; Wilson, D. J.; Cadix, A.; Violleau, F.; Destarac, M.; Polym. Chem. Low temperature RAFT/MADIX gel polymerization: access to controlled ultra-high molar mass polyacrylamides. Polym. Chem. 2014, 5(7), 2202-2207.

12. Kitayama, Y.; Okubo, M. A synthetic route to ultra-high molecular weight polystyrene ($>10^6$) with narrow molecular weight distribution by emulsifier-free, emulsion organotellurium-mediated living radical polymerization (emulsion TERP). Polym. Chem. 2016, 7(14), 2573-2580.

13. Jang, Y. C.; Choi, D. S.; Kim, J. G. First Emulsion Polymerization of Styrene with Sodium

Borohydride: Evidence of the Generation of Radical Intermediates by Sodium Borohydride in H_2O. Langmuir. 2004, 20(16), 6570-6574.
14. Zetterlund, P. B. Controlled/living radical polymerization in nanoreactors: compartmentalization effects. Polym. Chem. 2011, 2(3), 534-549.
15. Zetterlund, P. B.; Okubo, M. Compartmentalization in Nitroxide-Mediated Radical Polymerization in Dispersed Systems. Macromolecules. 2006, 39(26), 8959-8967.
16. Andrea, R. S; Michael, K. G. Chinese J. Aqueous stable free radical polymerization processes. Polym. Sci. 2004, 22(4), 309-312.
17. Jiang, Q. M.; Huang, W. Y.; Yang, H. J.; Xue, X. Q.; Jiang, B. B.; Zhang, D. L.; Fang, J. B.; Chen, J. H.; Yang, Y.; Zhai, G. Q.; Kong, L. Z.; Guo, J. Radical emulsion polymerization with chain transfer monomer: an approach to branched vinyl polymers with high molecular weight and relatively narrow polydispersity. Polym. Chem. 2014, 5(6), 1863-1873.
18. Gao, J.; Jang, F. C.; Zhai, G. G. Ultra-high molecular weight alpha-amino poly(methyl methacrylate) with high Tg through emulsion polymerization by using transition metal cation-tertiary amine pairs as a mono-centered initiator. Macromol. React. Eng. 2016, 10(3), 269-279.
19. Fan, X.; Jia, X.; Liu, Y.; Zhang, H.; Zhang, B.; Zhang, H.; Zhang, Q. Morphology evolution of poly(glycidyl methacrylate) colloids in the 1,1-diphenylethene controlled soap-free emulsion polymerization. Eur. Polym. J. 2017, 92, 220-232.
20. Zhan, M. G.; Li, S. Y.; Zhong, Y.; Shen, C. H.; Gao, S. J. Preparation and characterization of a foam regulator with ultra-high molecular weight. J. Appl. Polym. Sci. 2017, 134(7).

Chapter 2:

Polymerization of styrene in aqueous system using a diethylzinc and 1,10-Phenanthroline complex

2.1 Introduction

Organometallic compounds are widely used in organic synthesis [1,2], materials science [3,4], and so on [5,6]. Since Frankland synthesized alkylzinc compounds in 1849, these compounds have been extensively studied for various applications [7-9]. In particular, diethyl zinc is a very useful organometallic reagent for organic synthesis, and has been used for addition to carbonyl compounds [10,11], addition to double or triple bonds [12,13], cyclopropanation [15,16], and other miscellaneous reactions [16]. Diethylzinc (DEZ) is a known initiator of radical polymerization in nonpolar solvents such as toluene and hexane. As an oxygen sensitive material, dialkylzinc will form a complex with oxygen, followed by a rearrangement of the complex to an alkylperoxyzinc compound (C-O-O-Zn) that easily undergoes homolytic cleavage to generate an alkoxy radical at ambient temperature.

To achieve greater "green-ness" of the chemical process, it is necessary to develop reactions that further increase the reaction rate to minimize the amount of energy used and achieve polymerization at a temperature close to room temperature. The use of water as a safe and environmentally friendly solvent is also desirable. If water can be used instead of organic solvents for polymerization of vinyl monomers using DEZ, such reactions would be environmentally and economically advantageous [17,18]. However, because DEZ is an unstable compound that is spontaneously flammable in air and easily hydrolyzed in water [19], DEZ immediately reacts with protic polar solvents such as alcohol or water. Therefore, it has hitherto been impossible to carry out radical polymerization using DEZ in aqueous medium.

We recently attempted the emulsion polymerization of styrene with alkyl-9-borabicyclo[3.3.1]nonane (alkyl-9-BBN) in an aqueous solution of SDS. It was found that a stable borinate radical, which was generated from the oxidation adduct of alkyl-9-BBN, was able to initiate the polymerization of styrene by emulsion polymerization within a short reaction time at ambient temperature. Polystyrene with a high molecular weight were obtained in high yield by this method [20]. If the stability of alkyl zinc is similar to that of alkyl-9-BBN, it may be possible to achieve emulsion polymerization with the former in the same way as with the latter.

It is known that organic substrates having electron donor sites can form Lewis acid-base adducts with alkyl zinc [21]. In recent years, many researchers have tried to use different

ligands to form complexes with DEZ [6,22-23]. The photo-absorption behavior of 1,10-phenanthroline organozinc complex was confirmed in 1964 [24]. In 1977, the electrochemical behavior of organozinc complex with 1,10-phenanthroline was investigated by Electron Spin Resonance (ESR) analysis [25]. The use of 1,10-phenanthroline as a ligand is of considerable interest because the skeleton structure is fixed and commercially available. It is rigid and has a planar structure containing two cis-oriented nitrogen atoms, which allows strong affinity with zinc metal and does not easily deform during coordination [26]. Therefore, the stability of DEZ can be expected to increase by forming a Lewis acid-base adduct using 1,10-phenanthroline as a N-donor ligand; thus, the DEZ complex should not be as sensitive as DEZ. We therefore proposed that radical polymerization of the vinyl monomer can be carried out in aqueous solvent by using a stabilized diethylzinc-1,10-phenanthroline complex.

Herein, we report the emulsion polymerization of styrene with a diethylzinc-1,10-phenanthroline complex (Phen-DEZ) in aqueous sodium dodecyl sulfate (SDS) solution. Several parameters were identified as important for controlling the molecular weight and yield; namely, the reaction temperature, the amount of emulsifier, and the initiator-to-monomer ratio. These parameters and their influences are discussed in this study. Ultra-high-molecular-weight polystyrene ($Mw > 1 \times 10^7$) were obtained in high yield (80%) in this emulsion polymerization system. Emulsion polymerization of styrene initiated by Phen-DEZ has not been previously reported; therefore, we also perform a kinetics study of the emulsion polymerization of styrene initiated by Phen-DEZ.

2.2 Experimental

2.2.1 Materials

Diethylzinc was purchased from Nippon Aluminum Alkyls, Ltd. Tetrahydrofuran (THF), toluene, 1,10- phenanthroline, SDS, NaOH, $MgSO_4$, and hexane were supplied by Wako Pure Chemical Industry, Ltd. and used without further purification. Styrene, obtained from Wako Pure Chemical Industry, Ltd., was purified by washing with aqueous sodium hydroxide and then dried over anhydrous magnesium sulfate. A Millipore MilliQ Academic Water Purification System was used to prepare the deionized water with which all aqueous solutions were prepared.

2.2.2 Methods

(1). Synthesis of Diethylzinc Complexe with 1,10-Phenanthroline

1,10-Phenanthroline (540 mg) was slowly added to a solution of DEZ (0.3 mL) in hexane (10 mL). After stirring at 23°C for 24 h, the reddish-orange solid product was collected by filtration and dried overnight in vacuo. The stoichiometric ratio between 1,10-phenanthroline and DEZ was 1: 1, and this value is the same as in the literature [24].

(2). Polymerization Procedure

The procedure for emulsion polymerization is similar that used in our previous research [20]. In a typical experiment, 0.54g SDS was dissolved in 22.5mL deionized water (excessive oxygen was removed by 30 min argon bubbling) firstly. The prepared SDS solution was continuously stirred at 400 rpm. The styrene monomer (2.5mL) and Phen-DEZ (32mg) were sequentially added to the solution. The resulting solution was reacted for 24 h under inert gas at 23°C. A fixed amount of latex was taken from the reaction mixture and injected into excess methanol at regular time intervals. The precipitated polystyrene was collected, molecular weight and conversion of the polymer were measured. Synthesis and physical properties of the low molecular weight PS sample used for 1 H NMR measurement are described in support information. The polymerization reaction, under each set of conditions, was performed in triplicate. The equation used to calculate the reaction conversion is as follows:

$$\text{conversion (\%)} = m(\text{polymer})/m(\text{monomer}) \times 100\% \quad (1)$$

2.2.3 Sample Characterization

Size-exclusion chromatography (SEC) was performed using a system equipped with a Jasco UV-2075 Plus Intelligent UV-VIS detector and Jasco PU-2080 Plus pump. The SEC column used in the experiment is a TSKguardcolumn HHR(20) (7.5 mm I.D.×7.5 cm), followed by two TSKgel GMHHR-H(20) (7.8 mm I.D.×30 cm). The standard polystyrene with a molecular weight of 2.06×10^7, 9.84×10^6 and 4.48×10^6 were purchased from TOSOH Corporation and that with a molecular weight from 1.27×10^3 to 2.7×10^6 were purchased from SHOWA DENKO K.K. Polymer solutions at approx. 2 mg mL^{-1} were prepared and filtered through 0.45 μm filters prior to injection, and an eluent was THF at 40 °C at a flow rate of 1.0 mL min^{-1}.All SEC diagrams show the ultraviolet detector signal (Jasco UV-2075 Plus Intelligent UV detector). The number average molecular weight (Mn), weight average molecular weight (Mw) and molecular weight distributions (PDI) of the polymers were derived from a calibration curve based on a polystyrene standard using Chrom NAV software. The eluent was THF and the detector temperature was 40°C. Proton (^1H) nuclear magnetic resonance spectra (400 MHz) were collected on a Bruker Acsend 400 spectrometer.

2.3 Results and Discussion

2.3.1 Effect of Amount of Emulsifier on polymerization

The effect of the concentration of the SDS surfactant on the polymerization conversion in the emulsion polymerization of styrene was investigated (Figure 1). Emulsion polymerization was carried out using a constant monomer/initiator ratio of 1000:1, and the reaction

temperature was kept at 23°C. The polymerization conversions were compared by varying the surfactant concentration in the range of 1%-16% (SDS g/monomer g).

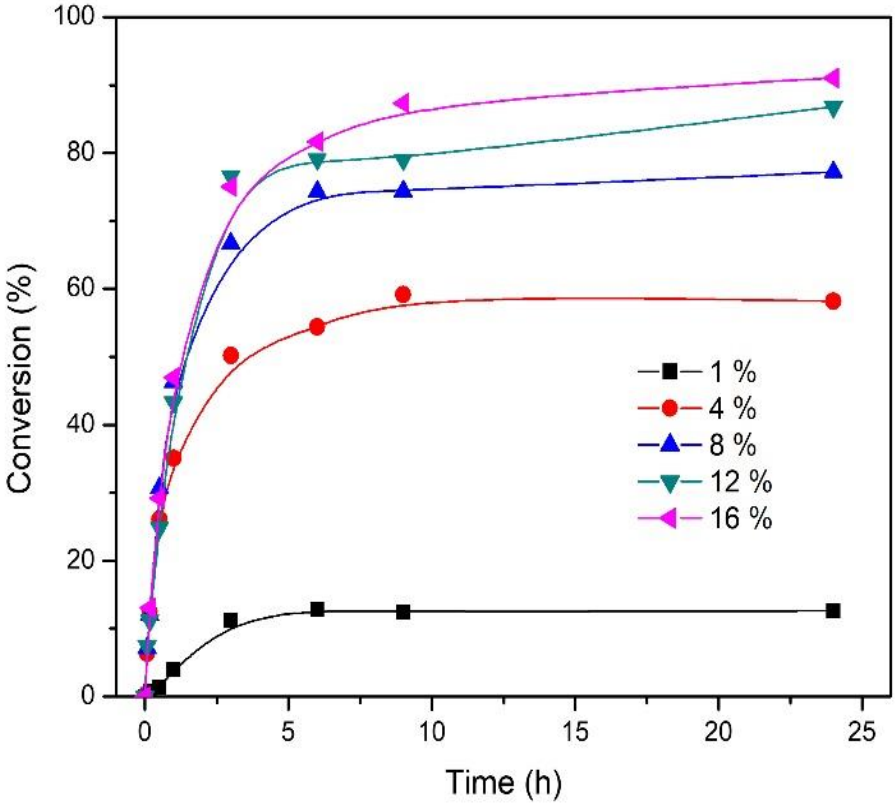

Figure 1. Effect of variation of the emulsifier concentration on the polymerization conversion.

Figure 1 shows that the polymerization conversion increased monotonically with the reaction time over the course of 3 h. When a small amount of emulsifier was used, the reaction conversion decreased remarkably. This is because the emulsion polymerization reaction occurs mainly inside the micelles and the number of micelles depends on the concentration of the emulsifier. As the emulsifier concentration increases, more micelles are formed and the number of latex particles per unit volume increases, and thus, the polymerization rate increases. In all cases, the polymerization rate was very high at the beginning of polymerization, but gradually became slower as polymerization progressed, and polymerization was almost complete in 9 h. Under the polymerization conditions employing SDS concentrations of 12% and 16%, the conversion after polymerization for 24 h reached about 90%. However, when the amount of SDS was small, especially when the concentration of SDS was reduced to 1%, the conversion was only 1/7 of that achieved with 16% SDS.

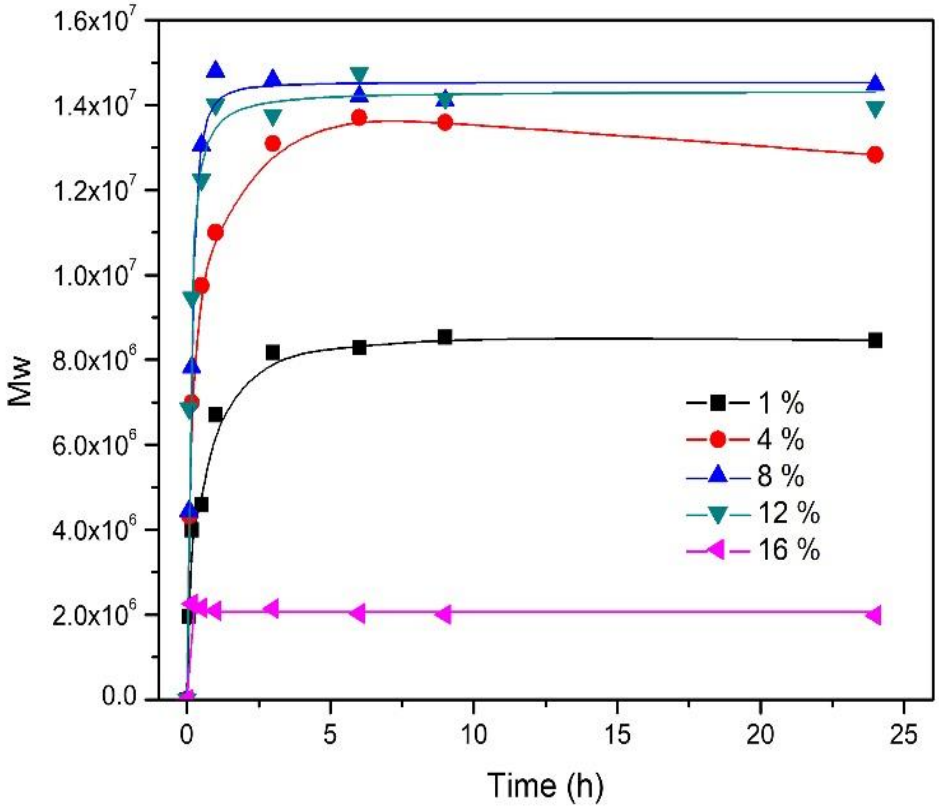

Figure 2. Effect of variation of the emulsifier concentration on the Mw.

Figure 2 shows the plots of the Mw versus the reaction time with different emulsifier concentrations. The profiles of the molecular weight were similar and ultra-high-molecular weight polystyrene were obtained in a short reaction time under all polymerization conditions. Because of the "segregation effect" [27-29] in emulsion system, the radicals can maintain activity for long time, making it possible to form ultra-high-molecular weight polystyrene. The molecular weight rapidly increased and became constant after several hours from the start of polymerization. When SDS concentration decreased to 1%, the maximum Mw of polystyrene was about 8×10^6. When the SDS concentration was increased to 4% or more, the Mw of polystyrene was higher than that obtained with 1% SDS. When the amount of SDS was further increased to 12%, there was no significant difference in the molecular weight of the obtained polymer. However, when the emulsifier amount increased to 16%, the Mw of polystyrene did not continue growing. The molecular weight of polystyrene reached 8×10^6 within 10 minutes and remained consistent at this value. This result is consistent with the result of emulsion polymerization using alkyl-9-BBN as initiator which we previously reported [20] and illustrates that using too much emulsifier may inhibit the growth of molecular chains. It is evident from Figures 1 and 2 that the reaction conversion and molecular weight of the polymer could be controlled by adjusting the amount of emulsifier.

Table 1 shows a comparison of the conversion and Mw of styrene polymerized with different concentrations of SDS for 9 h.

Table 1. Emulsion polymerization of styrene with Phen-DEZ in aqueous SDS solution at different SDS concentrations

SDS concentration (%)	conversion （%）	Mw (× 10^6)	PDI
1	12.5	8.5	2.5
4	59.2	13.6	2.5
8	74.4	14.1	2.4
12	79.0	14.2	2.4
16	87.3	2.0	1.9

Figure 3 shows the size exclusion chromatography (SEC) traces of these polystyrene samples.

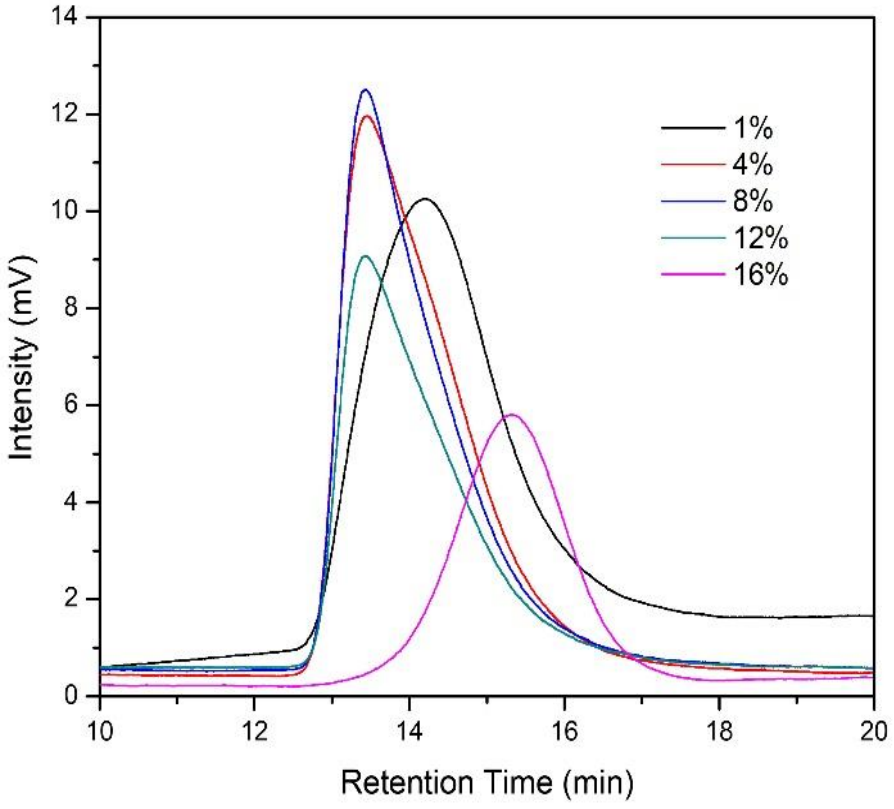

Figure 3. SEC profile of polystyrene polymerized with different emulsifier concentrations.

Based on the high conversion and the overall Mw trends, the proper concentration of SDS for the polymerization was 8%, and this was used for the subsequent experiments.

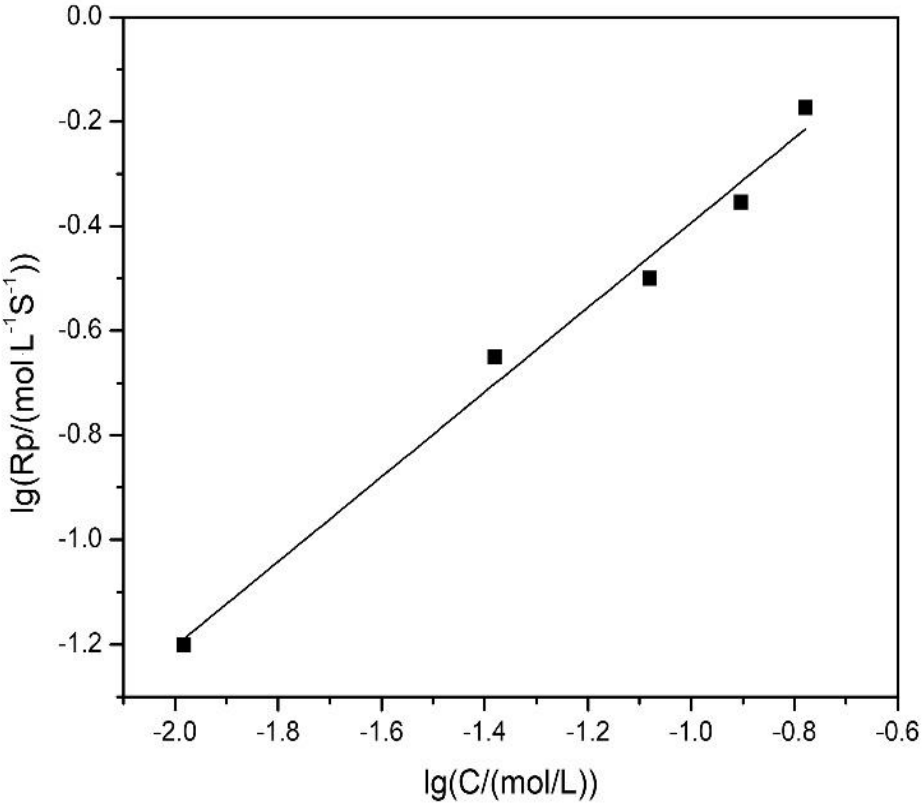

Figure 4. lg(Rp) versus lg[C] plot for samples containing different amounts of emulsifier.

The intriguing behavior prompted us to investigate the effect of the surfactant concentration on the emulsion polymerization. The influence of the concentration of the SDS surfactant on the polymerization of styrene initiated by the Phen-DEZ complex was investigated by dynamics computation.

Figure 4 presents a plot of lg[Rp] vs. lg[C], showing the influence of the SDS concentration on the polymerization rate. The polymerization rate (Rp) was calculated as：

$$Rp=-d[M]/dt \quad (2)$$

where [M] is the concentration of the monomer (mol/L).

The greater the amount of SDS used, the faster the reaction rate. To indicate the yield over time from the linear regression (Figure 4), the slope of the straight line was calculated as 0.81 with a correlation coefficient of 0.98. Thus, it can be concluded that $Rp \propto [SDS]^{0.81}$. Obviously, the concentration of the emulsifier has a great impact on the polymerization rate.

2.3.2 Effect of Monomer-to-Initiator Ratio on Polymerization

The effect of the proportion of the initiator on the conversion and Mw of the styrene emulsion polymerization was also investigated. Emulsion polymerization was carried out using a constant surfactant concentration of 8% and the reaction temperature was 23°C. The reaction conversion vs. time curves for styrene at several monomer/initiator molar ratios are shown in Figure 5. The monomer-to-initiator ratio (M/I) was changed by adding different amounts of Phen-DEZ. When the M/I ratio ranged from 2000:1 to 1000:1, an approximate linear variation of the conversion-time relation was obtained before three hours in each curve. The linearity indicated a constant polymerization rate during this reaction stage. 9 h later, the conversion became constant with a slight change as the reaction progressed. The reaction conversion increased with an increase in the amount of initiator. More initiator generates more radical species, and thus, the polymerization rate is higher than that achieved with a low initiator concentration. However, when the M/I ratio was further increased to 500:1, the conversion of $M/I_{500:1}$ was almost same as that of $M/I_{1000:1}$. The possible reason is that when the concentration of the initiator is increased to a certain extent, the concentration of the radicals dispersed in each micelle increases and the probability of bi-radical termination increases. The decrease in conversion is more pronounce when the M/I ratio increased to 100:1. This phenomenon is further supported by the Mw trends.

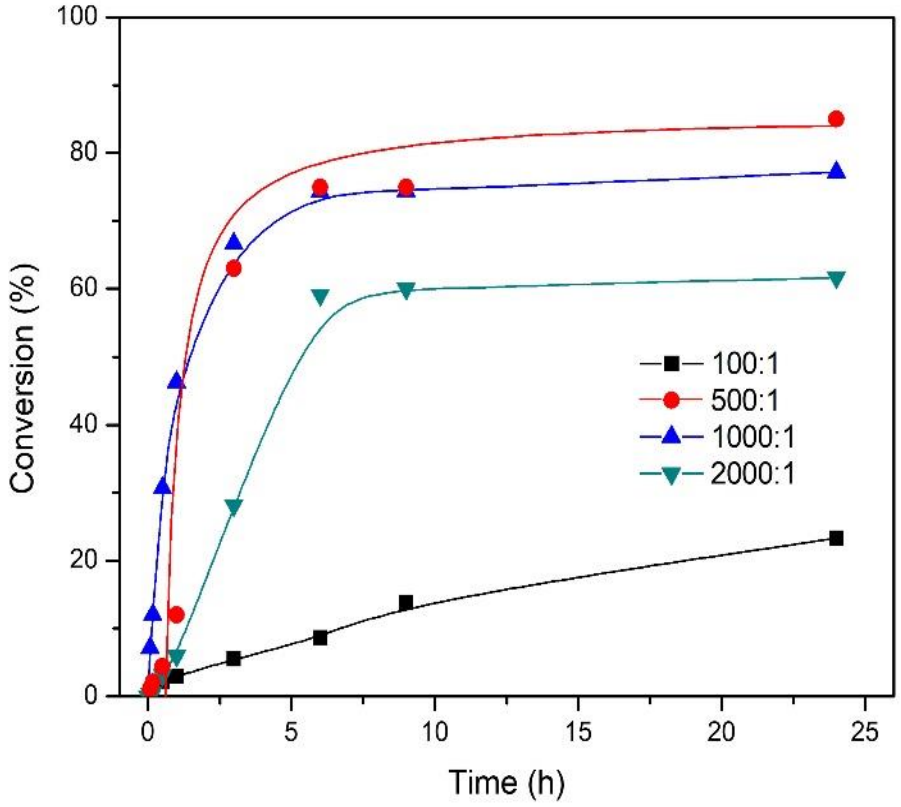

Figure 5. Effect of variation of the monomer-to-initiator ratio on polymerization conversion.

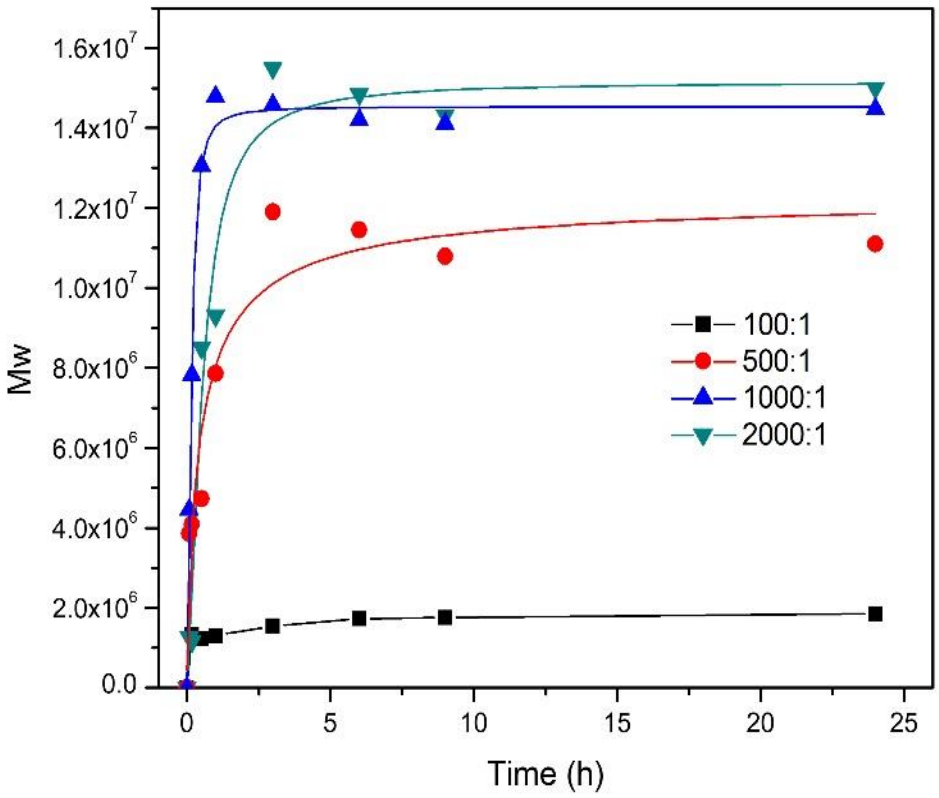

Figure 6. Effect of variation of the monomer-to-initiator ratio on Mw.

Figure 6 shows the molecular weight of polystyrene polymerized using different amounts of Phen-DEZ. For comparison, the ratio was varied from 100:1 to 2000:1. In all cases, the length of the molecular chains became constant after 3 h. The set with a high proportion (100:1) of initiator gave the lowest molecular weight (1.4×10^6), whereas in the case of 1000:1, the molecular weight was much higher (1.4×10^7). As discussed in the previous section, this is because the probability of free radical coupling termination increased with an increase in the amount of initiator, resulting in the relatively low molecular weight for a given reaction condition. When the initiator molar ratio dropped below 2000:1, the maximum Mw of polystyrene did not increase significantly. When the ratio of initiator to monomer was 1000:1 and 2000:1, the Mw of the polymer was around 1.2×10^7 to 1.3×10^7. This suggests that the termination of radical coupling was inhibited by a low initiator concentration. The conversion and Mw data of polystyrene polymerized for 9 h are summarized in Table 2.

Table 2. Emulsion polymerization of styrene with Phen-DEZ in aqueous SDS solution at different monomer-to-initiator ratio

Mole ratio (monomer:initiator)	conversion （%）	Mw ($\times 10^7$)	PDI
100:1	13.9	0.2	1.8
500:1	79.0	1.1	2.5
1000:1	74.4	1.4	2.4
2000:1	60.0	1.4	2.7

2.3.3 Effect of Temperature on Polymerization

Considering the previous results, the initiator-to-monomer ratio was kept at 1:1000. Polymerization was performed in the presence of 8% emulsifier with variation of the reaction temperature. The effect of the reaction temperature on the polymerization conversion is summarized in Figure 7. The results show that the polymerization rate increased with the reaction temperature, and the time needed to finish the reaction was shortened. When the reaction was carried out at 23°C, it took 6 h to finish the reaction. When the temperature was raised to 60°C, the reaction was almost complete after 3 h. When the temperature increased to 80°C, the reaction speed was significantly accelerated, and the polymerization was almost fully accomplished in 1 h with a yield of 75%. Because the rate of generation of free radicals at higher temperature was much higher than that at room temperature, the polymerization rate was enhanced by higher temperature. At the same time, the rate of monomer diffusion into the latex particles increased and the solution viscosity became lower at higher temperature [30], which resulted in an increase in the polymerization rate. In all cases, the polymerization was completed within 6 h. After six hours of reaction, the conversion did not vary significantly with the reaction temperature.

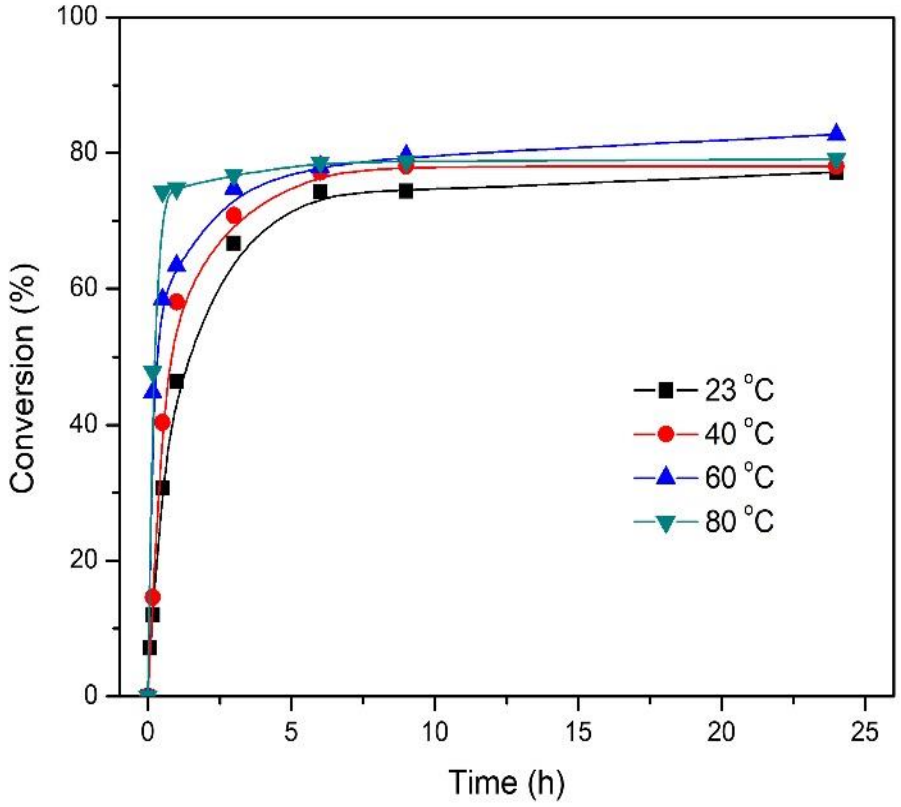

Figure 7. Effect of variation of the reaction temperature on the reaction conversion.

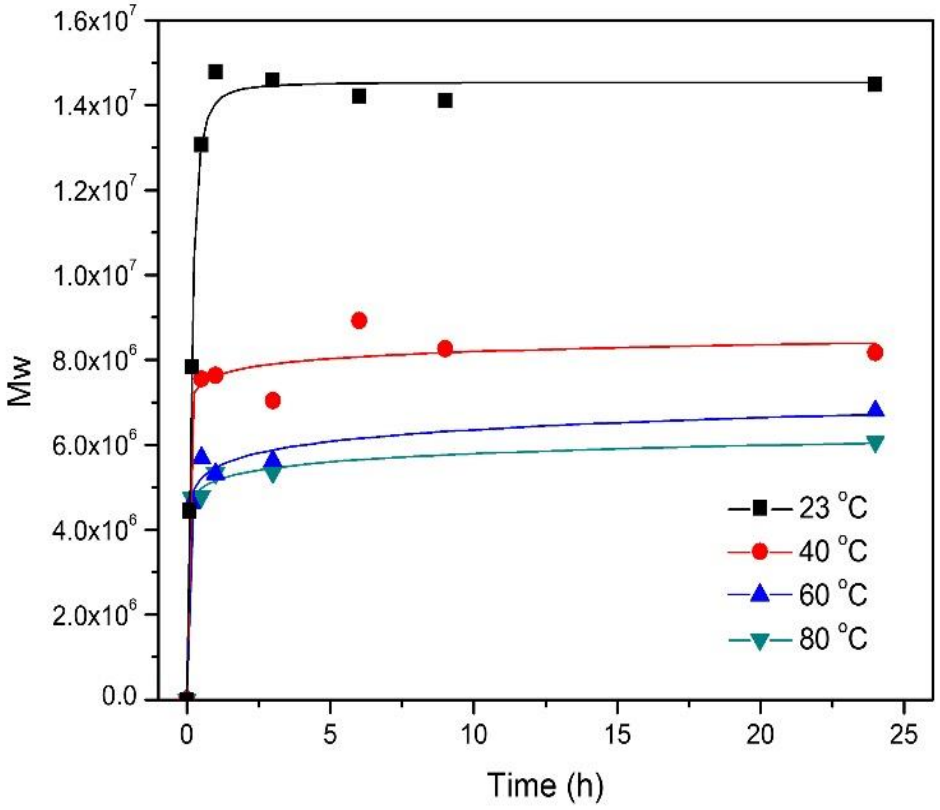

Figure 8. Effect of variation of the reaction temperature on Mw.

The Mw results are shown in Figure 8. As mentioned previously, the more the free radicals, the higher the probability of radical coupling, thus, the molecular weight decreased with an increase in the reaction temperature. Another possible reason is that the particles tend to aggregate and the bulk polymer increases, which also affects the decrease in the molecular weight. The Mw exceeded 1.2×10^7 when the polymerization temperature was 23°C, which may be because fewer radicals were produced and the probability of di-radical termination was reduced, therefore, the free radicals could remain active for a longer time.

Based on the above analysis, we can see this system retains the advantages of emulsion polymerization such as the ability to synthesize high molecular weight polymer, while combining the advantages of DEZ being able to initiate rapidly at low reaction temperatures.

2.3.4 Proposed initiation mechanism

Since the earliest discovery that alkylzinc can generate free radicals, many researchers tried to give a clear mechanism. However, due to the high activity of alkyl zinc and the complicated mechanism, the debate about the initiation mechanism has continued. In order to

make sure of the initiation mechanism, ^{1}H NMR was used to confirm the chain ends of polystyrene.

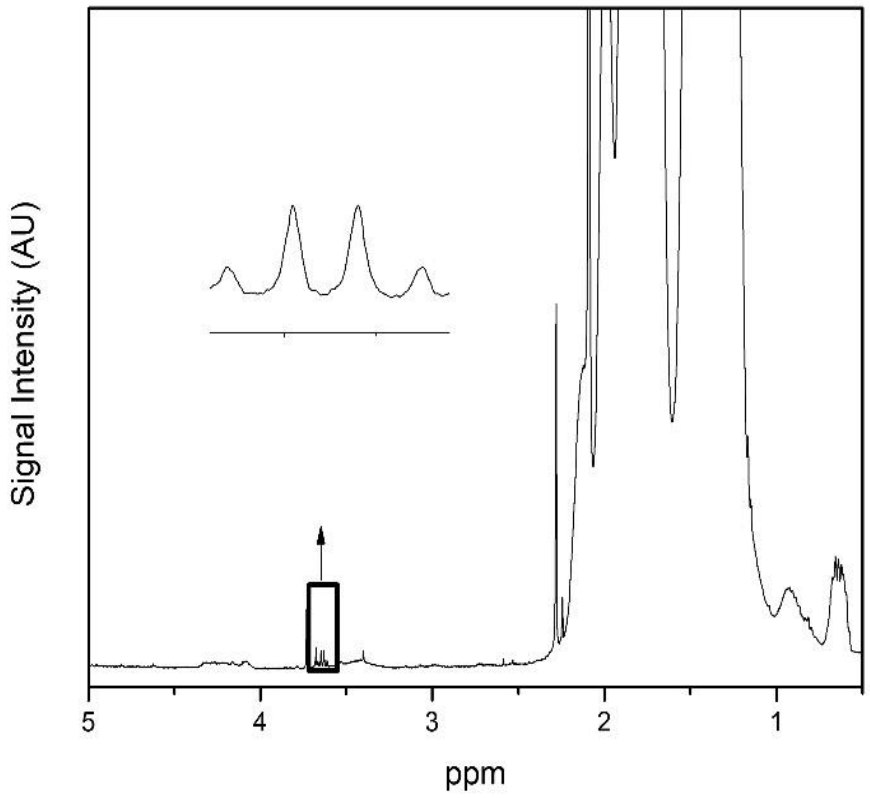

Figure 9. ^{1}H NMR spectrum of PS initiated by Phen-DEZ.

Figure 9 shows the ^{1}H NMR spectrum of homo polystyrene initiated by Phen-DEZ. The peaks at 0.36-0.37 ppm is assigned to the ethoxy group which is considered to show a characteristic the methylene proton signal from the initiator. Although the end group is weaker than the PS main chain due to the high molecular weight of polystyrene ($Mw=8.8\times10^{4}$). The proposed initiation mechanism of Phen-DEZ is shown in scheme 1. As introduced earlier, diethylzinc react with oxygen to form a peroxyzinc compound and the ethoxy radical (EtO•) that used to initiate the polymerization was generated from homolytic cleavage of the peroxyzinc. Then it seems that the end of the polymer chain contains ethoxy group.

However, several unknown radicals may be produced simultaneously while generating the ethoxy radical. At the present time, there is no evidence that a radical compound other than ethoxy radical is the initiator. Further analysis of the polymerization mechanism will be reported separately.

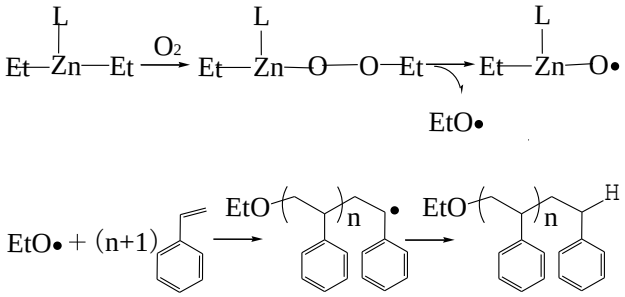

Scheme 1. Proposed reaction pathway.

2.3.5 Kinetic Studies

The kinetic behavior of emulsion polymerization of styrene initiated by Phen-DEZ has not been reported before. To achieve in-depth understanding, a kinetic study of the emulsion polymerization of styrene initiated by Phen-DEZ was conducted at four different polymerization temperatures (23−80 °C). The reaction rate versus the polymerization time is shown in Figure 10. In all cases, the rate increased to a maximum in a very short time then decreased sharply. With increasing the polymerization temperature, the highest Rp increases.

The dynamics of the initial stage of the styrene polymerization initiated by Phen-DEZ was investigated. The activation energy (Ea) of emulsion polymerization by Phen-DEZ can be directly obtained from the Arrhenius equation:

$$\ln k = -\frac{Ea}{RT} + \ln A \quad (4)$$

Where R is the gas constant, T is the temperature, and A is the pre-exponential factor.

As shown in the Arrhenius plot, there was a good linear relationship between ln k and 1/T, with an estimated Ea of approximately 31.0 kJ mol^{-1} for the emulsion polymerization of styrene, calculated from this plot (Figure 11).

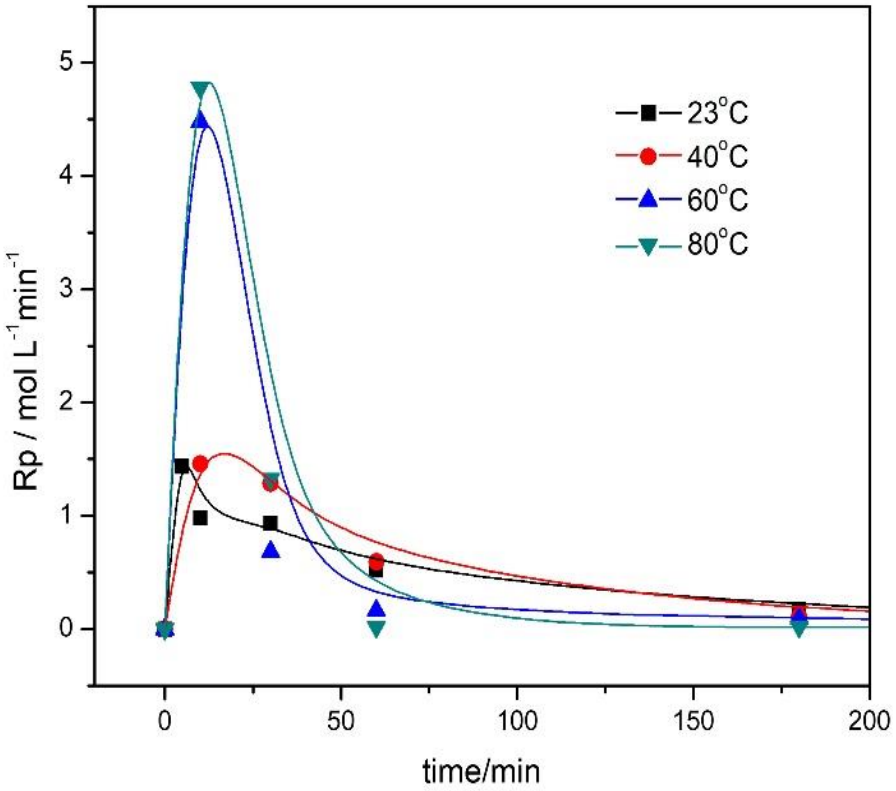

Figure 10. Time dependence of Rp 23 (■), 40 (●), 60 (▲), and 80°C (▼).

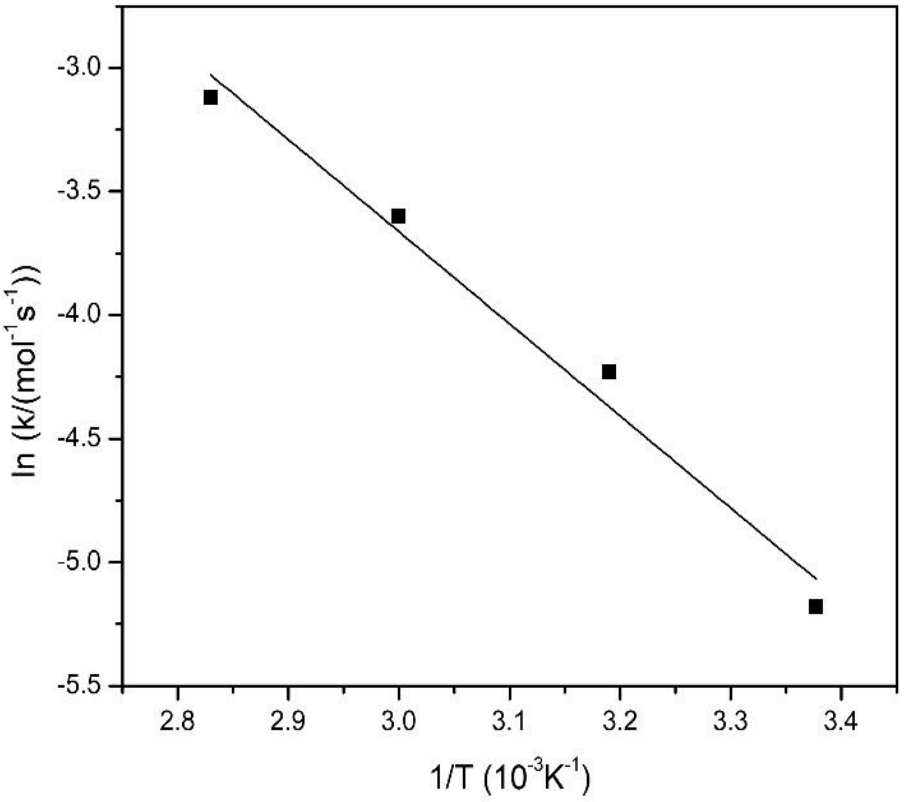

Figure 11. Arrhenius plot for the polymerization of styrene with Phen-DEZ in aqueous SDS solution at different temperatures.

The conversions and Mw of polystyrene that was polymerized at different temperatures for 24 h are compared in Table 3.

Table 3. Emulsion polymerization of styrene with Phen-DEZ in aqueous SDS solution at different temperatures

Temperature (°C)	conversion （%）	Mw (× 10^6)	PDI
23	78.7	14.3	2.5
40	78.0	8.2	2.7
60	82.7	6.8	2.5
80	79.1	6.1	2.8

2.4 Conclusions

The results reported in this paper highlight the possibility to synthesize polystyrene with ultra-high molecular weight by applying organozinc compound. Based on all the results, it is clear that Phen-DEZ is much stable than pure DEZ, this result can be linked to the formation of coordination during the process of synthesis. We demonstrated that extremely moisture-sensitive diethylzinc can be used as an initiator in emulsion polymerization after stabilized by 1,10-phenanthroline. Under our conditions, ultra-high-molecular-weight polystyrene can be prepared at ambient temperature with fast reaction speed in an aqueous solution. Calculated by kinetic study, the activation energy for this system was estimated to be 31.0 kJ/mol.

2.5 References

1. Bertinato, P.; Sorensen, E. J.; Meng, D. F.; Danishefsky, S. J. Studies toward a Synthesis of Epothilone A: Stereocontrolled Assembly of the Acyl Region and Modes for Macrocyclization. J. Org. Chem. 1996, 61,8000-8001.

2. Jeon, S. J.; Li, H. M.; Garcia, C.; Larochelle, L. K.; Walsh, P. J. Catalytic Asymmetric Addition of Alkylzinc and Functionalized Alkylzinc Reagents to Ketones, J. Org. Chem. 2005, 70, 448-455.

3. Fang, H. H.; Adjokatse, S.; Wei, H. T.; Yang, J.; Blake, G. R.; Huang, J. S. Ultrahigh Sensitivity of Methylammonium Lead Tribromide Perovskite Single Crystals to Environmental Gases. Sci. Adv. 2016, 2, e1600534/1-e1600534/9.

4. Ling, Y. C.; Yuan, Z.; Tian, Y.; Wang, X.; Wang, J. C.; Xin, Y.; Hanson, K.; Ma, B.; Gao, H. Bright Light-Emitting Diodes Bases on Organometal Halide Perovskite Nanoplatelets. Adv. Mater. 2016, 28, 305-311.

5. Hisano, K.; Keiichi, H.; Daisuke, K.; Naoyuki, T.; Masanobu, U. Dialkylzinc-Mediated Cross-Coupling Reactions of Perfluoroalkyl and Perfluoroaryl Halides with Aryl Halides. Chem. Eur. J. 2015, 21, 1-7.

6. Aleksanyan, D. V.; Kozlov, V. A.; Petrov, B. I.; Balashova, T. V.; Pushkarev, A. P.; Dmitrienko, A. O.; Fukin, G. K.; Gherkasov, A. V.; Bochkarev, M. N.; Lazarev, N. M.; Bessonova, Y. A.; Abakumov, G. A.; Lithium, Zinc and Scandium Complexes of Phosphorylated Salicylaldimines: Synthesis, Structure, Thermochemical and Photophysical Properties, and Application in OLEDs. RSC Adv. 2013, 46, 24484-24491.

7. Frankland, E. On the Isolation of Organic Radicals. Quart. J., Chem. Soc. 1850, 2, 263-296.

8. Sakata, R.; Tsuruta, T.; Saigusa, T.; Furukawa, J. Polymerization of Propylene Oxide and Vinyl Compounds with Diethylzinc in the Presence of Cocatalysts. Makromolekulare Chemie. 1960, 40, 64-78.

9. Ishimori, M.; Nakasugi, O.; Takeda, N.; Tsuruta, T. Diethylzinc/Water System for Epoxide Polymerization. Die Makromolekulare Chemie. 1968, 115, 103-118.

10. Botta, M. C.; Biava, H. D.; Spanevello, R. A.; Mata, E. G.; Suarez, A. G. Development of Polymer-Supported Chiral Aminoalcohols Derived from Biomass and Their Application to Asymmetric Alkylation. Tetrahedron Lett. 2016, 57, 2186-2189.

11. Anderson, J. C.; Harding, M. The Importance of Nitrogen Substituents in Chiral Amino Thiol Ligands for the Asymmetric Addition of Diethylzinc to Aromatic Aldehydes. Chem. Commun. 1998, 3, 393-394.

12. Ashraf, A.; El, S. Efficient Dual Catalytic Enantioselective Diethylzinc Addition to the Exocyclic CN Double Bond of Some 1,2,4-N-Triazinylarylimines Using Polymer-Supported Chiral β-Amino Alcohols Derived from Norephedrine. Tetrahedron. 2007, 63, 5490-5500.
13. Magali, V. A.; Alexakis, A. Influence of the Double-Bound Geometry of the Michael Acceptor on Copper-Catalyzed Asymmetric Conjugate Addition. Eur. J. Org. Chem. 2007, 35, 5852-5860.
14. Xu, J.; Samsuri, N. B.; Duong, H. A. Nickel-Catalysed Cyclopropanation of Electron-Deficient Alkenes with Diiodomethane and Diethylzin. Chem. Comm. 2016, 52, 3372-3375.
15. Ramirez, A.; Truc, V.; Lawler, M.; Ye, Y. K.; Wang, J.; Wang, C.; Chen, S.; Laporte, T.; Liu, N.; Kolotuchin, S. The Effect of Additives on the Zinc Carbenoid-Mediated Cyclopropanation of a Dihydropyrrole. J. Org. Chem. 2014, 79, 6233-6243.
16. Hansen, M. M.; Bartiett, P. A.; Heathcock, C. H. Preparation and Reactions of an Alkylzinc Enolate. Organometallics. 1987, 6, 2069-2074.
17. Hansen, M. M.; Bartlett, P. A.; Heathcock, C. H. Preparation and Reactions of an Alkylzinc Enolate. Organometallics. 1987, 6, 2069-74.
18. Filly, A.; Fabiano, T.; Anne, S.; Louis, C.; Femandez, X.; Chemat, F. Water as a Green Solvent Combined with Different Techniques for Extraction of Essential Oil from Lavender Flowers. C. R. Chim. 2016, 19, 707-717.
19. Wiley Online Library. Available online: https://onlinelibrary.wiley.com/doi/10.1002/047084289X.rd219 (accessed on 15 April 2001).
20. Zhao, C.; Sugimoto, R.; Naruoka, Y. A Simple Method for Synthesizing Ultra-High-Molecular-Weight Polystyrene Through Emulsion Polymerization Using Alkyl-9-BBN as an Initiator. Chin. J. Polym. Sci., 2018, 36, 592-597.
21. Lewinski, J.; Sliwinski, W.; Dranka, M.; Justyniak, I.; Lipkowski, J. Reaction of [$ZnR_2(L)$] Complexes with Dioxygen: A New Look at an Old Problem. Angew. Chem. Int. Ed. 2006, 45, 4826-4829.
22. Krahmer, J.; Beckhaus, R.; Saak, W.; Haase, D. Chelating Complexes of Diethylzinc and Zncl2 with 2,2-Bipyridine and 1,6,7,12,13,18-Hexaazatrinaphthylene (HATN) as Ligands. Z. Anorg. Allg. Chen. 2008, 634, 1696-1702.
23. Vaughan, B. A.; Arsenault, E. M.; Chan, S. M.; Waterman, R.; Synthesis and Characterization of Zinc Complexes and Reactivity with Primary Phosphines. J. Organomet. Chem. 2012, 696, 4327-4311.
24. Noltes, J. G.; Van den hurk, J. W. G.; Investigations on Organozinc Compounds. Ⅱ. Synthesis and Absorption Spectra of Some 2,2'-Bipyridine and 1,10-Phenanthroline Complexes of Organozinc Compounds. J. Organomet. Chem. 1965, 3, 222-228.

25. El-Shazly, M. F.; Electrochemical Reduction and Electron Spin Resonance Studies of Organozinc Complexes. Inorg. Chim. Acta. 1978, 26, 173-176.
26. Bencini, A.; Lippolis, V. 1,10-Phenanthroline: A Versatile Bulding Block for the Construction of Ligands for Various Purposes. Coord. Chem. Rev. 2010, 254, 2096-2180.
27. Kitayama, Y.; Okubo, M. A synthetic route to ultra-high molecular weight polystyrene (>10^6) with narrow molecular weight distribution by emulsifier-free, emulsion organotellurium-mediated living radical polymerization (emulsion TERP). Polym. Chem. 2016, 7, 2573-2580.
28. Per B, Z. Controlled/living radical polymerization in nanoreactors: compartmentalization effects. Polym. Chem. 2011, 2, 534-549.
29. Per B, Z.; Okubo, M. Compartmentalization in Nitroxide-Mediated Radical Polymerization in Dispersed Systems, Macromolecules. 2006, 39, 8959-8967.
30. Mao, B. W.; Gan, L. H.; Gan, Y. Y. Ultra High Molar Mass Poly[2-(dimethylamino)Ethyl Methacrylate] Via Atom Transfer Radical Polymerization. Polymer. 2006, 47, 3017-3020.

Chapter 3:

Graft polymerization of styrene on polypropylene initiated by a diethylzinc and 1,10-Phenanthroline complex

3.1 Introduction

Polypropylene is indispensable material and possesses many excellent features, such as high mechanical strength, low manufacturing costs and easy workability. However, lack of functional groups and highly non-polar nature results in poor dyeability, printability and paintability. Surface modification is an effective way to functionalize the surface of polymer materials, usually using grafting polymerization. Grafting polymerization offers an effective approach to introducing various kinds of monomers, thus empower the PP some desirable properties.

Grafting polymerization can be divided into “grafting from [1]”, “grafting onto [2]” and “grafting through [3]”. Since PP is a nonpolar substance, grafting reaction of a polar monomer is widely performed in order to increase the polarity of PP. For example, when acrylic acid is grafted onto PP, the hydrophilicity of the PP surface can be enhanced [4-6]. When grafting glycidyl methacrylate (GMA) [7-8], it is possible to introduce epoxy groups to PP and epoxy groups can be used for further reacting with various functional groups. Methyl methacrylate (MMA) [9-10] and styrene [11-12] have been used as graft monomer early and extensively studied. The most commonly used radical initiators such as BPO and AIBN require high temperature to initiate the reaction. Decomposition reaction of PP and crosslinking reaction of PE tend to occur in radical reaction of polyolefin such as high temperature radical reaction or strong irradiation. When the graft reaction is carried out under such conditions, the structure of the polyolefin is changed and the physical properties are decline. Furthermore, from the viewpoint of energy saving, it is very important to develop an initiator that can work at ambient temperature. Dating back to the 1960’s, Furukawa et al. reported that diethylzinc (DEZ) can serve as radical polymerization initiator of vinyl monomers at room temperature [13-15]. However, DEZ is highly combustible in air and difficult to handle, there are very few studies using DEZ as the radical polymerization initiator.

In our research, DEZ was stabilized by complexing with 1,10-Phenanthroline and the complex was used as radical initiator. This work offers a one-step simple method to graft

styrene onto PP and PE.

3.2 Experimental

3.2.1 Materials

Polypropylene (PP) film and linear low density polyethylene (PE) film were obtained from Toyobo (Pylen Film-CT and LIX Film-NP) and washed by refluxing $CHCl_3$ then dried under vacuum. Hexane, toluene, 1,10- phenanthroline, THF, $CHCl_3$, $MgSO_4$, NaOH, and styrene were purchased from Wako Pure Chemical Industry, Ltd. Styrene was washed by NaOH solution and treated with $MgSO_4$ to remove the stabilizer. Diethylzinc was supplied by Nippon Aluminum Alkyls, Ltd.

3.2.2 Characterization and measurements

The infrared spectra were obtained in the range of 4000-400 cm^{-1} by Jasco FT/IR-480 Plus. UV-Vis spectra were obtained by measuring the diffuse reflectance of the samples on a Jasco V-650 UV-Vis spectrometer. A thermogravimetry analyzer (Hitachi, STA 7200 RV) was carried out to determine the thermal stability of the films. The tests were performed in air from 25 to 550°C (10 °C/min) at a flow rate of 25 mL^{-1}. Size-exclusion chromatography (SEC) was performed with a Jasco PU-2080 Plus pump, a TOSOH UV-8020 detector. $CHCl_3$ was used as the eluent. Raman spectra were obtained on an HR800 Horiba Raman spectrometer. Atomic force microscope (AFM, Nanoscope II, Digital Instruments) was used to analyze the morphology of the surface of grafted PP films

3.2.3 Preparation of Phen-DEZ

Under the protection of argon gas, 1080mg 1,10-phenanthroline was added to a 50mL two-necked flask, followed by 20mL of hexane. DEZ (0.7mL) was added dropwise while stirring constantly. The mixture was stirred at 23°C for 24 h and the solid portion was collected by filtration. The reddish-orange Phen-DEZ was vacuum dried for 12 h.

3.2.4 Graft polymerization procedure

Typical graft polymerization of styrene to PP/PE film: PP/PE films (1 × 1 cm, thickness:

150μm), Phen-DEZ (90mg), toluene (3mL) and styrene (6mL) were added to an argon-filled flask. The mixture was gently stirred at room temperature (23°C). After reacting for 24 h, the polystyrene grafted PP / PE (PP-g-PS / PE-g-PS) films were taken out and further Soxhlet extracted with chloroform for 24 h. The graft polymerization was also carried out by a bulk polymerization method. The grafting yield was calculated using the FTIR absorbance. The internal reference peaks at 2720 and 699 cm^{-1} were used to determine the grafting yield of polystyrene.

3.3 Results and Discussion

The graft polymerization results are shown in Table 1.

Table 1. **Graft polymerization of styrene on PP/PE films**

Entry	Film	Solvent	Temperature (°C)	Time (h)	$Yield_{(graft)}$ (%)
1	PP	Toluene	23	24	1.7
2	PP	Bulk	0	24	0.4
3	PP	Bulk	23	24	3.4
4	PP	Bulk	60	24	4.9
5	PE	Toluene	23	24	1.2
6	PE	Bulk	23	24	1.4

The radicals generated from Phen-DEZ attacked the deactivated PP surface and formed active site, thus initiating the graft polymerization of styrene and resulting in styrene grafted on the PP surface. The grafting yield of PP-g-PS prepared in toluene solution at 23 ° C for 24 hours was 1.7%. However, the grafting yield increased to 3.4% by grafting styrene to PP surface under bulk polymerization condition. When the graft polymerization was carried out in bulk system, the viscosity of the mixture was significantly higher than that of solution system. Table 1 also shows the effect of temperature on the graft polymerization. The grafting yield increased as the increase of reaction temperature. When the temperature was 60° C, the grafting yield reached 4.9%. The concentration of free radicals increased with both bulk and high temperature reaction conditions, so the grafting yield seems to be improved.

The PP-g-PS (Entry 4) was used for the following series of tests.

The FT-IR transmittance method spectra of original PP and PP-g-PS (Figure 1) were used to confirm the grafting of PS onto the PP surface. As shown in Figure 1, the characteristic

absorption peak of aromatic can be detected at 699 cm^{-1} (out-of-plane C-H bending) and 1601 cm^{-1}. The absorption band at 1493 cm^{-1} belongs to the C=C deformation of the aromatic rings. The weak peaks at 3025 cm^{-1} and 3060 cm^{-1} correspond to C-H stretching in the benzene ring. All of these peaks were absent in the pure PP spectrum. These FTIR results demonstrated that polystyrene was successfully grafted onto the PP surface.

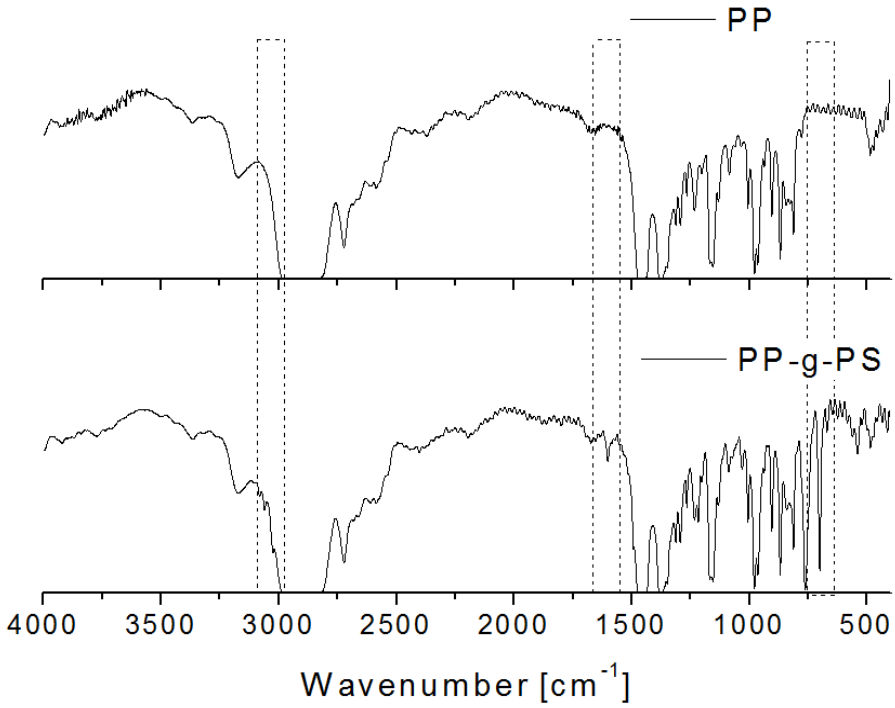

Figure 1. FTIR spectra of PP and PP-g-PS

Figure 2. shows the Raman spectra of original PP film and PP-g-PS. The original PP exhibits several typical Raman peaks at 1442, 1325, 1157, 869 and 825cm^{-1}[16]. The absorption bands at 1037 and 1062 corresponds to the C-C skeletal stretching bands [17]. The spectra of PP-g-PS shows a new peak near 1600 cm^{-1} which can be attributed to the C=C frequency of aromatic ring chain vibration of styrene. A weak peak at 3052 cm^{-1} assigned to the aromatic protons (C-H stretching in plane bending). The signal at 1000 cm^{-1} was assigned to the stretching of C-C aromatic. The band obtained at 620 cm^{-1} was assigned to C-H aromatic (stretching out of plane in opposite direction) [18].

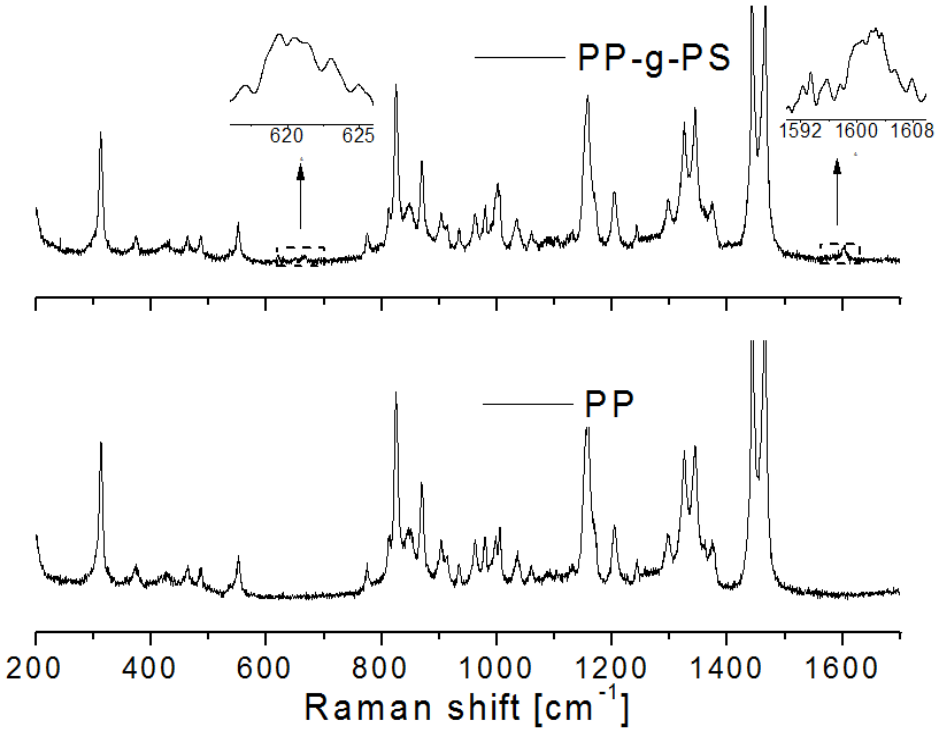

Figure 2. Raman spectra of PP and PP-g-PS

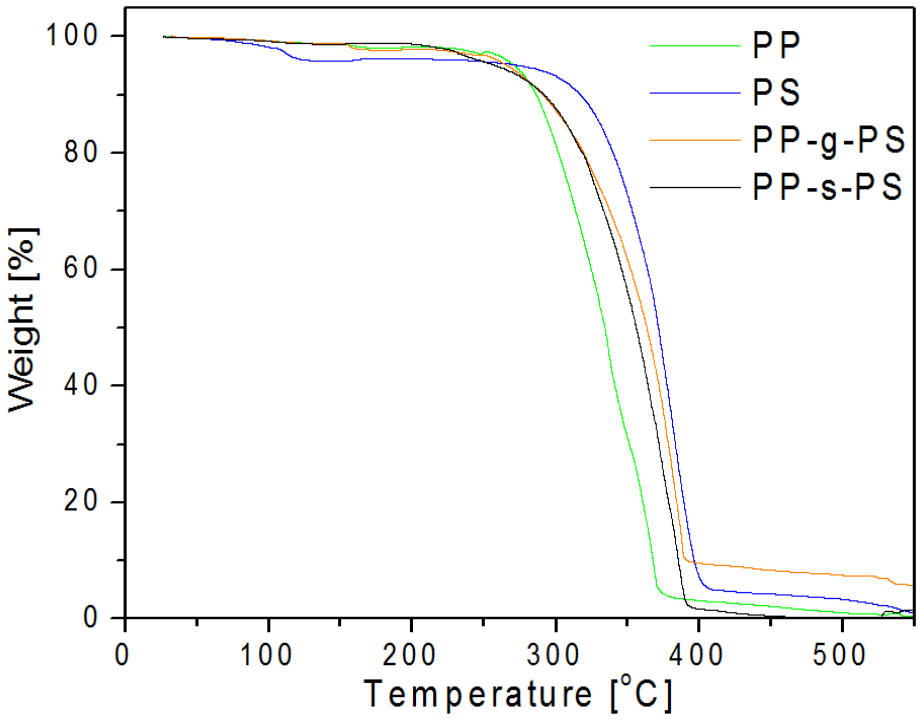

Figure 3. TG analysis of PP, PS, PP-g-PS and PP-s-PS

TG was performed to study the effect of grafting reaction on the thermal stability of PP. Figure 3 shows the TG results of PP, PS (homo polystyrene) and PP-g-PS films, which were measured in air. From the figure we can see that PS started to decompose at 270°C, which is slightly higher than that (250°C) of original PP film. By grafting styrene onto PP, the thermal stability of PP film has been improved. The possible reason is styrene replaced the tertiary hydrogen atoms and made electron cloud of macromolecules redistribution, the thermal stability of grafted PP was improved by strengthen the bond energy [19]. The grafting of styrene prompted the PP microradicals to react with styrene monomer before the degradation of the main chains of PP, by this way more stable radicals were formed and restrain the degradation of PP [20]. The thermal stability of the bulk structure of the grafted polymer depends not only on these microstructures but also on both the thickness of the PP substrate and the increase in that of the grafted PS polymer.

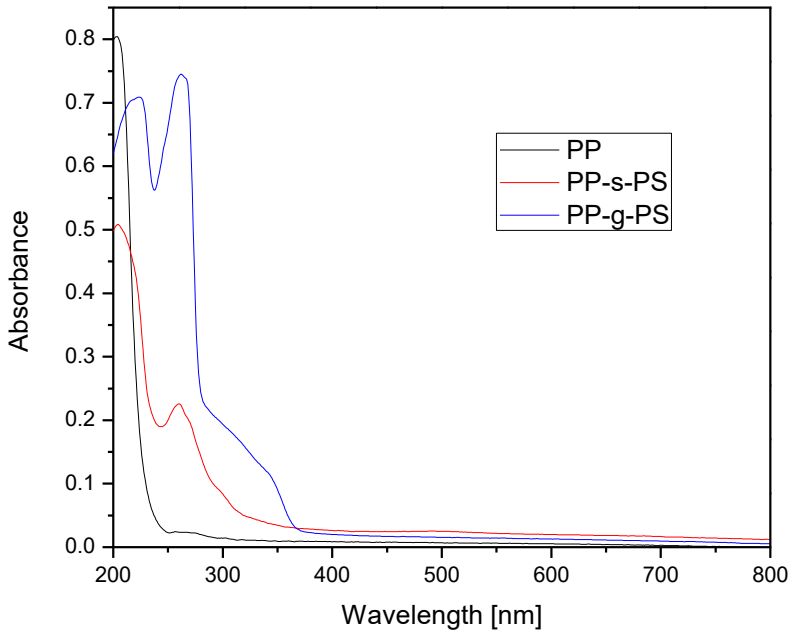

Figure 4. UV-vis spectra of PP, PP-g-PS and PP-s-PS films

The UV-Vis absorption of PP and PP-g-PS was recorded at room temperature. Two peaks at around 224 and 261 nm were observed on the PP-g-PS film, corresponding to the characteristic π-π* transition due to electron delocalization in the aromatic ring of polystyrene [18]. In order to compare with the PP-g-PS, another piece of PP was prepared for absorbing

PS. The film was immersed in polystyrene solution for 24 hours and then dried under vacuum (PP-s-PS). The UV-Vis spectra of PP-s-PS and PP-g-PS were compared in figure 4. From the difference in the positions of absorption peaks, it is clear that PS was grafted to the PP surface.

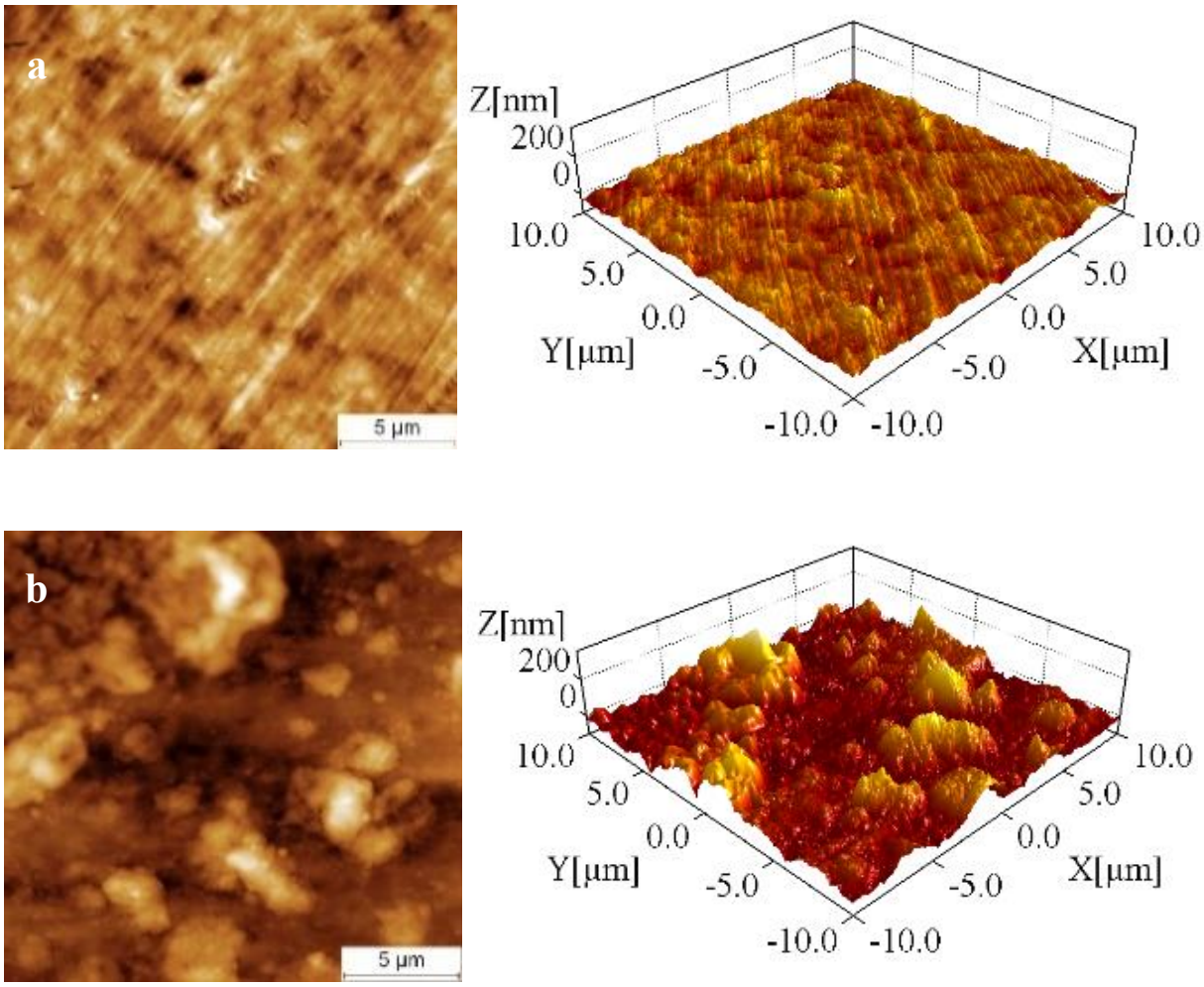

Figure 5. AFM of original (a).PP and (b).PP-g-PS

The surface morphology of PP and PP-g-PS were measured by AFM, the images are shown in Figure 5. Non-modified PP surface is smooth with the roughness value of 11.3 nm. By grafting styrene to the PP surface, the roughness of PP surface increased to 43.4 nm. The grafted PS macromolecular chains attached to the PP surface and formed homogeneous mountain-shaped structures. By grafting styrene onto PP film, the contact angle reduced from 106.1^{o} to 96.2^{o}.

Table 2. FTIR **Characteristic peak of PE**

Band (cm^{-1})	Assignment
2941-2835	CH2 asymmetric stretching
1473, 1463	Bending deformation
1366, 1351	Wagging deformation
1306	Twisting deformation
1176	Wagging deformation
731-720	Rocking deformation

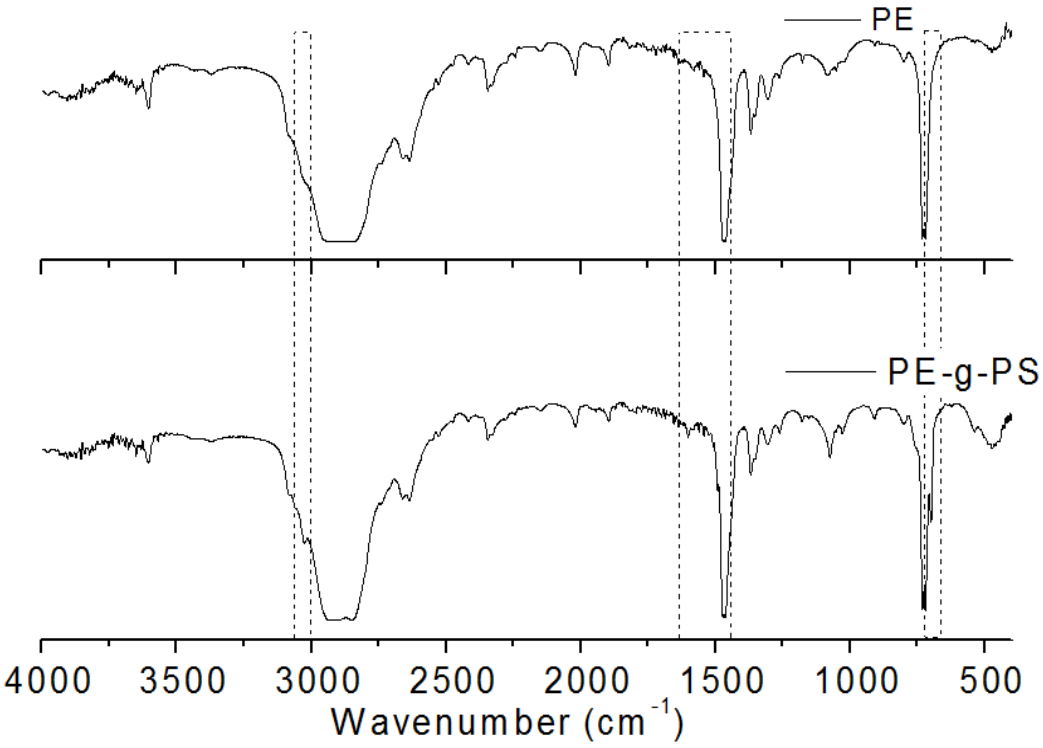

Figure 6. FTIR spectra of the PE and PE-g-PS (entry 6)

Under the same condition, Phen-DEZ can also initiated the graft polymerization of styrene on PE surface. The PE-g-PS film in figure 7 was prepared at 23° C in bulk system for 24 h (Entry 6). FTIR spectra of original PE and PE-g-PS are shown in figure 7. The original PE exhibits several typical FTIR peaks. Table 2 summarizes some of the characteristic peaks of PE [22]. IR spectra of PE-g-PS not only shows the characteristic peak of PE, but also shows the absorption at 3025, 1601, 1493 and 699 cm^{-1}. These peaks indicate that PS was successfully grafted onto the PE surface.

3.4 Conclusions

We have prepared PP-g-PS and PE-g-PS films initiated by Phen-DEZ complexe in one-step at ambient temperature. The grafting yield can be changed by changing the reaction conditions. At 60° C and bulk graft polymerization conditions, PP-g-PS films with higher grafting yield can be obtained. The surface roughness of PP has been greatly improved and morphology has also undergone significant changes. We believe that this technology can be developed not only into PP and PE but also various polyolefin and contributes to high function of polyolefin.

3.5 References

1. Pietrasik, J.; Sumerlin, B. S.; Lee, R. Y.; Matyjaszewski, K. Macromol. Chem. Phys. 2007, 208, 30-36.
2. Mandal, D. K.; Bhunia, H.; Bajpai, P. K.; Dubey, K. A.; Varshney, L.; Madhu, G. Thermo-oxidative degradation kinetics of grafted polypropylene films. Radiat. Eff. Defects Solids. 2017, 172(11-12), 878-895.
3. Hisada, K.; Matsuoka, M.; Tabata, I.; Hirogaki, K.; Hori, T. Two-step radical grafting onto polypropylene fiber initiated by active species prepared through the irradiation of electron beam. J. Photopolym. Sci. Technol. 2013, 26(2), 277-282.
4. Fasce, L. A.; Costamagna, V.; Pettarin, V.; Strumia, M.; Frontini, P. M. Poly(acrylic acid) surface grafted polypropylene films: near surface and bulk mechanical response. Express Polym. Lett. 2008, 2(11), 779-790.
5. Feng, G.; Wang, X.; Zhang, D.; Cao, H.; Qian, K.; Xiao, X. A comparative study on mechanical properties of surface modified polypropylene (PP) fabric reinforced concrete composites. Constr. Build. Mater. 2017, 157, 372-381.
6. Dogue, I. Louis Joseph; Mermilliod, N.; Boiron, G.; Staveris, S. Improvement of polypropylene film adhesion in multilayers by various chemical surface modifications. Int. J. Adhes. Adhes. 1995, 15(4), 205-10.
7. Kunita, M. H.; Girotto, E. M.; Muniz, E. C.; Rubira, A. F. Polypropylene grafted with glycidyl methacrylate using supercritical CO2 medium. Braz. J. Chem. Eng. 2006, 23(2), 267-271.
8. Xu, X.; Zhang, L.; Zhou, J.; Wang, J.; Yin, J.; Qiao, J. Thermal behavior of polypropylene-g-glycidyl methacrylate prepared by melt grafting. J. Macromol. Sci. B. 2015, 54(1), 32-44.
9. Zhang, Y.; Liu, Ji.; Hu, W.; Feng, Y.; Zhao, J. The chemical modification and characterization of polypropylene membrane with environment response by in-situ chlorinating graft copolymerization. Appl. Surf. Sci. 2017, 412, 627-637.
10. Dokolas, P.; Qiao, G. G.; Solomon, D. H. J. Graft copolymerization studies. III. Methyl methacrylate onto polypropylene and polyethylene terephthalate. Appl. Polym. Sci. 2002, 83(4), 898-915.
11. Hou, L. L.; Zhao, M. Studies on the preparation of multi-monomer grafted PP by one-step extrusion and the blends with PVC. Express Polym. Lett. 2008, 2(1), 19-25.
12. Caporaso, L.; Iudici, N.; Oliva, L. Synthesis of Well-Defined Polypropylene-graft-polystyrene and Relationship between Structure and the Ability To Compatibilize the Polymeric Blends. Macromolecules. 2005, 38(11), 4894-4900.

13. Makimoto, Ts.; Tsuruta, T.; Furukawa, J. Vinyl polymerization with organometallic compound carbon disulfide systems. Makromolekulare Chemie. 1962, 52, 239-41.
14. Saegusa, T.; Imai, H.; Furukawa, J. Metal alkyl catalysts for cationic polymerization of vinyl monomers. Makromolekulare Chemie. 1964, 79, 207-20.
15. Ishimori, M.; Nakasugi, O.; Takeda, N.; Tsuruta, T. Organometallic compounds as polymerization catalysts. II. Diethylzinc-water system for epoxide polymerization. Makromolekulare Chemie. 1968, 115, 103-18.
16. Masetti, G.; Cabassi, F.; Zerbi, G. Vibrational spectrum of syndiotactic polypropylene. Raman tacticity bands and local structures of iso- and syndiotactic polypropylenes. Polymer. 1980, 21(2), 143-52.
17. Sevegney, M. S.; Kannan, R. M.; Siedle, A. R.; Naik, R.; Naik, V. M. Vibrational spectroscopic investigation of stereoregularity effects on syndiotactic polypropylene structure and morphology. Vib. Spectrosc. 2006, 40(2), 246-256.
18. Pizarro, G. del C.; Marambio, O. G.; Jeria-Orell, M.; Gonzalez-Henriquez, C. M.; Sarabia-Vallejos, M.; Geckeler, K. E. Effect of annealing and UV-radiation time over micropore architecture of self-assembled block copolymer thin film. Express Polym. Lett. 2015, 9(6), 525-535.
19. Wang, J.; Ran, Y.; Zou, E.; Dong, Q. Supercritical CO2 assisted ternary-monomer grafting copolymerization of polypropylene. J. Polym. Res. 2009, 16(6), 739-744.
20. Zhu, B.; Dong, W.; Wang, J.; Song, J.; Dong, Q. Modification of polypropylene via the free-radical grafting ternary monomer in water suspension systems. J. Appl. Polym. Sci. 2012, 126(6), 1844-1851.
21. Liu, S.; Zheng, Z.; Li, M.; Wang, X. Effect of oxidation progress of tributylborane on the grafting of polyolefins. J. Appl. Polym. Sci. 2012, 125(5), 3335-3344.
22. Hou, L. L.; Zhao, M. Studies on the preparation of multi-monomer grafted PP by one-step extrusion and the blends with PVC. Express Polym. Lett. 2008, 2(1), 19-25.

Chapter 4:

Graft polymerization of MMA on polypropylene initiated by Phen-DEZ

4.1 Introduction

Polyolefins, such as polypropylene and polyethylene, are indispensable materials with many beneficial industrial uses. Their excellent properties, as represented by low specific density, high mechanical strength, high chemical resistance, and good processability, have led to the fabrication of objects for many different appliances. While they have many advantages, polyolefins do not contain polar groups, so they lack dyeability, printability, and adhesiveness unlike other functionalized polymers.

Various methods for the surface pretreatment of polyolefins have been developed with the aim of expanding their applications to high-performance fields; these pretreatment techniques include glow discharge [1], plasma treatment [2,3], corona discharge [4], and acid etching [5]. In addition, graft polymerization is a simple and efficient method for modifying the polymer surface. The surfaces of polyolefins can be modified with various kinds of vinyl monomers, and the products inherit many desirable properties from the monomers. Living graft polymerization is particularly noteworthy because it can precisely control the molecular weight and structure of the grafted chains. Ying et al. prepared multifunctional polyolefin-based elastomers via graft-from anionic living polymerization [6]. Ding et al. successfully synthesized photosensitive graft copolymers by living atom transfer radical polymerization [7]. Ye et al. summarized the recent developments in the area of Pd-diimine-catalyzed living ethylene polymerization [8].

Various monomers have been used for grafting onto various polyolefin backbones with different initiating systems. Jang et al. reported the UV-initiated radical graft polymerization of polypropylene fabrics. By grafting 2-hydroxyethyl methacrylate (HEMA) onto the polypropylene (PP) surface, the hydrophilic property of PP was significantly improved [9]. Grafting glycidyl methacrylate (GMA) onto the PP surface [10,11] is advantageous for the further modification of PP. The epoxy group of GMA is capable of reacting with many different functional groups, and the reactive compatibilization of PP/polyethylene terephthalate (PET) was improved while, at the same time, the blends exhibited better mechanical properties [12].

The heat distortion temperature and printing properties of PP can be improved by grafting styrene [13] and methyl methacrylate (MMA) [14-16] to the surface. The grafted PP can be used as a compatibilizer to improve the impact strength of its hybrid. However, most graft polymerizations must be carried out at high temperatures (i.e., >80 °C) because the initiator must absorb energy to initiate the reaction. Usually, in a radical reaction at high temperature, an intramolecular β-scission reaction occurs readily after hydrogen abstraction from the tertiary proton of the PP chain by the free radicals, and the PP chains are divided into two short PP chains. In addition, the use of these initiators is energy intensive, making them less attractive for industrial applications. Herein, we report a more convenient system that can be operated at room temperature for the grafting polymerization of vinyl monomers. Unlike commonly used initiators, diethylzinc (DEZ) shows superior properties for generating free radicals at low temperatures [17-19], which make it a promising initiator for materials that are prone to side reactions under high-temperature reaction conditions. This system does not require external stimulation such as corona discharge, plasma, or high temperatures. However, because DEZ is an unstable compound that is spontaneously flammable in air and vigorously hydrolyzed in water, it is challenging to carry out the radical graft polymerization of vinyl monomers using DEZ.

On the other hand, the reaction of DEZ with an N-donor ligand yields a Lewis acid–base complex, so it is expected that the stability of DEZ can be enhanced. Here, a complex of DEZ and 1,10-phenanthroline (Phen–DEZ) was synthesized using 1,10-phenanthroline as the N-donor ligand and the obtained Phen–DEZ complex is relatively stable and safe to handle. In this system, radicals are formed on the deactivated PP surface due to radicals generated from Phen–DEZ and oxygen, thus initiating the radical polymerization of the vinyl monomer and resulting in vinyl monomers grafted on the PP surface. In the present work, we provide a simple method to modify the PP surface by grafting in a one-step reaction under very mild conditions using MMA as the monomer.

4.2 Experimental

4.2.1 Materials

The PP film was provided by Toyobo (Pylen Film-CT), washed in refluxing chloroform, and dried under vacuum. PP fiber was provided by Zetta Ltd. Methyl methacrylate (MMA) and styrene monomer were purchased from Wako Pure Chemical Industry, Ltd., and the stabilizer was removed by washing with sodium hydroxide (NaOH) solution followed by treatment with

magnesium sulfate ($MgSO_4$). Diethylzinc was supplied by Nippon Aluminum Alkyls, Ltd. Hexane, toluene, 1,10-phenanthroline, tetrahydrofuran (THF), chloroform ($CHCl_3$), $MgSO_4$, and NaOH were purchased from Wako Pure Chemical Industry, Ltd.

4.2.2 Measurements

The Fourier transform infrared spectra (FT-IR) were obtained using a Jasco FT/IR-480 Plus spectrometer. Thermogravimetric analyses (TGA, Hitachi, STA 7200 RV) was carried out to determine the thermal stability of the films. The tests were performed in air from 25 to 550 °C (10 °C/min) at a flow rate of 25 mL^{-1} min^{-1}. Size-exclusion chromatography (SEC) was performed with a Jasco PU-2080 Plus pump and an RI-2031 Plus Intelligent RI detector. $CHCl_3$ was used as the eluent. X-ray diffraction (XRD) patterns were recorded under ambient conditions with Cu-K_α radiation. Raman spectra were obtained on an HR800 Horiba Raman spectrometer. Atomic force microscopy (AFM, Nanoscope II, Digital Instruments) was used to analyze the morphology of the grafted PP films. The contact angle study was analyzed using a portable contact angle analyzer (PGX). Scanning electron microscopy (SEM) images were obtained using a field emission (FE)-SEM (Hitachi SU-8020) microscope.

4.2.3 Synthesis of Phen–DEZ

The Phen–DEZ complex was synthesized in a 50 mL two-neck flask under the protection of argon gas. First, 1,10-phenanthroline (1080 mg) and hexane (20 mL) were added to the flask, and the mixture was gently stirred while diethyl zinc (0.7 mL) was slowly injected. After stirring the mixture for 24 h at 23 °C, the solution was filtered. The reddish-orange Phen–DEZ complex was treated by vacuum desiccation and the yield of Phen-DEZ complex was 90%.

4.2.4 Grafting and sample preparation

All the graft polymerization process was performed under an argon atmosphere. Several pieces of PP film (15 mg, 1 × 1 cm, 0.15 mm thickness)/PP fibers (50 mg) were placed in an oven-dried Schlenk flask fitted with a stopcock. Then, toluene (3 mL) and Phen–DEZ (90 mg, 0.3mmol) were added to the flask, followed by the monomer (6 mL), and the resulting solution was gently stirred for 24 h under argon. Subsequently, Phen–DEZ was reacted with diffused oxygen to form radicals. In this stage, graft polymerization of the monomer on the surface of PP and self-homopolymerization of the monomer occurred simultaneously. The free

homopolymer was removed from the grafted PP by Soxhlet extraction with chloroform for 24 h. The grafting yield was calculated using the integration of FTIR absorbance peak area [20,21]. Different ratio of PP and PMMA were mixed and measured by FTIR. A linear relationship between the ratio of PP/PMMA and the area of reference peaks was obtained. The internal reference peaks at 2720 and 1732 cm^{-1} were used to determine the grafting yield of MMA.

4.3 Results and Discussion

The graft polymerization was carried out in toluene solution and via bulk polymerization. Under both conditions, PP was miscible with the reaction solution. Moreover, weak van der Waals forces between DEZ and toluene result in the absorption of DEZ onto the PP surface. The reaction of DEZ with diffused oxygen produces free radicals, and MMA could be grafted to the surface of PP successfully. The influences of various reaction conditions on the graft yield (G) were investigated by carrying out a series of graft polymerizations with different reaction times, solvents, and temperatures. Table 1 summarizes the results of graft polymerization obtained under various reaction conditions. Phen–DEZ can initiate graft polymerization at relatively low temperatures compared to commonly used initiators such as azobisisobutyronitrile (AIBN) and benzoyl peroxide (BPO), which require high reaction temperatures.

Table 1. Graft polymerization of MMA onto PP films by the Phen–DEZ initiator.

Entry	Solvent	Temperature (°C)	Polymerization time (h)	G (%)	$Yield_{homo}$ (%)
1	Tol	23	24	4.2	1.6
2	Tol	23	120	6.4	1.6
3	Tol	60	24	5.8	4.1
4	bulk	0	24	0.1	0.2
5	bulk	23	24	7.6	3.5
6	bulk	60	24	27.0	9.9

Graft polymerization in toluene solution at 23 °C for 24 h gave a grafting yield of 4.2% (Table 1, entry 1). On increasing the reaction time or temperature, the grafting yield improved to 6.4% and 5.8%, respectively. MMA could be grafted onto PP even by graft polymerization carried out at 0 °C under bulk polymerization conditions. That is, despite the absence of

reactive sites on PP polymer chains, Phen–DEZ can also cleave some stable CH bonds at 0 °C and form radicals for the grafting reaction. In addition, the grafting yield was 7.6% at room temperature (23 °C), reaching a maximum (G = 27.0%) at 60 °C in the bulk system. The grafting yield increased with increase in the reaction temperature, and this was also observed for solution graft polymerization. By comparing the G of grafted PP prepared in solution and bulk, we can conclude that the grafting yield was affected by the monomer concentration. The SEC measurements of the homopolymer indicate that the molecular weight (M_w) of the PMMA prepared at 60 °C was 380000, which is slightly lower than that obtained from the reaction performed at room temperature (M_w = 470000). This can also be explained by the accelerated rate of generation of free radicals.

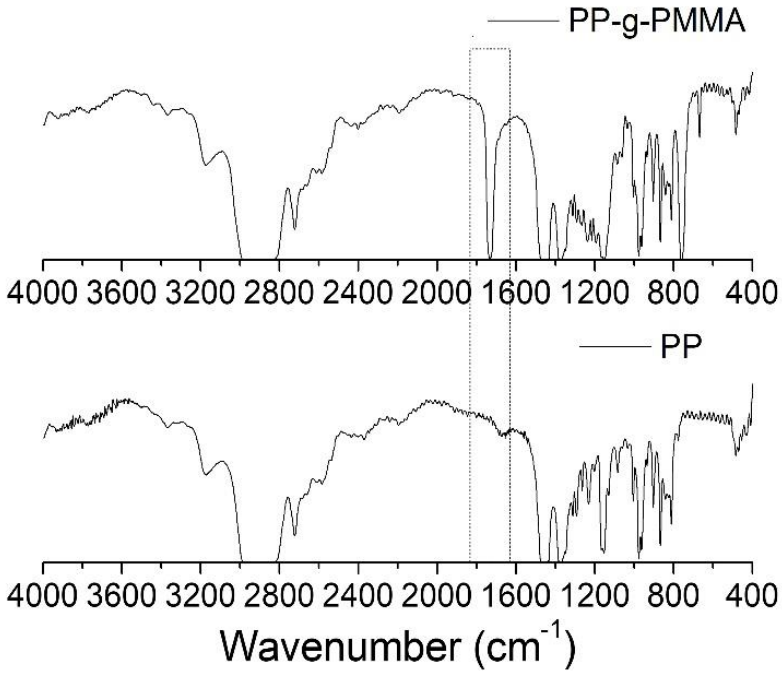

Figure 1. FTIR spectra of PP film (a) and PP-g-PMMA (b) (Table 1, entry 6).

The FT-IR (Figure 1) and Raman (Figure 2) spectra of the PP film and polymethyl methacrylate-*graft*-polypropylene (PP-g-PMMA) film were used to confirm the grafting of PMMA onto the surface of PP. The IR and Raman spectra of PP can be found in several reports [22-28]. The characteristic absorption peaks at 973 and 997 cm^{-1} are assigned to the rocking vibrations of the -CH_2- [22] groups. The intense peaks observed in the range of 2758–3037 cm^{-1} arise from the strong alkane C-H stretch [29]. The FTIR spectra also indicate the presence of C-H bend/scissoring and C-H methyl rocking at 1454 and 1373 cm^{-1}, respectively [23]. The graft polymerization of PP and PP-*g*-PMMA was confirmed by FTIR analysis (Figure 1)

because the spectrum of the graft polymer clearly shows a band at 1732 cm^{-1} that is attributable to the ester carbonyl stretching vibration. The weak characteristic absorption band at 1275 cm^{-1} corresponds to the C-O stretching of PMMA. The absorption bands at 1193 and 753 cm^{-1} correspond to CH_2 twisting and rocking modes. The peaks at 1395 cm^{-1} (OCH_3 deformation), 1481 cm^{-1} (CH_2 scissoring), and 1447 cm^{-1} (CH_3 asymmetric stretching) overlap with the characteristic absorption bands of PP. The CH- bending peak was chosen as an internal reference, and the relative amount of grafted PMMA was calculated from the ratio of the peak intensity of the C=O group to that of the CH group [20].

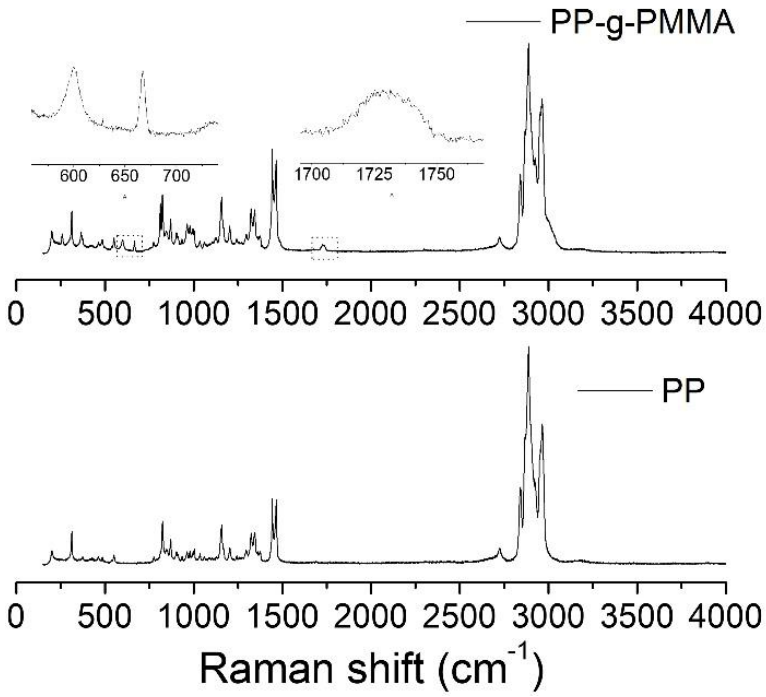

Figure. 2. Raman spectra of the PP film (a) and PP-g-PMMA sample (Table 1, entry 6).

In addition to the IR results, the Raman spectra also provided overwhelming evidence that MMA was grafted onto PP. The Raman spectra of PP and PP-*g*-PMMA are shown in Figure 2. The weak C-C skeletal stretching bands appear at 1037, 1062, 1087, and 1104 cm^{-1} [24]. Other peaks, such as those at 825, 869, 1157, 1325, and 1442 cm^{-1}, are also consistent with literature observations [28]. The Raman bands at 1728 and 603 cm^{-1} can be ascribed to the C=O stretching vibrations and the O-C=O deformation in PMMA, respectively [30]. The spectrum of grafted PMMA contains a band at 2952 cm^{-1} (the C-H stretching). The band at 602 cm^{-1}

arises from υ(C-COO) and υ_s(C-C-O) vibrations. The other bands appearing at 814, 999, 1460, 2848, and 3001 cm^{-1} are also consistent with literature reports [31, 32].

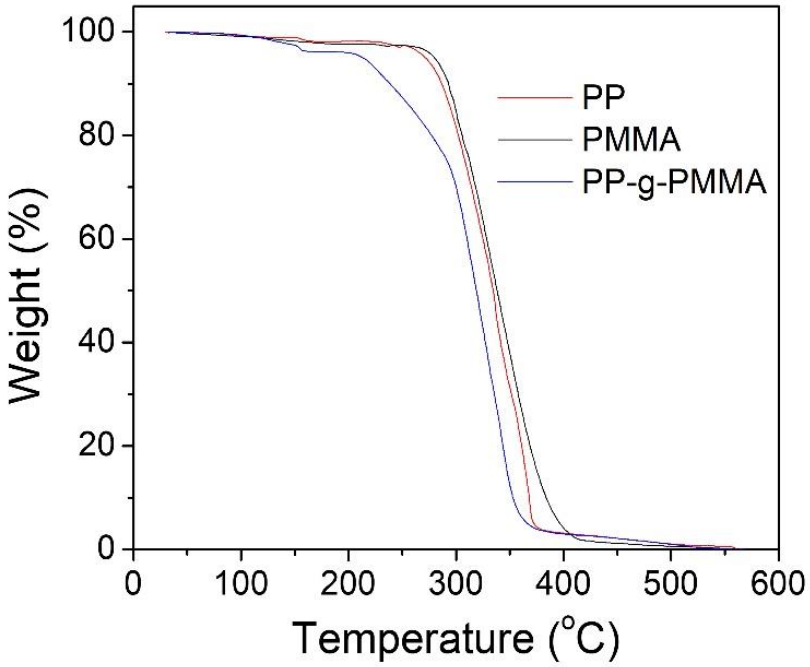

Figure 3. TGA curves for PP, PMMA homopolymer, and PP-g-PMMA.

The effect of grafting on the thermal stability of PP was studied by carrying out TGA measurements in air. Figure 3 shows the TGA results for pristine PP, homo PMMA, and PP-*g*-PMMA. The thermal decomposition of PP-*g*-PMMA occurred in two stages. The first stage of degradation occurred from 200 to 295 °C with a weight loss of 3–30%. The second stage of degradation occurred from 295 to 525 °C, showing a weight loss of 30–98%. The first decomposition stage is attributed to the scission of the grafted PMMA chains, whereas the second degradation stage may be due to the thermal scission of PP. The thermal stability of the graft-modified PP film was remarkably changed. The temperature at which the original PP film began to decompose was 250 °C, but the decomposition temperature of the grafted PP is 260 °C. On the other hand, the initial decomposition temperature of PP-*g*-PMMA was lower than that of the PMMA homopolymer. This can be explained by the elimination of the stabilizing effect of oxygen on the vinylidene end group of MMA [33,34]. Although the initial decomposition temperature of graft PMMA was reduced, the onset temperature of the PP matrix was increased (280 °C). The grafted PP lost 27% of its mass in the initial decomposition stage, followed by the decomposition of PP. This result is consistent with the value of the grafting yield of MMA.

Thus, the TGA curves showed that MMA was grafted onto the PP film.

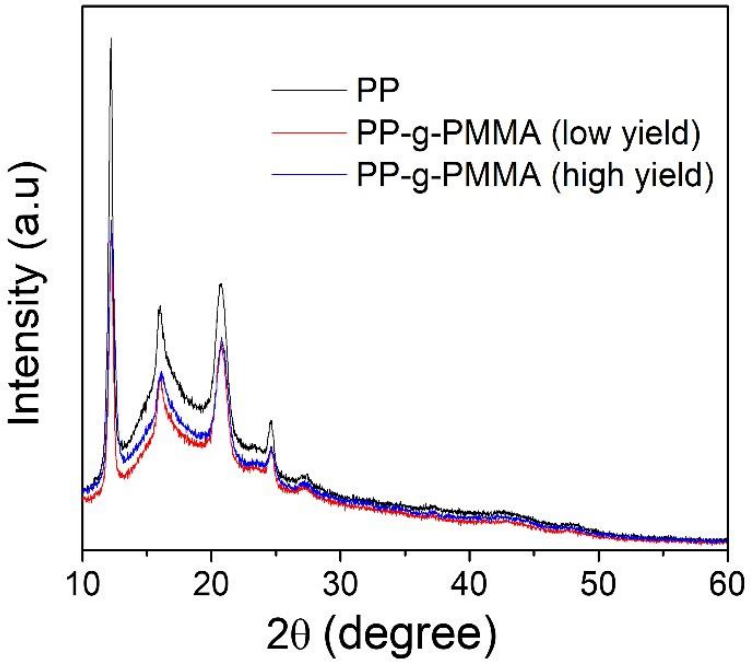

Figure 4. XRD patterns of PP, PP-g-PMMA (G = 4.2%), and PP-g-PMMA (G = 27%).

Figure 4 shows the XRD spectra of the original PP and those of grafted PP with a high grafting yield (G = 27.0%) and a low grafting yield (G = 4.2%). Several characteristic peaks that arise from the semi-crystalline structure of PP were observed ranging from 12° to 25°. However, the diffraction pattern of grafted PP is similar to that of PP, except for the peak intensities. With increase in grafting yield, the peak intensity was reduced. The reason for this reduction in intensity was that the grafted PP contained a large number of branched chains; these chains were entwined with each other, which affected the tacticity [35]. The results show that the internal structure of PP film is not destroyed by MMA grafting, and the grafting reaction seems to be restricted to the PP surface.

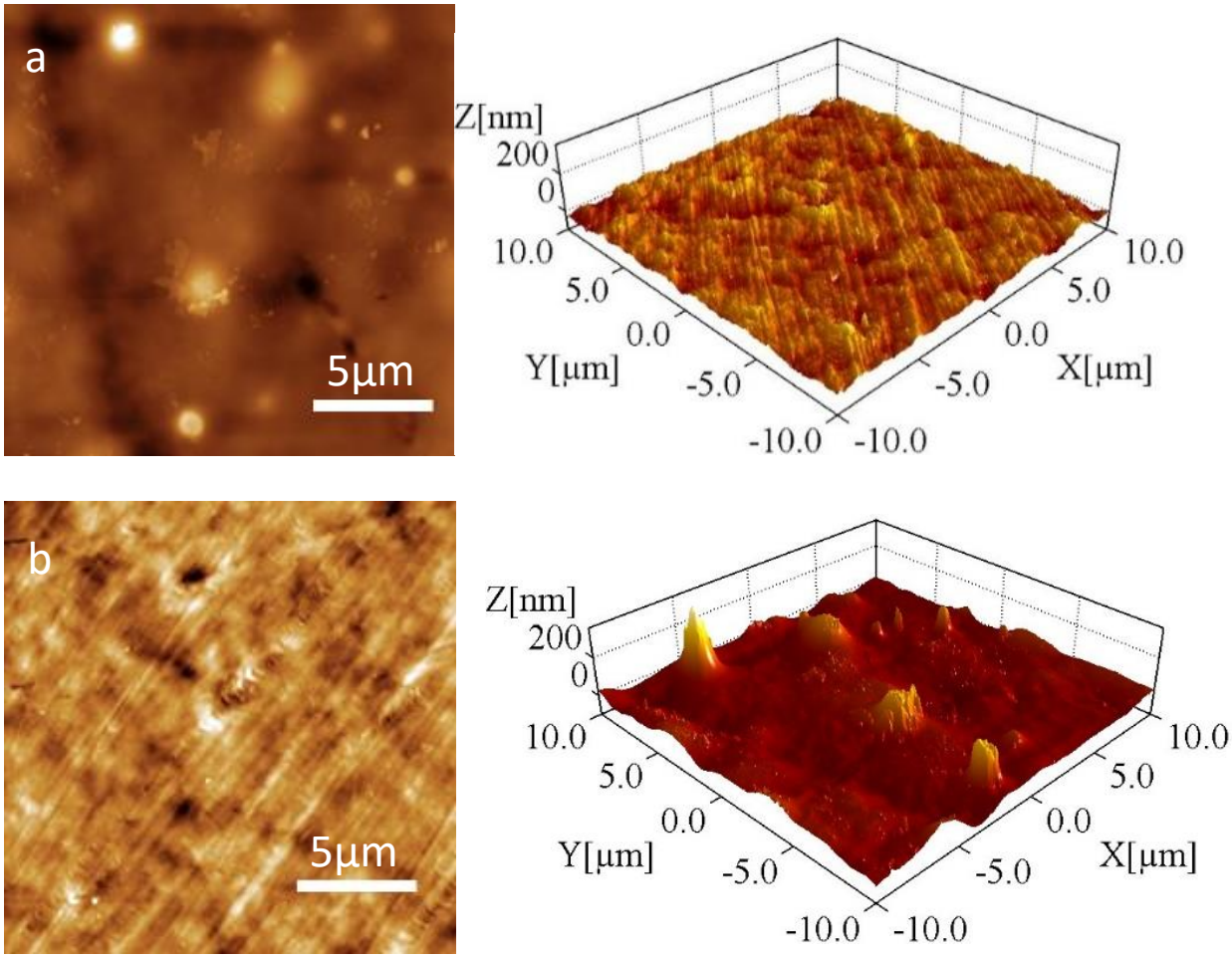

Figure 5. The AFM topologies of the PP (a) and PP-g-PMMA (b) samples.

Figure 5 shows the surface morphology of the original PP film (a) and grafted PP film (b). The roughness of PP film was 11.3 nm. However, the PP-g-PMMA surface did not reproduce the structure of the PP film, and the roughness values increased to 36.4 nm. In addition to the surface becoming uneven, there were some large mastoid structures on the PP surface. These observations suggest that MMA had been successfully grafted onto the PP film. However, the transplanted MMA is distributed sparsely, either because the amount of grafted MMA was low or because long molecular chains formed on the PP surface, impeding the reaction between the monomer and the PP matrix.

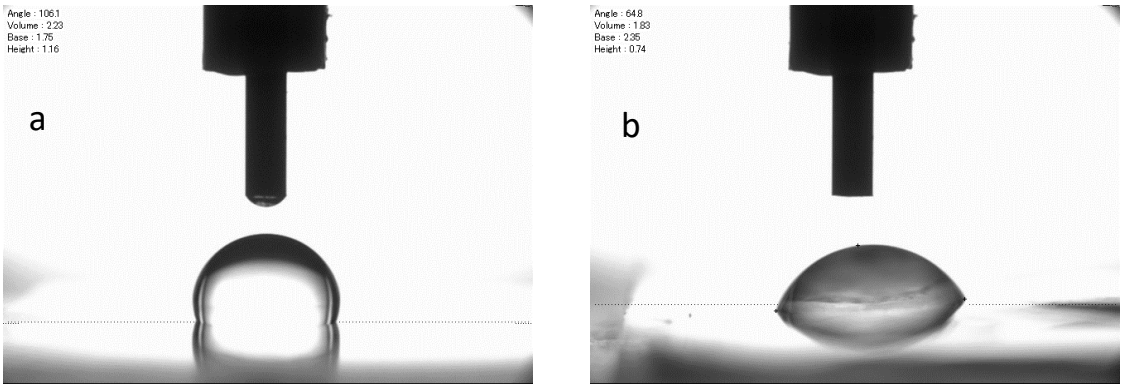

Figure 6. Contact angles on the (a) PP (contact angle = 106.1°) and (b) PP-g-PMMA (contact angle = 64.8°).

The effect of grafting PMMA on the surface of PP was also tested using contact angle measurements (as shown in Figure 6), which provide a measure of the wettability of a solid by water. The contact angle of PP was 106.1°. After grafting MMA onto the PP, a contact angle of 64.8° was obtained, a substantial decrease arising from the presence of the ester groups in the PMMA layer on the surface of PP. That is, the contact angle of PP-*g*-PMMA was significantly improved after the grafting of MMA to PP, indicating that the presence of PMMA increased the hydrophilicity of the PP film.

We also confirmed the grafting of MMA on PP microfibers, where PMMA covers the PP surface. Compared to conventional materials, microstructured materials generally exhibit superior mechanical properties and physical properties [36]. However, particular attention should be paid to the reaction conditions during the modification process to prevent damaging the microstructure. Thus, PMMA was grafted onto PP fibers in a bulk system using mild reaction conditions (23 °C); this protected the microstructure of the PP fibers. Because PMMA was grafted onto the PP fibers under mild polymerization conditions using Phen–DEZ, there was no effect on the microstructure of the PP fibers.

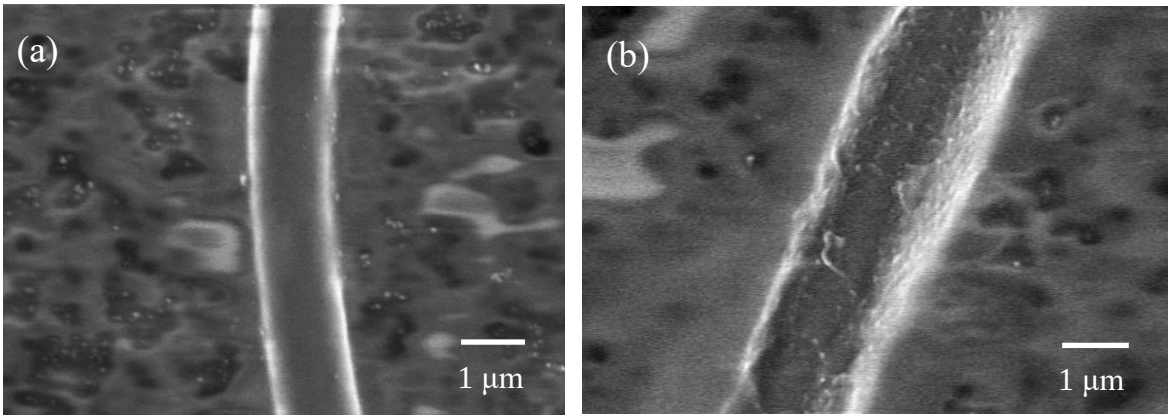

Figure 7. SEM micrographs of PP fibers: (a) original PP fiber and (b) PP-g-PMMA fibers.

Figure 7 shows the SEM images of an untreated PP fiber (a) and a grafted PP fiber (b). From the SEM images, the difference in PP fiber surface morphology before and after treatment can be seen clearly. The original PP fibers exhibited smooth surfaces, while the grafted PP fibers showed roughened surfaces. By grafting PMMA on PP fibers, as shown in Figure 7(b), several nodules formed on the surface of the fiber. Aside from the increase in the surface roughness of the PP fiber, the grafting reaction did not affect the original fiber structure.

4.4 Conclusions

A simple one-step radical system for the grafting polymerization of MMA onto PP films and fibers was developed using an alkylzinc complex (Phen–DEZ) as the radical source. By using this initiator, the graft polymerization can not only occur at a high temperature (60 °C) but can also take place at low temperature (0 °C). FTIR, Raman, and XRD measurements confirmed the presence of grafted monomer. AFM images showed the changes in PP morphology before and after grafting. In addition, the introduction of PMMA to the PP film improved the wettability. Furthermore, Phen–DEZ can be applied for the grafting modification of PP nanofibers at ambient temperature without changing the nanostructure.

4.5 References

1. Vashurin, A.; Kuzmin, I.; Titov, V.; Pukhovskaya, S.; Razumov, M.; Golubchikov, O.; Koifmanc, O. The surface modification of the polypropylene by aqueous soluble CoII phthalocyanine to obtain materials for Catalysis. Macroheterocycles. 2015, 8, 351-357.
2. Domagala, W. U. Pretreatment of polypropylene films for following technological processes, part 2: The use of low temperature plasma method. J. Appl. Polym. Sci. 2011, 122, 2529-2541.
3. Moosheimer, U.; Bichler, Ch. Plasma pretreatment of polymer films as a key issue for high barrier food packagings. Surf. Coat. Technol. 1999, 116, 812-819.
4. Green, M. D.; Guild, F. J.; Adams, R. D. Characterisation and comparison of industrially pre-treated homopolymer polypropylene, HF 135M. Int. J. Adhes. Adhes. 2002, 22, 81-90.
5. Blais, P.; Carlsson, D. J.; Csullog, G. W.; Wiles, D. M. The chromic acid etching of polyolefin surfaces, and adhesive bonding. J. Colloid Interface Sci. 1974, 47, 636-649.
6. Ying, W. B.; Lee, M. W.; Yang, H. S.; Moon, D. S.; Ko, N. Y.; Lee, B.; Zhu, J.; Zhang, R.; Lee, K. J. Synthesis of Multifunctionalized Graft-Type Polyolefin-Based Elastomers with a High Utility Temperature, Macromol. Chem. Phys. 218 (2017) https://doi.org/10.1002/macp.201700298.
7. Ding, L.; Li, J.; Wang, C.; Lin, L. Controlled synthesis of photosensitive graft copolymers with high azobenzene-chromophore loading densities in the main and side chains by combining ATRP and ADMET polymerization. React. Funct. Polym. 2015, 91-92, 85-92.
8. Ye, Z.; Xu, L.; Dong, Z.; Xiang, P. Designing polyethylenes of complex chain architectures via Pd-diimine-catalyzed "living" ethylene polymerization. Chem. Commun. 2013, 49, 6235-6255.
9. Jang, J.; Go, W. Continuous Photografting of HEMA onto Polypropylene Fabrics with Benzophenone Photoinitiator. Fiber. Polym. 2008, 9, 375-379.
10. Kunita, M. H.; Girotto, E. M.; Muniz, E. C.; Rubira, A. F. Polypropylene grafted with glycidyl methacrylate using supercritical CO_2 medium. Braz. J. Chem. Eng. 2006, 23, 267-271.
11. Zhuang, L.; Chen, S.; Lin, R.; Xu, X. Preparation of a solid amine adsorbent based on polypropylene fiber and its performance for CO_2 capture. J. Mater. Res. 2013, 28, 2881-2889.
12. Champagne, M. F.; Huneault, M. A.; Roux, C.; Peyrel, W. Reactive compatibilization of polypropylene/polyethylene terephthalate blends. Polym. Eng. Sci. 1999, 39, 976-984.
13. Vahdat, A.; Bahram, H.; Ansari, N.; Ziaie, F. Radiation grafting of styrene onto polypropylene fibres by a 10 MeV electron beam. Radiat. Phys. Chem. 2007, 76, 787-793.
14. Zhang, Y.; Liu, J.; Hu, W.; Feng, Y.; Zhao, J. The chemical modification and characterization of polypropylene membrane with environment response by in-situ

chlorinating graft copolymerization. Appl. Surf. Sci. 2017, 412, 627-637.
15. Dokolas, P.; Qiao, G. G.; Solomon, D. H. Graft copolymerization studies. III. Methyl methacrylate onto polypropylene and polyethylene terephthalate. J. Appl. Polym. Sci. 2002, 83, 898-915.
16. Sehgal, T.; Rattan, S. Synthesis, characterization and swelling characteristics of graft copolymerized isotactic polypropylene film. Int. J. Polym. Sci. 2010. http://dx.doi.org/10.1155/2010/147581.
17. Furukawa, J.; Saigusa, T.; Tsuruta, T.; Kakogawa, G.; New catalyst for the polymerization of alkylene oxides, Makromol. Chem. 1959, 36, 25-39.
18. Saegusa, T.; Imai, H.; Furukawa, J. Metal alkyl catalysts for cationic polymerization of vinyl monomers, Makromol. Chem. 1964, 79, 207-220.
19. Nakayama, Y.; Tsuruta, T.; Furukawa, J. Catalytic reactivity of organometallic compounds in olefin polymerization V. the co-catalytic action of oxygen on the vinyl polymerization induced by organometallic compounds. Makromol. Chem. 1960, 40, 79-90.
20. Liu, S.; Zheng, Z.; Li, M.; Wang, X. Effect of oxidation progress of tributylborane on the grafting of polyolefins. J. Appl. Polym. Sci. 2012, 125, 3335-3344.
21. Hou, L. L.; Zhao, M. Studies on the preparation of multi-monomer grafted PP by one-step extrusion and the blends with PVC. Express. Polym. Lett. 2008, 2, 19-25.
22. Hajfarajollah, H.; Mehvari, S.; Habibian, M.; Mokhtarani, B.; Noghabi, K. A. Rhamnolipid biosurfactant adsorption on a plasma-treated polypropylene surface to induce antimicrobial and antiadhesive properties Noghabi. RSC. Adv. 2015, 5, 33089-33097.
23. Wujcik, E. K.; Duirk, S. E.; Chase, G. G.; Monty, C. N. A visible colorimetric sensor based on nanoporous polypropylene fiber membranes for the determination of trihalomethanes in treated drinking water. Sens. Actuators, B-Chem. 2016, 223, 1-8.
24. Sevegney, M. S.; Kannan, R. M.; Siedle, A. R.; Naik, R.; Naik, V. M. Vibrational spectroscopic investigation of stereoregularity effects on syndiotactic polypropylene structure and morphology. Vib. Spectrosc. 2006, 40, 246-256.
25. Loos, J.; Bonnet, M.; Petermann, J. Morphologies and mechanical properties of syndiotactic polypropylene (sPP)/ polyethylene (PE) blends. Polymer. 1999, 41, 351-356.
26. Hahn, T.; Suen, W.; Kang, S.; Hsu, S. L.; Stidham, H. D.; Siedle, A. R. An analysis of the Raman spectrum of syndiotactic polypropylene. 1. Conformational defects. Polymer. 2001, 42 , 5813-5822.
27. Thakur, V. K.; Vennerberg, D.; Madbouly, S. A.; Kessler, M. R. Bio-inspired green surface functionalization of PMMA for multifunctional capacitors. RSC. Adv. 2014, 4, 6677-6684.
28. Masetti, G.; Cabassi, F.; Zerbi, G. Vibrational spectrum of syndiotactic polypropylene.

Raman tacticity bands and local structures of iso- and syndiotactic polypropylenes. Polymer 1980, 21(2), 143-152.
29. Lee, C. C.; Proust, G.; Alici, G.; Spinks, G. M.; Cairney, J. M. Three-dimensional nanofabrication of polystyrene by focused ion beam. J. Microsc-Oxford. 2012, 248, 129-139.
30. Bruckmoser, K.; Resch, K.; Kisslinger, T.; Lucyshyn, T. Measurement of interdiffusion in polymeric materials by applying Raman spectroscopy. Polym. Test. 2015, 46, 122-144.
31. Matsushita, A.; Ren, Y.; Matsukawa, K.; Inoue, H.; Minami, Y.; Noda, I.; Ozaki, Y. Two-dimensional Fourier-transform Raman and near-infrared correlation spectroscopy studies of poly(methyl methacrylate) blends 1. Immiscible blends of poly(methyl methacrylate) and atactic polystyrene. Vib. Spectrosc. 2000, 24, 171-180.
32. Thomas, K. J.; Sheeba, M.; Nampoori, V. P. N.; Vallabhan, C. P. G.; Radhakrishnan, P. Raman spectra of polymethyl methacrylate optical fibres excited by a 532 nm diode pumped solid state laser, J. Opt. A: Pure Appl. Op. 10 (2008) 055303/1-055303/5.
33. Peterson, J. D.; Vyazovkin, S.; Wight, C. A. Kinetic Study of Stabilizing Effect of Oxygen on Thermal Degradation of Poly(methyl methacrylate). J. Phys. Chem. B. 1999, 103, 8087-8092.
34. Kashiwagi, T.; Inaba, A.; Brown, J. E.; Hatada, K.; Kitayama, T.; Masuda, E. Effects of weak linkages on the thermal and oxidative degradation of poly(methyl methacrylates). Macromolecules. 1986, 19, 2160-2168.
35. Zhu, B.; Dong, W.; Wang, J.; Song, J.; Dong, Q. Modification of polypropylene via the free‐radical grafting ternary monomer in water suspension systems. J. Appl. Polym. Sci. 2012, 126, 1844-1851.
36. Rong, M. Z.; Zhang, M. Q.; Zheng, Y. X.; Zeng, H. M.; Friedrich, K. Improvement of tensile properties of nano-SiO_2/PP composites in relation to percolation mechanism. Polymer. 2001, 42, 3301-3304.

Chapter 5:

Graft polymerization of MMA on cotton initiated by Phen-DEZ

5.1 Introduction

Recently, due to the environmental crises, the demand for replacing synthetic materials with natural resources has increased. Cellulose is an organic raw material that has received widespread attention, and cotton which is composed of 95% cellulose is commonly used, natural, and inexpensive material. Because of its comfortability and breathability, cotton is extensively used in the manufacture of personal care items, bedding products, clothing, and underwear. However, cotton also suffers from inherent flammability, low abrasion durability, and poor interfacial compatibility with other matrices. With the development and progress of technology, the benefits of cotton are no longer limited to its softness and warmth. Nevertheless, novel methods must be developed to further enhance the functional diversity of cotton materials. To expand the number of applications of cotton, its structure and properties can be modified by introducing polymer chains with various functional groups on the cellulose backbone. Among the many methods of modifying cotton, graft polymerization can modify the cellulose structure, tailor its properties, and increase the functionality of cotton without compromising the intrinsic properties of cellulose. Grafting functional monomers onto cotton to improve various aspects has been widely studied.

The flammability of cotton is a critical issue that has been specifically considered for various applications. Many researchers have devoted great efforts to improving the flame retardancy of cotton [1, 2]. It is generally believed in the clothing industry that increased water vapor permeability signifies higher comfort of the fabric. Recently, owing to the potential industrial applications, superhydrophobic cotton surface have generated tremendous research interest [3-6]. By grafting non-fluorinated methacrylate, waterproof, windproof and breathable cotton fabrics have been prepared [7]. The textile industry has stringent requirement for the mechanical properties of cotton, including abrasion resistance and tensile properties. The physical and mechanical properties of cotton can be greatly improved through graft modification [8]. In addition, antimicrobial properties [9] and dyeability [10, 11] can be imparted to the grafted cotton.

The grafting of vinyl monomers on cotton has been studied in detail and in most cases the reaction has been performed at 60°C or higher using ordinary radical initiators [3, 12].

Previously, we reported a novel organic zinc complex, diethyl(1,10-phenanthroline N^1,N10)zinc (Phen-DEZ), and investigated its initiation behavior [13-15]. As a highly reactive initiator, Phen-DEZ rapidly initiated homopolymerization and graft polymerization at room temperature without additional heating or other stimulation. However, whether this novel initiator can efficiently initiate graft polymerization in an emulsion system has not been tested. In emulsion systems, polymers with high molecular weights can be obtained. Therefore, graft modification of cotton in an emulsion system can enable uniform grafting of long polymer chains onto its surface. In this study, the graft polymerization of methyl methacrylate (MMA) onto cotton was performed under various conditions, and FTIR, XRD, TG and SEM analyses were performed for the grafted and original cotton.

5.2 Experimental

5.2.1 Materials

The cotton (gossypium herbaceum) provided by Hamayuan was purified by extraction with hot acetone under boiling for 5 h. MMA was purchased from Wako Pure Chemical Industry, Ltd., and the stabilizer was removed according to previously published methods [15]. Diethylzinc was supplied by Nippon Aluminum Alkyls, Ltd. and 1,10-phenanthroline, chloroform (CHCl3), methanol, acetone, magnesium sulfate, sodium dodecyl sulfate (SDS), sodium hydroxide were purchased from Wako Pure Chemical Industry, Ltd. Ultrapure distilled water was obtained using a Milli-Q laboratory system.

5.2.2 Equipment and instrumentation

The FTIR spectra of modified and unmodified cotton were obtained using a Jasco FT/IR-480 Plus spectrometer from 400 to 4000 cm^{-1}. The surface morphology of the cotton was observed by SEM (Hitachi SU-8020). The molecular weight of the free polymer was determined by size-exclusion chromatography (SEC, Jasco PU-2080 Plus pump) equipped with an RI-2031 Plus Intelligent RI detector. CHCl3 was used as the eluent (40°C) and XRD patterns were recorded under ambient conditions with Cu-Kα radiation. The thermal behaviors of the prepared cotton samples were analyzed by TGA (Hitachi, STA 7200 RV) in air at a heating rate of 10°C /min. The surface morphology of the cotton fiber was examined using a field emission (FE)-SEM (Hitachi SU-8020).

5.2.3 Synthesis of Phen-DEZ

The synthesis method for Phen-DEZ was the same as that employed in the literature [13]. A certain amount of DEZ was slowly injected into a mixture of 1,10-phenanthroline and hexane. The reaction was performed at 23°C for 24 h. The reddish-orange Phen-DEZ solid was collected by filtration and dried in vacuo. All processes were performed under an argon atmosphere.

5.2.4 Preparation of modified cotton fabrics

Grafted cotton was prepared via emulsion polymerization. The cotton (50mg), SDS (180 mg), and 7.5 mL water were added to a 50 mL flask and stirred. After the materials were sufficiently blended, the flask was degassed using two freeze-pump-thaw cycles. A defined amount of monomer (2.5mL) was then added to the flask. Continuous stirring of the mixture was performed for 1 h and 80 mg of Phen-DEZ was added to the stable emulsion system under an Ar flow. Polymerization was performed at room temperature (23°C) for 24 h. The grafted cotton was extracted to a constant weight with chloroform and vacuum drying. The extract was poured into methanol and the recovered homo-PMMA was dried and weighed.

The graft yield (Yg) was calculated using the weight increase in the original cotton according to the following equation:

$$Yg = (m1-m0)/m0 \times 100\%$$

where, m0 is the weight of the original cotton sample and m1 is the weight of the cotton after graft polymerization.

5.3 Results and discussion

Graft polymerization was performed at room temperature (23 °C) in an emulsion system with a constant emulsifier concentration. Cotton is compatible with water, resulting in full contact with the initiator and monomer during graft polymerization. The initiator gained access to the cotton fabric via the many reactive sites available for graft polymerization. To compare with the emulsion polymerization method, bulk and solution graft polymerizations were also performed. The ratio of monomer to initiator was fixed at 90:1 and the other conditions were identical to those used for emulsion polymerization.

Table 1. Graft polymerization of MMA onto cotton fibers by Phen-DEZ.

Entry	Molar ratio (initiator:monomer)	System	Graft yield%
1	1:500	Emulsion	16.7
2	1:180	Emulsion	69.7
3	1:90	Emulsion	89.1
4	1:30	Emulsion	35.3
5	1:90	Bulk	7.1
6	1:90	Solution	2.1

Table 1 shows the changes in the grafting yield and molecular weight of the free PMMA with varying ratios of monomer to initiator. The graft yield with a Phen-DEZ/MMA ratio of 1:500 was 16.7%, and when the ratio was increased to 1:180 and 1:90, the graft yields were 69.7% and 89.1%, respectively. However, when the molar ratio of Phen-DEZ/MMA was 30:1, the graft yield decreased to 35.3%. That is, only within a certain initiator concentration does the yield of grafting increases with increasing initiator content. When the initiator concentration is excessively high, the probability of bi-radical termination increases and the graft yield decreases. After measuring the molecular weight of the free polymer, the molecular weight of the homopolymer obtained using this method was very high. For example, under the conditions of Entry 3, Mw reached 1.53×106Da. It is generally believed that the molecular weight of a grafted polymer is close to that of the free polymer [3, 16]. Therefore, Phen-DEZ as an initiator in an emulsion system can result in higher grafting yields and high molecular weight of the grafted polymer chains.

For comparison with the emulsion system, we also grafted cotton in a solution system with toluene as a solvent and a bulk polymerization system. By comparing the data in Table 1 (Entries 3, 5, and 6), it is clear that the cotton modified in the emulsion system exhibited a higher graft yield. This is likely because, for cotton, water is good swelling medium and can break the hydrogen bonding and increase the accessibility of the cotton fiber to the grafted monomer [17]. Therefore, emulsion graft polymerization, which is environmentally friendly and efficient, is suitable for cotton surface modification while depositing long polymer chains on the surface. Table 1 shows that when the ratio of monomer to initiator is 90:1, the graft yield is the highest among all the tested conditions. Therefore, that the samples prepared under these conditions were used for subsequent measurements.

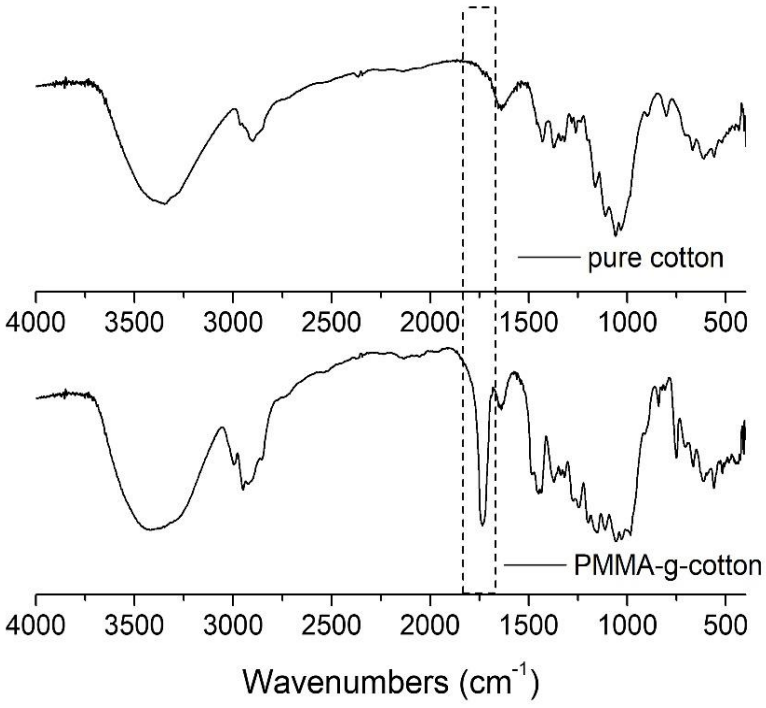

Figure 1. FTIR spectra of (a) pristine cotton and (b) PMMA-g-cotton

Figure 1 shows FTIR spectra of the pure and modified cotton samples. Figure 1(a) and (b) shows the same cotton characteristic FTIR peaks [18, 19]. The band at 3000–3500 cm-1 is attributed to the stretching vibration of –OH and that at 2900 cm-1 is assigned to the stretching vibration of C-H. The weak absorption at 2852 cm-1 is associated with the symmetric stretching of -CH2. The bands at 1429 and 1318 cm-1 are assigned to C-H wagging. The bands at 1161 and 1110 cm-1 correspond to C-O-C asymmetric stretching. The band at 1032 cm-1 is characteristic of C-O stretching, while that at 1058 cm-1 is attributed to asymmetric in-plane ring stretching.

In Figure 1(b), all characteristic absorption peaks of PMMA are observed [20], including the peak at 1732 cm-1 which is attributed to the C=O stretching vibration of the ester groups of grafted PMMA [21]. The bands at 2994 and 2950 cm-1 are attributed to C-H bond stretching vibrations of the –CH3 and –CH2– groups. The distinct band at 753 cm-1 is assigned to the α-methyl group vibration. The bands at 1151 and 1246 cm-1 correspond to the C-O-C stretching vibration. However, all these peaks are absent in the pure cotton samples, indicating that MMA was successfully grafted onto the cotton fabric.

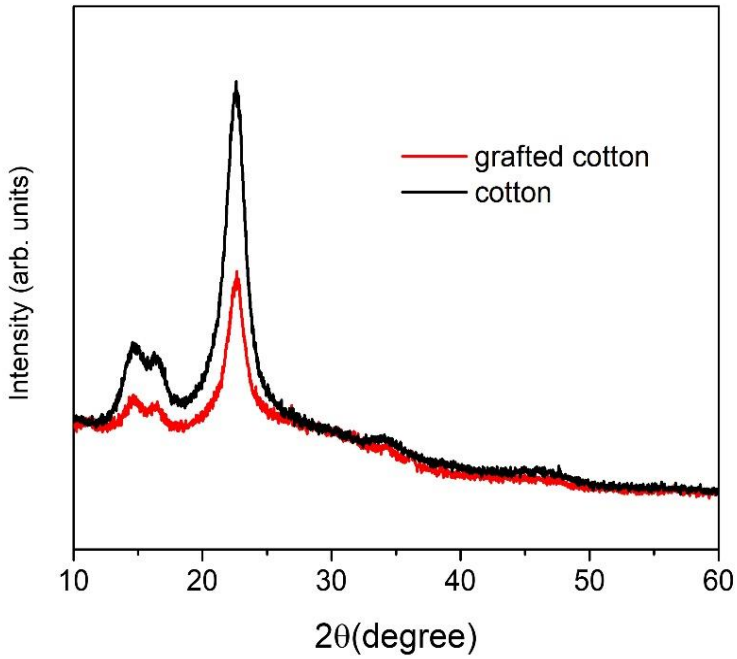

Figure 2. XRD patterns of the pure and PMMA-g-cotton samples.

The XRD spectra of the natural (pure) and grafted cotton are shown in Figure 2. The XRD patterns of the cotton before and after graft modification show diffraction peaks at 2θ=14.9°, 16.6° and 22.7°, arising from the typical structure of native cotton fibers [17, 22]. The characteristic peak positions of the two curves are identical, but the peak intensity is significantly reduced by graft modification. Because cellulose is semicrystalline, the hydroxyl groups in the amorphous regions are modified, resulting in the decrease of percentage crystallinity. This result indicates that the crystallization properties of the cotton fibers change upon graft modification.

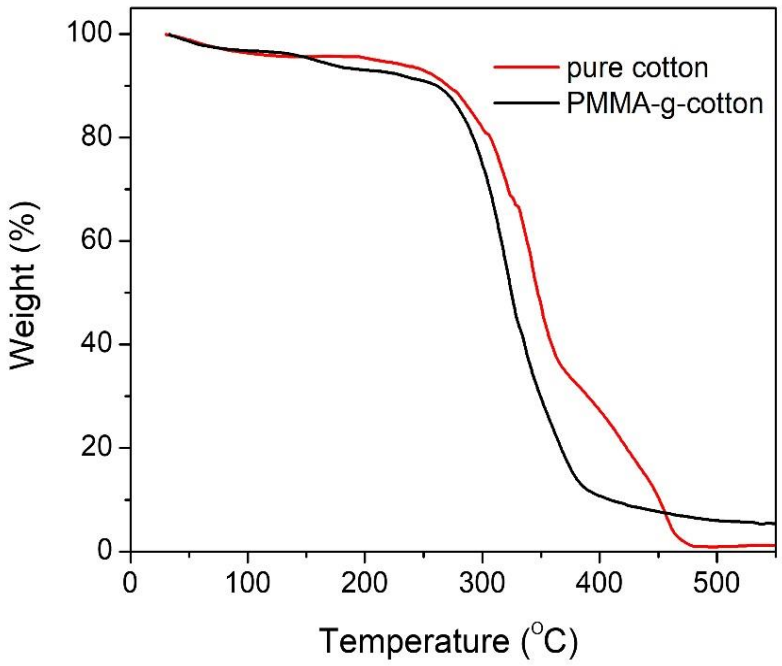

Figure 3. TG profiles of pure cotton and PP-g-PMMA (89.1%).

The thermal stabilities of the pure cotton and grafted cotton samples were assessed by TGA in air and the results are presented in Figure 3. The weight loss during the initial stage is attributed to the loss of water and solvent remaining on the surface and inner cavities of the cotton fiber. When the temperature increased to > 300 °C, both, the pure and modified cotton, start decomposing. The initial decomposition temperatures of the two cotton samples are similar, as is their decomposition behavior. However, when the temperature is increased to > 480 °C, the unmodified cotton completely decomposes, but the grafted cotton still retains approximately 8% of its original weight. This is likely because the amount of grafted PMMA on the cotton surface is relatively large, thereby covering it uniformly. The grafted PMMA and cotton start to decompose with increasing temperature, but the grafted PMMA layer can protect the cotton during decomposition. Therefore, when the temperature is increased to 500 °C, 8% of the residue remains.

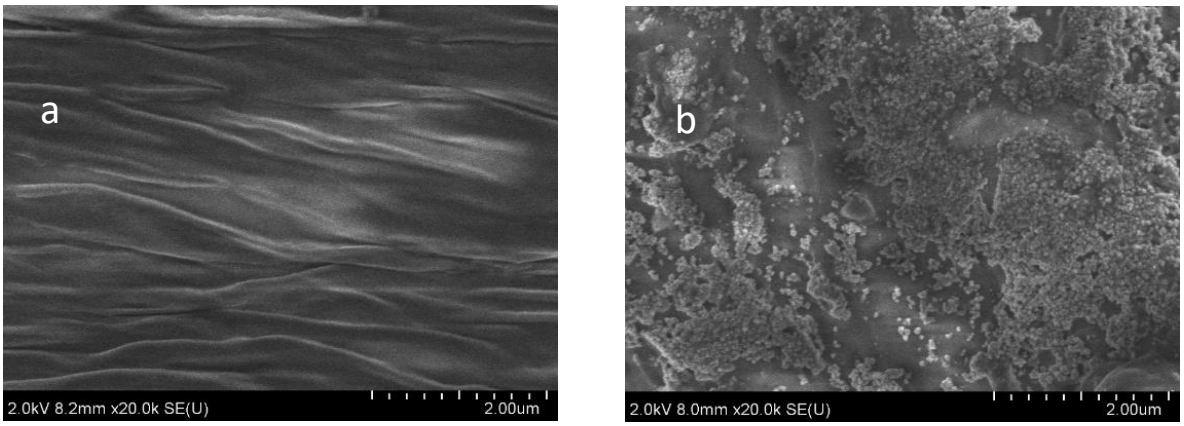

Figure 4. SEM micrographs of the pure cotton (a) and cotton-g-PMMA samples (b)

The surface of pure cotton and cotton-g-PMMA was examined by SEM (Figure 4). As shown in Figure 4 (a), pure cotton exhibits a texture with striations and nanogrooves [23]. Compared to the images of the grafted cotton, it is evident that the texture of cotton after surface modification disappears, and the surface is covered with a rough polymer film. Because of this significant morphological change, it is easily concluded that MMA was grafted to the cotton by the Phen-DEZ initiator.

Because the cotton used in the experiment is a fiber, it is difficult to prepare a uniform and flat sample; consequently, the cotton before and after modification cannot be used to measure the contact angle. To study the surface properties of the cotton fiber after modification, two cotton balls (raw cotton and grafted cotton) were added to a mixture of pure water and MMA monomer, shaken, and allowed to stand until settlement lamination. The significant differences in wettability can be seen in Figure 5. The unmodified cotton sinks to the water layer at the bottom of the bottle, indicating the hydrophilicity of the cotton fiber. The grafted cotton is completely immersed in the MMA solution because the cotton surface after graft modification is covered with a layer of PMMA, making its dispersion in MMA more favorable. Based on these results, it can be concluded that surface graft modification changed the surface properties of cotton, improving its compatibility with polymers.

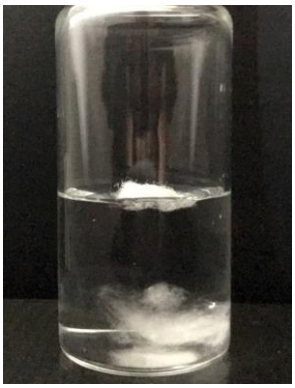

Figure 5. Immersion of pure and grafted cotton fibers in water

Figure 5. Immersion of pure and grafted cotton fibers in a water/MMA mixture

(upper: MMA layer, lower: water layer).

5.4 Conclusion

A highly efficient, green, and nonpolluting method for the surface modification of cotton was developed. MMA was grafted onto cotton fibers using Phen-DEZ as an initiator in an emulsion system at ambient temperature. This method is an environmentally friendly process for the surface modification of cotton. FTIR, XRD, TG, and SEM measurements confirmed the success of graft polymerization. By comparing the compatibility of the grafted and unmodified cotton samples in water and MMA solvent, the affinity of the modified cotton for the MMA solvent was evident. The hydrophilicity of the modified cotton decreased, while the grafted polymer chains on the cotton increased its compatibility with polymeric materials.

5.5 References

1. Verma, S. K.; Kaur I. Gamma-induced polymerization and grafting of a novel phosphorus-, nitrogen-, and sulfur-containing monomer on cotton fabric to impart flame retardancy. J. Appl. Polym. Sci. 2012, 125, 1506-1512.
2. Kaur, I.; Bhati, P.; Sharma, B. Antibacterial, flame retardant, and physico-chemical properties of cotton fabric graft copolymerized with a binary mixture of acrylonitrile and 4-vinylpyridine. J. Appl. Polym. Sci. 2014, 131, 40415/1-40415/14.
3. Li, Y.; Li, Q.; Zhang, C.; Cai, P.; Bai, N.; Xu, X. Intelligent self-healing superhydrophobic modification of cotton fabrics via surface-initiated ARGET ATRP of styrene. Chem. Eng. J. 2017, 323, 134-142.
4. Jiang, B.; Chen, Z.; Sun, Y.; Yang, H.; Zhang, H.; Dou, H.; Zhang, L. Fabrication of superhydrophobic cotton fabrics using crosslinking polymerization method. Appl. Surf. Sci. 2018, 441, 554-563.
5. Yu, Y.; Wang, Q.; Yuan, J.; Fan, X.; Wang, P.; Cui, L. Hydrophobic modification of cotton fabric with octadecylamine via laccase/TEMPO mediated grafting. Carbohyd. Polym. 2016, 137, 549-555.
6. Periolatto, M.; Ferrero, F. Cotton and polyester surface modification by methacrylic silane and fluorinated alkoxysilane via sol-gel and UV-curing coupled process. Surf. Coat. Tech. 2015;271:165-173.
7. Wu, J.; Li, J.; Wang, Z.; Yu, M.; Jiang, H.; Li, L.; Zhang, B. Designing breathable superhydrophobic cotton fabrics. RSC Adv. 2015, 5, 27752-27758.
8. Effenberger, F.; Schweizer, M.; Mohamed, W. S. Elucidation of the nanoparticle effect on the grafting of vinyl monomers onto cotton fabric. J. Appl. Polym. Sci. 2009, 113, 492-501.
9. Nogueira, F.; Vaz, J.; Mouro, C.; Piskin, E.; Gouveia, I. Covalent modification of cellulosic-based textiles: A new strategy to obtain antimicrobial properties. Biotechnol. Bioproc. E. 2014, 19, 526-533.
10. Maulik, S. R.; Das, D.; Bhattacharya, S. C. Modification of cotton fabric with acrylamide in the presence of $K_2S_2O_8$ for improving dyeability of natural dyes. J. Text. I. 2011, 102, 131-139.
11. Ibrahim, N. A.; E-Zairy, W. R.; Eid, B. M. Novel approach for improving disperse dyeing and UV-protective function of cotton-containing fabrics using MCT-β-CD. Carbohyd. Polym. 2010, 79, 839-846.
12. Klimov, V. V.; Bryuzgin, E. V.; Le, M. D.; Zelenova, E. A.; Nguyen, T. H.; Navrotskii, A. V.; Nishide, H.; Novakov, I. A. An investigation of the hydrophobic property stability of grafted

polymeric coatings on a cellulose material surface. Polym. Sci. Ser. D. Glues Sealing Mater. 2016, 9, 364-367.
13. Zhao, C.; Okada, H.; Sugimoto, R. Polymerization of styrene in aqueous system using a diethylzinc and 1,10-phenanthroline complex. Polymer. 2018, 154, 211-217.
14. Zhao, C.; Okada, H.; Sugimoto, R. Diethyl(1,10-phenanthroline-N1,N10)zinc initiated grafting of styrene on polypropylene/ polyethylene. Bull. Chem. Soc. Japan. 2018, 91, 1576-1578.
15. Zhao, C.; Okada, H.; Sugimoto, R. Surface modification of polypropylene with poly(methyl methacrylate) initiated by a diethylzinc and 1,10-phenanthroline complex. React. Funct. Polym. 2018, 132, 127-132.
16. Matyjaszewski, K.; Dong, H.; Jakubowski, W.; Pietrasik, J.; Kusumo, A. Grafting from Surfaces for "Everyone": ARGET ATRP in the Presence of Air. Langmuir. 2007, 23, 4528-4531.
17. Parikh, D. V.; Thibodeaux, D. P.; Condon, B. X-ray crystallinity of bleached and crosslinked cottons. Text. Res. J. 2007, 77, 612-616.
18. Jiang, B.; Chen, Z.; Sun, Y.; Yang, H.; Zhang, H.; Dou, H.; Zhang, L. Fabrication of superhydrophobic cotton fabrics using crosslinking polymerization method. Appl. Surf. Sci. 2018, 441, 554-563.
19. Lin, J.; Zheng, C.; Ye, W. J.; Wang, H. Q.; Feng, D. Y.; Li, Q. Y.; Huan BW. A facile dip-coating approach to prepare SiO2/fluoropolymer coating for superhydrophobic and superoleophobic fabrics with self-cleaning property. J. Appl. Polym. Sci. 2015, 132, 41458/1-41458/9.
20. Duan, G.; Zhang, C.; Li A.; Yang, X.; Lu, L.; Wang X. Preparation and characterization of mesoporous zirconia made by using a poly(methyl methacrylate) template. Nanoscale. Res. Lett. 2008, 3, 118-122.
21. Dokolas, P.; Qiao, G. G.; Solomon, D. H. Graft copolymerization studies. III. Methyl methacrylate onto polypropylene and polyethylene terephthalate. J. Appl. Polym. Sci. 2002, 83, 898-915.
22. Palama, I. E.; D'Amone, S.; Arcadio, V.; Caschera, D.; Toro, R. G.; Gigli, G.; Cortese, B. Underwater Wenzel and Cassie oleophobic behavior. J. Mater. Chem. A. 2015, 3, 3854-3861.
23. Cortese, B.; Caschera, D.; Padeletti, G.; Ingo, G. M.; Gigli, G. A brief review of surface-functionalized cotton fabrics. Surf. Innov. 2013, 1, 140-156.

Chapter 6:

Graft polymerization of MMA on silk initiated by Phen-DEZ

6.1 Introduction

Silk is one of the most highly sought nature fibers, which presents many excellent properties, such as high moisture absorbency, good biocompatibility, and graceful luster [1-2]. Owing to these features, silk fibers are widely used for decorations, clothes, and other products useful for the human body [3]. However, there are some limitations to the applications of silk, which are mainly attributed to its poor crease recovery, low limiting oxygen index, easy yellowing, fibrillation, and poor color fastness [1,4]. Therefore, finding ways to overcome these shortcomings is important for expanding the application of silk fibers. Many papers on the physical and chemical modification of silk have been published recently. Compared with other methods of modifying silk fiber, graft polymerization involves low energy consumption, leads to long-lasting modification effects, imparts excellent properties to the final product, and improves the existing properties of the parent polymer without degrading its original properties [5]. Free radical polymerization has been widely used for graft polymerization owing to its mild reaction conditions and the simplicity of the procedure. Many monomers were grafted onto silk fiber using graft polymerization, including 2-hydroxyethyl methacrylate [6], methacrylamide (MAA) [6], octafluoropentyl [7], and diethylene glycol dimethacrylate [8]. Of all vinyl monomers, MMA is the most widely used monomer for silk grafting and still represents an attractive model for studying the physicochemical and structural changes caused by grafting [9,10].

In some of our previous published papers, we reported that diethyl(1,10-phenanthroline N^1,N^{10})zinc (Phen-DEZ) was used as a radical initiator for the successful graft modification of polypropylene and polyethylene [11,12]. However, there is no literature report has been published regarding the use of diethylzinc (DEZ) to initiate graft polymerization of silk. As the original intention of this study was to extend the applications of diethylzinc, silk was selected as graft polymerization matrix.

6.2 Experimental

6.2.1 Materials

Silk fibers from Bombyx mori silkworms were used as MMA grafting substrate after degumming and cleaning them for 12 h in a Soxhlet extractor using acetone and water to remove impurities. Nippon Aluminum Alkyls, Ltd. supplied DEZ. Sodium dodecyl sulfate (SDS), MMA, MgSO4, NaOH, hexane, chloroform, acetone, methanol, and 1,10-phenanthroline were purchased from Wako Pure Chemical Industry, Ltd. To remove the stabilizer, MMA was washed with NaOH. Deionized water was used to prepare all solutions. Resin dye (SDN blue) was purchased from Osaka Kaseihin. Co., Ltd.

6.2.2 Characterization and measurements

The Fourier transform infrared (FTIR) spectra of modified and unmodified silk were recorded on a Jasco FT/IR–480 Plus spectrometer, in the range of 400–4000 cm^{-1}. The surface morphology of silk was examined using a Hitachi SU-8020 scanning electron microscopy (SEM) instrument. Thermogravimetric analysis (TGA) of silk was carried out using a Hitachi STA7200 RV analyzer in air at the heating rate of 10 °C/min. The surface morphology of silk fiber was analyzed using a Hitachi SU-8020 field emission-SEM apparatus.

6.2.3 Preparation of Phen-DEZ.

We used the same method reported in one of our previously published papers to synthesize Phen-DEZ [13]. The reaction was performed in a two-necked 50 mL round bottom flask equipped with a stirrer. Hexane (20 mL) and 1,10-phenanthroline (1080 mg) were added to the reaction system, while slowly injecting 0.7 mL DEZ at 23 °C. After allowing the mixture to react for 24 h under argon atmosphere for protection, the mixture was filtered and the obtained Phen-DEZ was collected and dried in vacuo.

6.2.4 Graft polymerization procedure.

Since silk fiber can be fully dispersed in water and using water as solvent presents advantages (water is a low cost, non-polluting substance), an emulsion polymerization system was selected in this study. Silk fiber (100 mg), SDS (180 mg) and deionized water (7.5 mL) were added to a 50 mL flask. The excess oxygen was removed using freeze-pump-thaw cycles. Then, 2.5 mL MMA was added to the reaction system using a syringe. After fully mixing the

reactants, the required amount of Phen-DEZ (33mg–500mg) was added to the solution. The graft polymerization systems were maintained at the desired temperature (see Table 1) for 24 h. The grafted silk samples were extracted using chloroform for 100 h to remove the homopolymer and were subsequently dried and weighted.

The grafting yield (Yg) was calculated using to the following equation:

$Yg = (m_1 - m_0) / m_0 \times 100\%$

where m_0 and m_1 are the initial weight of pure silk and weight of the grafted silk, respectively.

6.2.5 Dyeing

The degummed, pure silk, and MMA-grafted silk (silk-g-MMA) were dyed using commercial resin dye (SDN blue). The ratio of dye solution to water was maintained at 1:20. Dyeing was performed at 60 °C for 5 min and was followed by ultrasonic cleaning and washing using running water. Soap solution was used to further clean the dyed silk fiber. Lastly, both silk fibers were dried in vacuum at 23 °C, and the dried silk was directly used for color comparison.

6.3 Results and discussion

By changing the reaction conditions, such as the initiator concentration and temperature, it was possible to obtain grafted silk fiber featuring different graft ratios. The results are summarized in Table 1.

Table 1. Graft polymerization of methyl methacrylate onto silk fiber (I:M is the initiator to monomer molar ratio)

Entry	Temperature (°C)	I:M (molar ratio)	Graft yield (%)
1	23	1:15	23.0
2	23	1:30	97.6
3	23	1:90	222.6
4	23	1:300	280.8
5	50	1:300	1230.6
6	80	1:300	959.3

As the initiator to monomer (I:M) molar ratio increased from 1:300 to 1:15, the graft yield decreased. When the I:M ratio increased from 1:300 and 1:90, the graft yield decreased, but remained above 200%. However, when the I:M ratio was further increased to 1:30, the graft yield was significantly reduced to 97.6%. These results suggested that within the range of I:M ratios selected in this study, increasing the amount of initiator caused the bi-radical termination of excessive radicals, and thus, caused the grafting rate to decrease.

The effect of temperature on the graft yield was more pronounced than that of the initiator concentration. When the reaction temperature was increased from 23 to 50 and 80 °C, the graft yield greatly increased. That could be attributed to the increase in temperature leading to more grafting sites being produced on the surface of the silk fibers, and consequently to the increase in graft yield. On the other hand, increasing the temperature also increased the rate of bi-radical termination. Therefore, when the temperature was further increased from 50 to 80 °C, the graft yield decreased again.

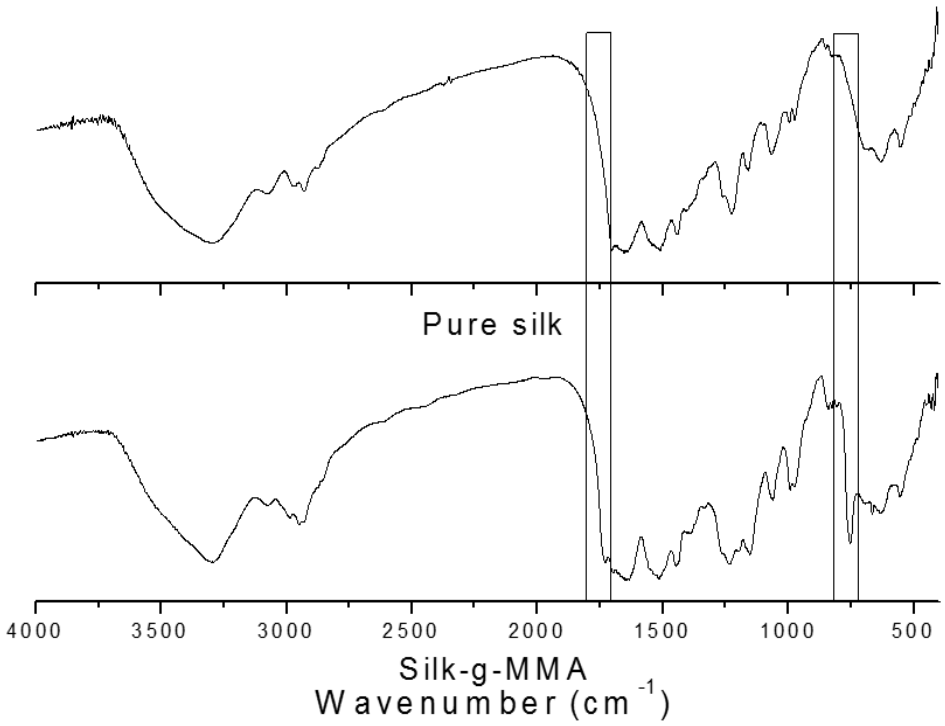

Figure 1. FTIR spectra of pure silk and methyl methacrylate-grafted silk (silk-g-MMA)

The FTIR spectra of pure and grafted silk are shown in Figure 1. The characteristic absorption peak at 3300 cm^{-1} was assigned to the N–H hydrogen bonds, and the peak at

approximately 3080 cm^{-1} was ascribed to the N–H stretching vibrations. The spectra for the silk samples showed absorption bands at 1653, 1543, and 669 cm-1 (amides I, II, and V, respectively), which were assigned to the silk I structure [7,14-16]. In comparison of the FTIR spectra of the pure and grafted silk, the characteristic peaks of poly MMA (PMMA) were only identified in the spectrum of modified silk, which demonstrated that MMA was grafted onto silk [17,18]. In addition, the peak at 1732 cm^{-1} was attributed to the stretching vibrations of the ester carbonyl group, the absorption band at 2948 cm^{-1} corresponded to the $–CH_2–$ groups, the weak absorbance peaks at 1632 and 1261 cm^{-1} were identified to be the absorbance of the C–C stretching and –C–O–C groups of PMMA, respectively, the peaks at 1193 and 752 cm^{-1} were associated with the $–CH_2–$ group twisting and rocking modes, and the band at 1447 cm^{-1} represented the asymmetric stretching of the $–CH_3$ groups.

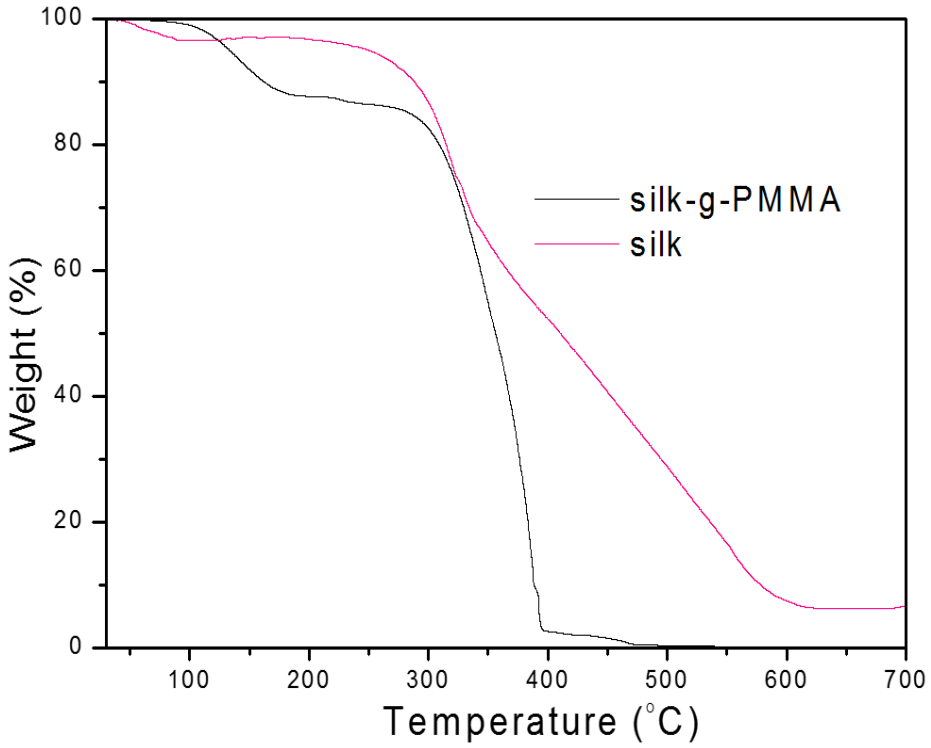

Figure 2. TGA curves for silk and silk-g-PMMA

Figure 2 illustrates the comparison of the TGA results for pure and grafted silk. The thermal behaviors of untreated and modified silk were quite different. The untreated silk fibers experienced a 4% weight loss at temperatures below 100 °C, while the grafted silk fibers did not exhibit significant weight loss. This occurred because the unmodified silk fibers absorbed moisture from the air, however the hygroscopicity of the grafted silk fibers was lowered by the grafted PMMA. Pyrolysis of untreated silk started at 250 °C, and when the temperature

exceeded 350 °C, the weight loss rate decreased and gradually stabilized. The two thermal decomposition stages could be attributed to the cleavage of silk fiber macromolecules and oxidation of carbon, respectively [1]. Two distinct mass loss processes can be observed in the TGA curve of silk-g-PMMA. The first weight loss stage was due to the least stable head to head linkage of grafted PMMA, which has been reported in previously published papers [19,20]. When the temperature reached 290 °C, the grafted silk fiber underwent random scission degradation of the grafted PMMA, which began to thermally decompose. This temperature was 40 °C higher than that of unmodified silk fiber, which indicated that the thermal stability of the grafted silk fiber was improved.

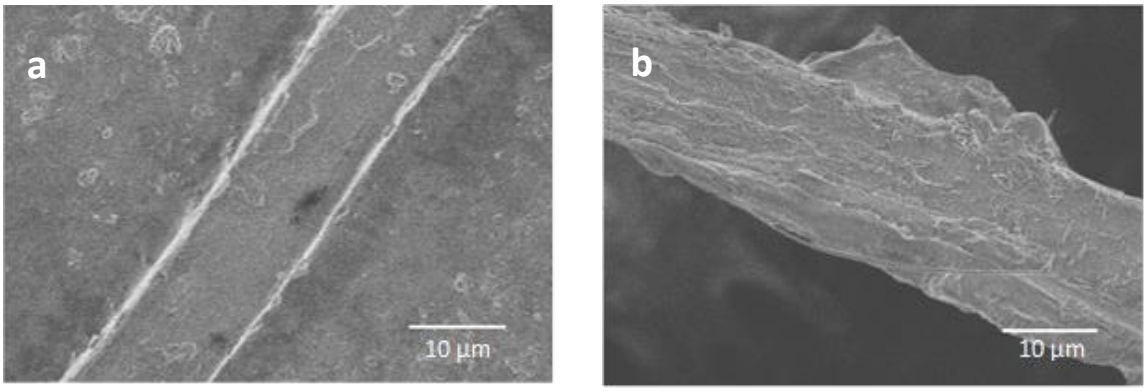

Figure 3. Scanning electron microscopy images of (a) pure silk fiber and (b) poly(methyl methacrylate)-grafted silk featuring 97.6% weight gain

Figure 3 presents the surface morphology of untreated silk (a) and silk-g-PMMA (b). Pure, untreated silk presents a clean and smooth surface and no obvious sediments and texture, while silk-g-PMMA exhibits a rough and uneven appearance. This demonstrated that MMA was successfully grafted onto the silk fiber. Using the SEM images, we concluded that the diameter of the pure silk fiber was approximately 12 µm, while the diameter of the grafted fiber was 16 µm. The increase in diameter was attributed to the grafted PMMA layer, which further demonstrated the success of the graft polymerization.

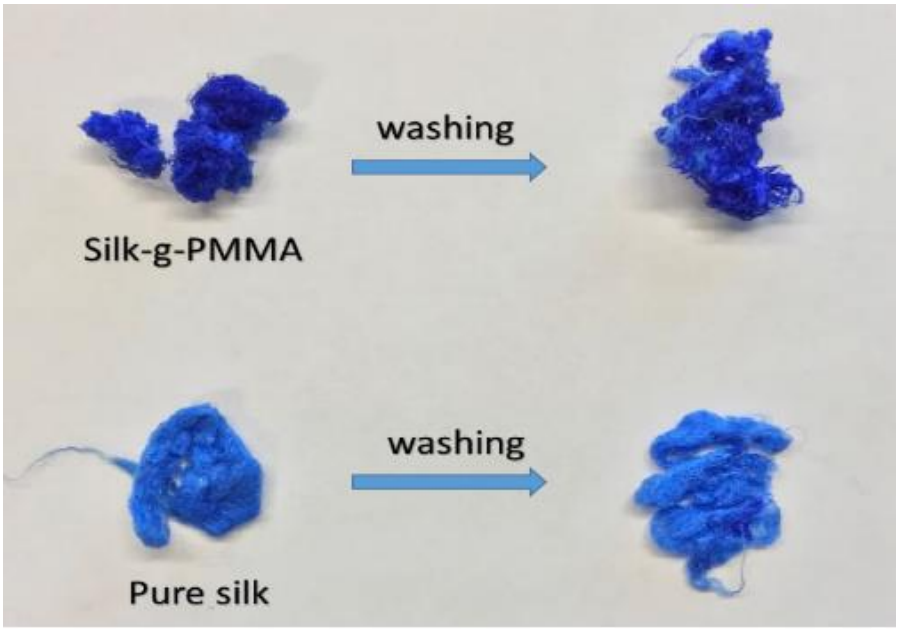

Figure 4. Dyeability of pure and poly(methyl methacrylate)-grafted silk (silk-g-PMMA).

Silk presents good dyeing performance, and its color is bright after dyeing. However, silk fiber exhibits poor color fastness performance and its color easily fades after washing. From figure 4, we observed that the dyeing performance of silk fiber before and after grafting was good, and the dyed silk fiber presented brilliant blue color. Compared with the pure silk fiber, the grafted one was more easily dyed and exhibited superior dyeing performance. However, after ultrasonic washing and soaping, both silk fibers presented different degrees of fading. Comparing the fading degrees of silk fibers before and after grafting, we concluded that the silk-g-PMMA fiber exhibited better dyeing properties than pure silk, and grafting could improve the color fastness of silk fiber. This could be attributed to the grafted PMMA molecules filling in the amorphous areas of silk, which resulted in higher free volumes inside the amorphous areas [4].

6.4 Conclusion

Graft polymerization of MMA onto silk fiber in an aqueous system using the Phen-DEZ complex as initiator was carried out, and the reaction presented high graft yield. The FTIR spectra confirmed the grafting of PMMA onto silk fiber. Moreover, the SEM images illustrated the changes in silk surface morphology before and after grafting. It was also found that the grafted silk presented higher thermal stability, better dyeability, as well as better color fastness than pure silk.

6.5 Reference

1. Liu, C.; Xing, T.; Wei, B.; Chen, G. Synergistic Effects and Mechanism of Modified Silica Sol Flame Retardant Systems on Silk Fabric. Materials. 2018, 11(10).
2. Cheng, X. W.; Guan, J. P.; Yang, X. H.; Tang, R. C. Improvement of flame retardancy of silk fabric by bio-based phytic acid, nano-TiO2, and polycarboxylic acid. Prog. Org. Coat. 2017, 112, 18-26.
3. Guan, J.; Chen, G. Flame resistant modification of silk fabric with vinyl phosphate. Fiber Polym. 2008, 9(4), 438-443.
4. Jutarat, P.; Watthana, K. Dyeing properties of Bombyx mori silks grafted with methyl methacrylate and methacrylamide. J. Appl. Polym. Sci. 2006, 100(2), 1169-1175.
5. Prachayawarakorn, J.; Boonsawat, K. Physical, chemical, and dyeing properties of Bombyx mori silks grafted by 2-hydroxyethyl methacrylate and methyl methacrylate. J. Appl. Polym. Sci. 2007, 106(3), 1526-1534.
6. Basri, M.; Harun, A.; Ahmad, M. B.; Razak, C. N. A.; Salleh, A. B. Immobilization of lipase on poly(N-vinyl-2-pyrrolidone-co-styrene) hydrogel. J. Appl. Polym. Sci. 2001, 82(6), 1404-1409.
7. Li, Z.; Jin, F.; Cao, B.; Wang, X. Modification of silk fibers via emulsion graft copolymerization with fluoroacrylate. Chinese J. Polym. Sci. 2008, 26(3), 353-362.
8. Chen, G.; Guan, J.; Xing, T.; Zhou, X. Properties of silk fibers modified with diethylene glycol dimethacrylate. J. Appl. Polym. Sci. 2006, 102(1), 424-428.
9. Das, A.; Saikia, C. N.; Hussain, S. Grafting of methyl methacrylate (MMA) onto Antheraea assama silk fiber. J. Appl. Polym. Sci. 2001, 81(11), 2633-2641.
10. Masuhiro, T.; Nobutami, K.; Giuliano, F. Structural analysis of methyl methacrylate-grafted silk fibers. J. Appl. Polym. Sci. 1993, 50(5), 885-90.
11. Zhao, C.; Okada, H.; Sugimoto, R. Diethyl(1,10-phenanthroline-N1,N10)zinc initiated grafting of styrene on polypropylene/ polyethylene. Bull. Chem. Soc. Japan. 2018, 91, 1576-1578.
12. Zhao, C.; Okada, H.; Sugimoto, R. Surface modification of polypropylene with poly(methyl methacrylate) initiated by a diethylzinc and 1,10-phenanthroline complex. React. Funct. Polym. 2018, 132, 127-132.
13. Zhao, C.; Okada, H.; Sugimoto, R. Polymerization of styrene in aqueous system using a diethylzinc and 1,10-phenanthroline complex. Polymer. 2018, 154, 211-217.
14. Liu, Y.; Qian, J.; Liu, H.; Zhang, X.; Deng, J.; Yu, T. Blend membrane of regenerated silk fibroin, poly(vinyl alcohol), and peroxidase and its application to a ferrocene-mediating

hydrogen peroxide sensor. J. Appl. Polym. 1996, 61(4), 641-647.
15. Qian, J.; Liu, Y.; Liu, H.; Yu, T.; Deng, J. An amperometric new methylene blue N-mediating sensor for hydrogen peroxide based on regenerated silk fibroin as an immobilization matrix for peroxidase. Anal. Biochem. 1996, 236(2), 208-14.
16. Hu, Y.; Zhang, Q.; You, R.; Wang, L.; Li, M. The relationship between secondary structure and biodegradation behavior of silk fibroin scaffolds. Adv. Mater. Sci. Eng. 2012, 185905.
17. Shang, S.; Zhu, L.; Chen, W.; Yi, L.; Qi, D.; Yang, L. Reducing silk fibrillation through MMA graft method. Fiber. Polym. 2009, 10(6), 807-812.
18. Thakur, V. K.; Vennerberg, D.; Madbouly, S. A.; Kessler, M. R. Bio-inspired green surface functionalization of PMMA for multifunctional capacitors. RSC Adv. 2014, 4(13), 6677-6684.
19. Diego, L.; Nogueira, M. F. J.; Elaine, M. S. Thermal evaluation of cashew nutshell liquid as new bioadditives for poly(methyl methacrylate). J. Therm. Anal. Calorim. 2013, 111(1), 619-626.
20. Takashi, K.; Atsushi, I.; Brown, J. E.; Koichi, H.; Tatsuki, K.; Eiji, M. Effects of weak linkages on the thermal and oxidative degradation of poly(methyl methacrylates) Macromolecules. 1986, 19(8), 2160-8.

List of Figures

List of Tables